DESIGN, SYNTHESIS AND APPLICATIONS OF FUNCTIONALIZED IONIC LIQUIDS

THÈSE N^{O} 3531 (2006)

PRÉSENTÉE LE 2 JUIN 2006

À LA FACULTÉ SCIENCES DE BASE

Laboratoire de chimie

SECTION DE CHIMIE ET GÉNIE CHIMIQUE

ÉCOLE POLYTECHNIQUE FÉDÉRALE DE LAUSANNE

POUR L'OBTENTION DU GRADE DE DOCTEUR ÈS SCIENCES

PAR

Dongbin ZHAO

M.Sc. in Chemistry, Xinan Petroleum University, Nanchong, Chine
et de nationalité chinoise

acceptée sur proposition du jury:

Prof. P. Vogel, président du jury
Prof. P. Dyson directeur de thèse
Prof. C. Chiappe, rapporteur
Prof. K. Severin, rapporteur
Prof. I. Tkatchenko, rapporteur

ÉCOLE POLYTECHNIQUE
FÉDÉRALE DE LAUSANNE

Lausanne, EPFL
2007

Contents

Summary……..1

Résumé……3

Acknowledgements……..5

Abbreviations……...6

Compounds synthesized in this thesis……..7

1 Introduction……11

1.1 Preface...……...12

1.2 Basics of ILs……12

1.3 IL functionalization……..13

1.3.1 IL functionalization via imidazolium cation modification……13

1.3.1.1 ILs containing alkene and alkyne functionality……14

1.3.1.2 ILs containing alcohol, ether and carboxyl functionalities substituents……14

1.3.1.3 ILs containing silicon, nitrogen, phosphous and transition metal ……15

1.3.1.4 N,N-bis(functionalized)-imidazolium ILs (double armed)……16

1.3.1.5 Alternative methods……17

1.3.2 Non-imidazolium based functionalized ILs……18

1.4 References……22

2 Synthesis and Characterization of Imidazolium ILs Incorporating the Nitrile Functionality…….25

2.1 Introduction……..26

2.2.1.1 Structural characterisation of **1a**, **3a**, **3b** and **5b** in the solid state……28

2.2.1.2 Physical properties of the ILs……34

2.2.2 Double armed imidazolium ILs bearing nitrile functionality……37

2.2.2.1 Solid state structures of **6a**, **6b**, **6c**, **7a** and **7b**……...39

2.2.4 Concluding remarks……..41

2.2.5 Experimental……41

2.3 References……51

3 Palladium Complexes of Nitrile Functionalized Imidazolium ILs and their Applications in Catalysis……54

3.1 Introduction……..55

3.2 Results and Discussion……55

3.2.1 Reaction of Nitrile Functionalized Ionic Liquids with $PdCl_2$……...55
3.2.2 Carbon-Carbon coupling reactions……59
3.2.3 Hydrogenation of cyclohexadiene…….66
3.3 Concluding remarks……..67
3.4 Experimental…….67
3.5 References……74
4 Synthesis and Characterization of Pyridinium ILs Incorporating the Nitrile Functionality and Applications in C-C coupling reactions…….77
4.1 Introduction……..78
4.2 Results and Discussion…….78
4.2.1 Synthesis of the ILs……...78
4.2.2 Reactions of **13a – 13d** with palladium(II) chloride…….79
4.2.3 Solid state structures of 13a and 14a…….80
4.2.4 Carbon-carbon coupling reactions…….82
4.3 Concluding remarks……..86
4.4 Experimental…….87
4.5 References……93
5 Synthesis, Characterization and Reactivity of Allyl F-ILs……..95
5.1 Introduction……..96
5.2 Results and discussion……..97
5.2.1 Synthesis and characterization of allyl F-ILs and their reactivity with palladium chloride…..97
5.2.2 Reactivity of the allyl functionalised ILs……101
5. 3 Concluding remarks……..103
5. 4 Experimental…….104
5.5 References……..109
6 “Dual-functionalized” ILs: synthesis and characterization of imidazolium salts with the butyronitrile-trifluoroborate anion……111
6.1 Introduction……...……..112
6.2 Results and discussion……...…….113
6.2.1 Synthesis and characterization of inoic liquids with the nitrile functionalized anion $[CH_3CH(BF_3)CH_2CN]^-$……113

6.2.2 Physical properties……..115
6.3 Concluding remarks……115
6.4 Experimental……...116
6.5 References……..121
7 Development of an IL Polymer as Metal Nanoparticle Stabilizer……122
7.1 Introduction……123
7.2 Results and Discussion……...124
7.3 Concluding Remarks……..132
7.4 Experimental……...132
7.5 References……..142
8 Conclusions……144

Summary

Room temperature ionic liquids (RTILs), considered as “designers’ solvents”, are attracting a great attention because of their possibility to be tailored based on property requirements. The ionic liquids designed and synthesized for carrying out specified task are referred as functionalized ionic liquids, which show great application potential in various processes. The efforts to produce functionalized ionic liquids, characterize them, and evaluate their properties and applications are presented in this thesis.

In chapter 1 the recent developments in ionic liquid functionalization are highlighted.

Chapter 2 describes the synthesis and characterization of imidazolium salts in which a nitrile group is attached to the alkyl side chain (single-armed as well as double-armed). The nitrile group was chosen as it is a promising donor to transition metals such as palladium and platinum. The physicochemical properties of these new ionic liquids are described and it is shown how the length of the alkyl unit linking the imidazolium ring and the CN group influences the melting point of the ionic liquid.

The third chapter describes palladium complexation reactions with the nitrile functionalized imidazolium ionic liquids (prepared as described in Chapter 2). Their application in C-C coupling and hydrogenation reactions are described. It will be shown that the palladium complexes serve as precursors to nanoparticle catalyst reservoirs and are very efficiently stabilized by the nitrile-functionalized ionic liquids.

In chapter 4, the synthesis of a series of nitrile functionalized ionic liquids based on the *N*-butylnitrile pyridinium cation is reported and their suitability as solvents for palladium-catalyzed biphasic Suzuki and Stille coupling reactions is demonstrated. TEM images reveal that nanoparticles are formed *in situ* in Stille reactions and show that the nitrile-functionalized ionic liquid exert a superior nanoparticle-stabilizing effect compared to non-functionalized ionic liquids. This allows excellent catalyst lifetimes.

In the fifth chapter the synthesis and characterization of a series of ionic liquids incorporating the allyl functionality and some nascent reactions that they undergo, indicating that they are useful precursors to a wide range of other functionalized ionic liquids, will be described.

Chapter 6 reports on a concept of "dual-functionalized" ionic liquids. Specifically imidazolium cations with various functionalities are combined with the nitrile functionalized anion $[CH_3CH(BF_3)CH_2CN]^-$, aiming at reducing the melting point and visocity of ionic liquids

In the final chapter the ionic liquid, 1-methyl-3-(4-vinylbenzyl)-imidazolium chloride, is prepared and polymerized to form a macromolecule that is subsequently used as a transition metal nanoparticle stabilizer. A methodology that enables transition metal nanoparticle transfer between liquid phases, via surface modification of the nanoparticles by anion exchange, is described.

Keywords: ionic liquids, synthesis, catalysis, nanoparticles

Résumé

Les liquides ioniques de température ambiante, considérés en tant que "dissolvants des concepteurs", attirent une grande attention en raison de la possibilité à travailler ont basé sur la condition de propriété. Les liquides ioniques conçus et synthétisés pour la tâche indiquée de mise en oeuvre sont la plupart du temps référés comme functionalizée les liquides ioniques, qui montrent de grands potentiels d'application dans divers processus. Les efforts de produire functionalizée les liquides ioniques, les caractérisent et évaluent leurs propriétés et des applications sont présentées dans cette thèse.

En chapitre 1 les développements récents dans le functionalization liquide ionique sont accentués.

Le chapitre 2 décrivent la synthèse et la caractérisation des sels d'imidazolium en lesquels un groupe de nitriles est attaché à la chaîne latérale alkylique (simple-armée comme double-armée). Le groupe de nitriles a été choisi car c'est un donateur prometteur aux métaux de transition tels que le palladium et le platine. Les propriétés physico-chimiques de ces nouveaux liquides ioniques est décrites et on lui montre comment la longueur de l'unité alkylique liant l'anneau d'imidazolium et le groupe de CN influencent le point de fusion du liquide ionique.

Le troisième chapitre décrit des réactions de complexation de palladium à des nitriles functionalizée les liquides ioniques d'imidazolium (préparés comme décrit en chapitre 2). Leur application dans des réactions d'accouplement et d'hydrogénation de cc sont décrites. On lui montrera que les complexes du palladium servent de précurseurs aux réservoirs de catalyseur de nanoparticle et sont stabilisés fortement efficacement par les nitriles-functionalizée IL.

En chapitre 4, la synthèse d'une série de nitriles functionalized les liquides ioniques basés sur *le N* - le cation butylnitrile de pyridinium est rapporté et leur convenance comme les dissolvants des réactions pour accouplement biphasé palladium-catalysé de Suzuki et de Stille ont démontré. Les images de TEM indiquent que des nanoparticles sont formés *in situ* dans des réactions de Stille et prouvent que les nitriles-functionalizée le liquide qu'ionique exerce un effet nanoparticle-stabilisant supérieur comparé au non-functionalizée le liquide ionique. Ceci tient compte d'excellentes vies de catalyseur.

Dans le cinquième chapitre la synthèse et la caractérisation d'une série de liquides ioniques incorporant la fonctionnalité d'allylique et quelques réactions naissantes qu'elles subissent,

indiquant qu'elles sont les méthodes utiles à un éventail d'autre functionalizée les liquides ioniques seront décrits.

Les rapports du chapitre 6 sur un concept des liquides ioniques "duels-functionalized" et de l'IL comportant des cations d'imidazolium avec de diverses fonctionnalités et les nitriles functionalized un nion $[CH_3CH(BF_3)CH_2CN]^-$ le point de la fusion d'IL réducteur visant et le visocity, seront décrits.

Dans le chapitre final le liquide ionique, chlorure 1-méthylique-3-(4-vinylbenzyl)-imidazolium, est préparé et polymérisé pour former un macromoléculaire qui a plus tard employé comme stabilisateur de nanoparticle en métal de transition. Une méthodologie permet le transfert de nanoparticle en métal de transition entre les phases liquides, y compris la modification extérieure des nanoparticles par l'intermédiaire de l'échange anionique, est décrite.

Mots-clés : liquides ioniques, synthèse, catalyse, nanoparticles

Acknowledgements

Without all these people this thesis would not have been possible.

Firstly, I would like to thank my supervisor, Professor **Paul J. Dyson**, who gave me the opportunity to join his group in the EPFL, and directed me through nearly four years of thesis work. His supportive discussions and enthusiasm for chemistry always replenished my energy to work. I would also like to thank his mercy tolerating the impurity of my ILs.

Dr. **Fei Zhaofu**, who has shared the same work place with me, is thanked for helping me with synthetic techniques, and in valuable research proposals. He really helped me a great deal in my thesis work. I am also grateful to him for joining me in cleaning the remains of the "fridge-bomb experiment".

Dr **Gabor Laurenczy** is thanked for helping me with high pressure NMR experiments.

Collegues Dr **Tilmann Geldbach**, for great help in NMR and catalysis; Major **Wee Han Ang**, for his delicious food taken from Singapore and MALDI expertise. **Adrian Chaplin** for his help in conducting safe chemistry, **Corinne Daguenet** for her help in the operation of the autoclave, **Antoine Dorcier** for his mass spectrometer management, **Céline Fellay** for her work with me as a project student and the lovely Christmas gift, **Ana Vidis** for briefly sharing the lab and **Claudine Scolaro** for her orderly lab work style. Dr. **Rosario Scopellitti** for X-ray single crystal analysis. Professor **Buffat Philippe**, Dr **Hessler Aïcha** and **Guido Milanezi** of CIME-EPFL for their help in TEM analysis. Professor **Cinzia Chiappe** and **Daniela Pieraccini** for providing in-depth investigation on the application of functioanlized ILs.

Catherine Droz and **Talya Van Woerden**, our secretaries, are greatly thanked for their work that kept my thesis research going smoothly.

My wife, **Ling Duan**, and my parents, for their long time support and encouragement.

Abbreviations

Original term	*Abbreviation*
Room temperature ionic liquid	RTIL
IL	IL
Functionalized ionic liquid	F-IL
Dual-functionalized ionic liquid	DF-IL
Tetrahydrofuran	THF
Dimethyl sulfoxide	DMSO
Methyl	m
Imidazolium	im
1-butyl-3-methyl-imidazolium	C_4mim
bis(trifluoromethanesulfonyl)imide	Tf_2N
Nanoparticle	NP
XRD	X-ray diffraction analysis
EDX	Energy Dispersive X-ray Analysis
TEM	Transition electronic microscopy

Compounds synthesized in this thesis

Compound name/Abbreviation/Number

1-methyl-3-ethylnitrile-imidazolium chloride/[CCNmim]Cl/**1a**

1-methyl-3-propylnitrile-imidazolium chloride/[C_2CNmim]Cl/**2a**

1-methyl-3-butylnitrile-imidazolium chloride/[C_3CNmim]Cl/**3a**

1-methyl-3-pentylnitrile-imidazolium chloride/[C_4CNmim]Cl/**4a**

1,2-dimethyl-3-butylnitrile-imidazolium chloride/[C_3CNdmim]Cl/**5a**

1-methyl-3-ethylnitrile-imidazolium hexafluorophosphate/[CCNmim][PF_6]/**1b**

1-methyl-3-propylnitrile-imidazolium hexafluorophosphate/[C_2CNmim][PF_6]/**2b**

1-methyl-3-butylnitrile-imidazolium hexafluorophosphate/[C_3CNmim][PF_6]/**3b**

1-methyl-3-pentylnitrile-imidazolium hexafluorophosphate/[C_4CNmim][PF_6]/**4b**

1,2-dimethyl-3-butylnitrile-imidazolium hexafluorophosphate/[C_3CNdmim][PF_6]/**5b**

1-methyl-3-ethylnitrile-imidazolium tetrafluoroborate/[CCNmim][BF_4]/**1c**

1-methyl-3-propylnitrile-imidazolium tetrafluoroborate/[C_2CNmim][BF_4]/**2c**

1-methyl-3-butylnitrile-imidazolium tetrafluoroborate/[C_3CNmim][BF_4]/**3c**

1-methyl-3-butylnitrile-imidazolium bis(trifluoromethanesulfonyl)imide/[C_3CNmim][Tf_2N]/**3d**

1-methyl-3-pentylnitrile-imidazolium tetrafluoroborate/[C_4CNmim][BF_4]/**4c**

1,2-dimethyl-3-butylnitrile-imidazolium tetrafluoroborate/[C_3CNdmim][BF_4]/**5c**

1,2-dimethyl-3-butylnitrile-imidazolium
bis(trifluoromethanesulfonyl)imide/[C_3CNdmim][Tf_2N]/**5d**

1,3-diethylnitrile-imidazolium chloride/[$(CCN)_2$im]Cl/**6a**

1,3-dibutylnitrile-imidazolium chloride/[$(C_3CN)_2$im]Cl/**7a**

1,3-dipentylnitrile-imidazolium chloride/[$(C_4CN)_2$im]Cl/**8a**

1,3-diethylnitrile-imidazolium hexafluorophosphate/[$(CCN)_2$im][PF_6]/**6b**

1,3-dibutylnitrile-imidazolium hexafluorophosphate/[$(C_3CN)_2$im][PF_6]/**7b**

1,3-dipentylnitrile-imidazolium hexafluorophosphate/[$(C_4CN)_2$im][PF_6]/**8b**

1,3-diethylnitrile-imidazolium tetrafluoroborate/[$(CCN)_2$im][BF_4]/**6c**

1,3-dibutylnitrile-imidazolium tetrafluoroborate/$[(C_3CN)_2im][BF_4]$/**7c**

1,3-dipentylnitrile-imidazolium tetrafluoroborate/$[(C_4CN)_2im][BF_4]$/**8c**

1,3-diethylnitrile-imidazolium bis(trifluoromethanesulfonyl)imide/$[(CCN)_2im][Tf_2N]$/**6d**

1,3-dibutylnitrile-imidazolium bis(trifluoromethanesulfonyl)imide/$[(C_3CN)_2im][Tf_2N]$/**7d**

1,3-dipentylnitrile-imidazolium bis(trifluoromethanesulfonyl)imide/$[(C_4CN)_2im][Tf_2N]$/**8d**

di-(1-methyl-3-butylnitrile-imidazolium) palladium tetrachloride/$[C_3CNmim]_2PdCl_4$/**9a**

di-(1,2-dimethyl-3-butylnitrile-imidazolium) palladium tetrachloride/$[C_3CNdmim]_2PdCl_4$/**10a**

di-(1,3-dibutylnitrile-imidazolium) palladium tetrachloride/$[(C_3CN)_2im]_2PdCl_4$/**11a**

1-methyl-3-butylnitrile-imidazolium palladium dichloride hexafluorophosphate complex/$[(C_3CNmim)_2PdCl_2][PF_6]_2$/**9b**

1-methyl-3-butylnitrile-imidazolium palladium dichloride tetrafluoroborate complex/$[(C_3CNmim)_2PdCl_2][BF_4]_2$/**9c**

1-methyl-3-butylnitrile-imidazolium palladium dichloride bis(trifluoromethanesulfonyl)imide complex/$[(C_3CNmim)_2PdCl_2][Tf_2N]_2$/**9d**

1,2-dimethyl-3-butylnitrile-imidazolium palladium dichloride hexafluorophosphate complex/$[(C_3CNdmim)_2PdCl_2][PF_6]_2$/**10b**

1,2-dimethyl-3-butylnitrile-imidazolium palladium dichloride tetrafluoroborate complex/$[(C_3CNdmim)_2PdCl_2][BF_4]_2$/**10c**

1,2-dimethyl-3-butylnitrile-imidazolium palladium dichloride bis(trifluoromethanesulfonyl)imide complex/$[(C_3CNmim)_2PdCl_2][Tf_2N]_2$/**10d**

di-(1-methyl-3-butylnitrile-imidazolium) palladium tetrachloride palladium dichloride complex/$[PdCl_2(C_3CNmim)_2][PdCl_4]$/**11b**

di-(1,2-dimethyl-3-butylnitrile-imidazolium) palladium tetrachloride palladium dichloride complex/$[PdCl_2(C_3CNdmim)_2][PdCl_4]$/**12b**

N-butylnitrile-pyridinium chloride/$[C_3CNpy]Cl$/**13a**

N-butylnitrile-pyridinium hexafluorophosphate/$[C_3CNpy][PF_6]$/**13b**

N-butylnitrile-pyridinium tetrafluoroborate/$[C_3CNpy][BF_4]$/**13c**

N-butylnitrile-pyridinium bis(trifluoromethanesulfonyl)imide/$[C_3CNpy][Tf_2N]$/**13d**

di-(N-butylnitrile-pyridinium) palladium tetrachloride/$[C_3CNpy]_2PdCl_4$/**14a**

N-butylnitrile-pyridinium palladium dichloride hexafluorophosphate complex/$[(C_3CNpy)_2PdCl_2][PF_6]_2$/**14b**

N-butylnitrile-pyridinium palladium dichloride tetrafluoroborate complex/$[(C_3CNpy)_2PdCl_2][BF_4]_2$/**14c**

N-butylnitrile-pyridinium bis(trifluoromethanesulfonyl)imide palladium dichloride complex/$[(C_3CNmim)_2PdCl_2][Tf_2N]_2$/**14d**

Bis-[di-(N-butylnitrile-pyridinium) palladium tetrachloride] palladium dichloride complex/$([C_3CNpy]_2PdCl_4)_2PdCl_2$/**14e**

1-allyl-3-methyl-imidazolium bromide/[allymim]Br/**15a**

1-allyl-3-methyl-imidazolium tetraphenylborate/$[allymim][BPh_4]$/**15b**

1-allyl-3-methyl-imidazolium tetrafluoroborate/$[allymim][BF_4]$/**15c**

1,3-diallyl-imidazolium bromide/$[(ally)_2im]$Br/**16a**

1,3-diallyl-imidazolium tetraphenylborate/$[(ally)_2im][BPh_4]$/**16b**

1,3-diallyl-imidazolium tetrafluoroborate/$[(ally)_2im][BF_4]$/**16c**

di-(1-allyl-3-methyl-imidazolium) palladium dibromide-dichloride/$[allymim]_2PdCl_2Br_2$/**17a**

di-(1,3-diallyl-imidazolium) palladium dibromide-dichloride/$[(ally)_2im]_2PdCl_2Br_2$/**18a**

di-1-methylimidazole palladium bromide complex/$[mim]_2PdBr_2$/**19**

1-*iso*-propyl-phenyl-3-methyl-imidazolium trifluoromethanesulphonic/[*i*ppmim]$[CF_3SO_3]$/**20**

Potassium butylnitrile 3-trifluoroborate/$K[CH_3(BF_3)CHCH_2CN]$/**21**

1-butyl-3-methylimidazolium butylnitrile 3-trifluoroborate/$[C_4mim][CH_3(BF_3)CHCH_2CN]$/**21a**

1-allyl-3-methyl-imidazolium butylnitrile 3-trifluoroborate/$[allymim][CH_3(BF_3)CHCH_2CN]$/**21b**

1-propyne-3- methyl-imidazolium butylnitrile 3-trifluoroborate/[propynemim]$[CH_3(BF_3)CHCH_2CN]$/**21c**

1-butylcarboxyl acid-3-methyl-imidazolium butylnitrile 3-trifluoroborate/$[C_3COOHmim][CH_3(BF_3)CHCH_2CN]$/**21d**

1-butylnitrile-3-methyl-imidazolium butylnitrile 3-trifluoroborate/$[C_3CNmim][CH_3(BF_3)CHCH_2CN]$/**21e**

1,3-di-allyl-imidazolium butylnitrile 3-trifluoroborate/$[(ally)_2im][CH_3(BF_3)CHCH_2CN]$/**21f**

1,3-di-propyne-imidazolium butylnitrile-3-trifluoroborate/[(propyne)$_2$im][$CH_3(BF_3)CHCH_2CN$]/**21g**

1,3-butylcarboxyl acid-imidazolium butylnitrile 3-trifluoroborate/[($C_3COOH)_2$im][$CH_3(BF_3)CHCH_2CN$]/**21h**

1,3-di-butylnitrile-imidazolium butylnitrile 3-trifluoroborate/[($C_3CN)_2$mim][$CH_3(BF_3)CHCH_2CN$]/**21i**

1-methylstyrene-3-methylimidazolium chloride/[mstyr-mim]Cl/**22**

Poly-(1-methylstyrene-3-methylimidazolium chloride)/ILPCl/**23**

Poly-(1-methylstyrene-3-methylimidazolium hexafluorophosphate)/ILPPF_6/**24**

Poly-(1-methylstyrene-3-methylimidazolium bis(trifluoromethanesulfonyl)imide)/ILPTf_2N/**25**

1

Introduction

1.1 Preface

The first chapter intends to give a brief summary of F-ILs. Curiosity in ILs has increased significantly over the last decade, evoked by the growth of new synthetic routes to ILs (especially the air and moisture stable ones), as well as having many potential applications. The design and synthesis of functionalized ILs, especially functionalized cations, will be summarized in this chapter.

1.2 Basics of ILs

The history of ILs dates back nearly one hundred years,[1] however, research developed quietly for many years[2] until Wilkes and co-workers reported air and moisture stable imidazolium based room temperature ILs that inspired much interest in the field.[3] Chemists with a range of different interests were attracted by the ready accessibility and unique properties of ILs, resulting in a huge number of publications during the past decade. Some typical structures of ILs are shown in Scheme 1.1. Heteroatomic cations such as imidazolium, pyridinium, ammonium and phosphinium ions are the most widely used cations of the IL family, with the most widely applied synthetic strategy involving the cationization of the heteroatomic compound followed by anion metathesis.

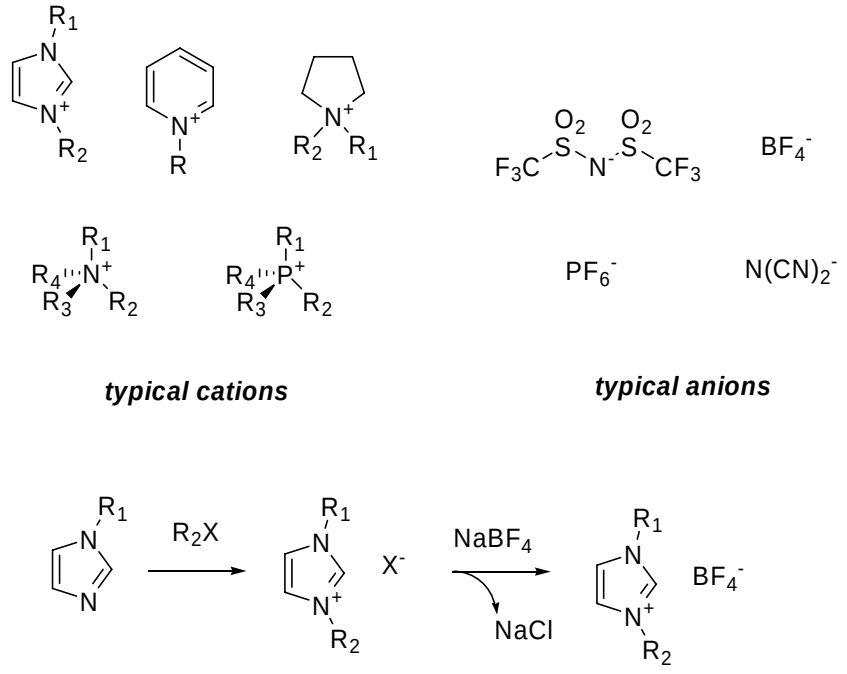

Scheme 1.1 Examples of some typical ILs and the most common synthetic route

The unique properties of ILs, eg. their wide liquid range (over 300°C), high stability, wide electrochemical window, high density (usually > 1.0 g/ml), negligible vapour pressure, high viscosity (from 50 to over 3000 cp), distinguish them from traditional organic solvents.

1.3 IL functionalization

The chemophysical properties of ILs depend on the combination of cation and anion; in addition, the length of the alkyl chain and functionality have a striking influence on their properties. Thus, the preparation of "task-specific" or functionalized ILs is normally realized through the incorporation of functional groups on the cations, to date, mostly the imidazolium cation, although a few examples involving functionalized anions are known.[4]

1.3.1 IL functionalization via imidazolium cation modification

Starting from 1-alkylimidazoles and using functionalized alkyl halides, the quaternization method usually gives the desired functionalized ILs as imidazolium halides in good yield (Scheme 1.2). Both components are often commercially available and the reaction is usually facile. In many cases solvent is not required unless the reaction is highly exothermic. However, in most cases, solvent is required to purify the imidazolium halide from unreacted starting materials. If a long chain alkyl halide is used, longer reaction times are needed and heating is also necessary. Electron-withdrawing groups attached to the alkyl halide enhance electrophilicity, and consequently shorten the reaction time.

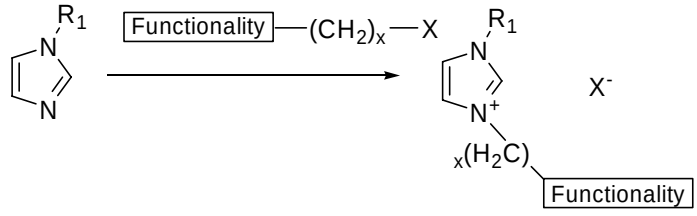

R_1, R_2 = alkyl

X = I, Br, or Cl

Scheme 1.2 Synthetic route used to prepare functionalized ILs precursors

This method is suitable for the synthesis of nearly all the ILs which are stable towards base, however, because of the relatively strong basicity of imidazole, elimination of hydrogen halide or Hoffmann elimination can occur in some cases.[5]

So far most functional groups have been introduced directly to the imidazolium moiety using this direct quartinazation route. For example, imidazolium cations with hydroxyl groups,[6] carboxylic groups,[7] thiol groups[8], alkyne groups,[9] alkene groups,[10] diene groups,[11] and fluorous chains were successfully prepared.[12, 13]

Certain functionalities requires alternative synthetic routes to be attached to the imidazole backbone, for example, amine[14] and amide groups,[15] phosphine,[16] urea and thiourea groups,[17] and chiral

centres.[18] The imidazolium centre is relatively inert and functional groups can after be further reacted, eg. carboxylic ester groups can be converted to carboxylic acid groups,[19] and sulphides can be converted into thiol groups.[20]

1.3.1.1 ILs containing alkene and alkyne functionality

Alkene and alkynes can be easily introduced into imidazole ring systems using the quaternization method.[21] Chart 1.1 illustrates some examples of such ILs. Alkene ILs are often less viscous than their saturated counterparts.[22] Due to the highly developed chemistry of C=C and C≡C bonds, they are very good precursors for the preparation of further functionalized ILs. For example, they can be brominated to give dense halogenated ILs.[23] The resulting brominated ILs with $[PF_6]^-$or $[Tf_2N]^-$ anions are immiscible with water and miscible with dichloromethane, however, they are hardly miscible with chloroform. They are more thermally stable than the non-halogenated imidazolium ILs and therefore have potential applications in separation processes.

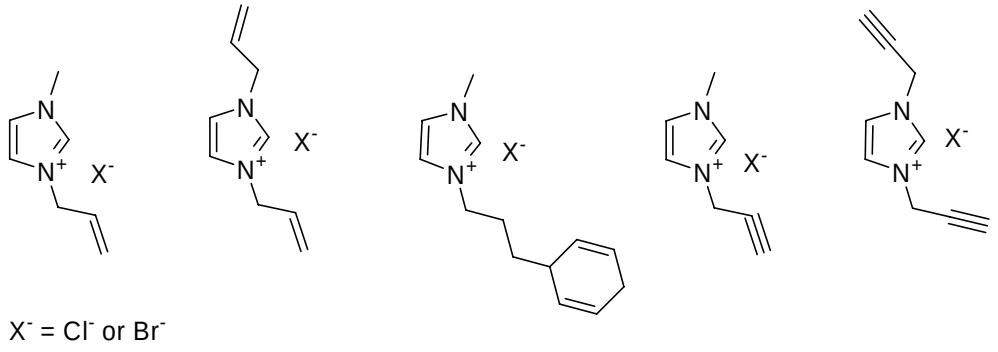

Chart 1.1 Examples of ILs containing alkene and alkyne functionalities.

1.3.1.2 ILs containing alcohol, ether and carboxyl functionalities

Direct quaternisation of imidazole with chloroalkylalcohol afford OH or OMe[4d] functionalized ILs. Similarly, ester groups can be introduced into imidazolium systems, which can be converted into carboxylic acid groups by reaction with HCl. They dissolve a wide range of transition metal salts and react to form coordination polymers.[24] Chart 1.2 presents some examples of these ILs.

Chart 1.2 Examples of ILs of containing alcohol, ether and carboxyl groups

1.3.1.3 ILs containing silicon, nitrogen, phosphous and transition metal substituents

Many other functional groups have also been introduced onto the imidazolium backbone using standard quaternization reactions. For example, the imidazolium salts with $SiOMe_3$ groups can be prepared in high yield. By anion exchange the hydrophillicity of these salts can be controlled on Si/SiO_2 surface (Chart 1.3).[25, 26]

Chart 1.3 Examples of imidazolium salts of functionality containing $SiOMe_3$ group

The thiol group was also incorporated into the imidazolium moiety. Reduction of disulfide ILs gives thiol-functionalized ILs that can be used to stabilize gold nanoparticles, which can be transferred from water to ILs through anion exchange (Scheme 1.3).

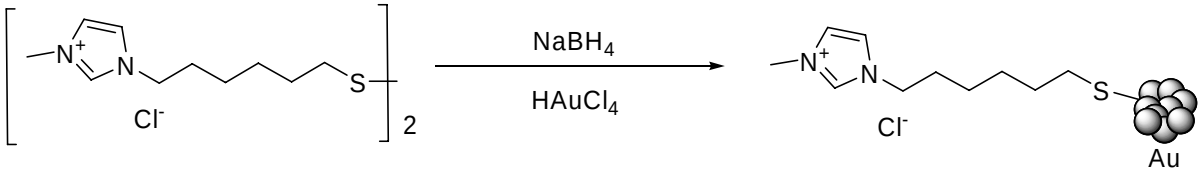

Scheme 1.3 Synthesis of gold nanoparticles using a thiol IL as stabilizer

Imidazolium salts with the SO_3H group are strong Brønsted acids, they can serve as catalyst for Fischer esterification, dehydrodimerization and the pinacol rearrangement.[27] Amino, amido[28], and have also been introduced into the imidazolium backbone. Chart 1.4 presents some of the functionalized ILs bearing these groups.

Chart 1.4 Examples of ILs of functionality containing amino and amido groups

The biphenyl phosphine fragment was introduced into the imidazolium unit,[29] and used in hydroformylation reactions.[30] (Chart 1.5 left) Phosphonate can also be introduced to the imidazole system (Chart 1.5 right), which is stable in air and can be used as mechanic lubricant.[31]

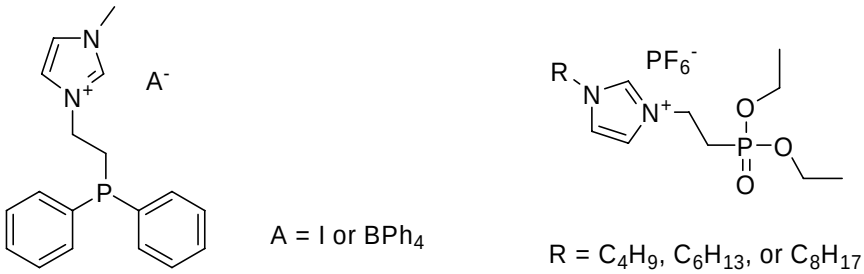

Chart 1.5 Imidazolium salts with phosphine functionality and ILs with phosphonate functionality

Transition metals can also be incorporated into ILs. For example, the cobalt carbonyl moiety was introduced into imidazolium to form a compound with a melting point of 100°C, which is designated as the criteria to distinguish ILs from other salts (Scheme 1.4).

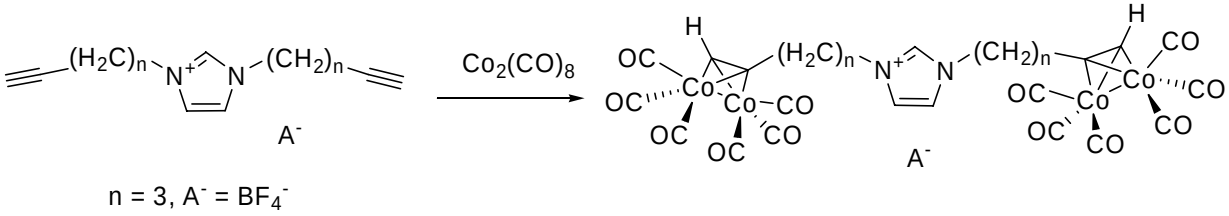

Scheme 1.4 ILs containing cobalt carbonyl fragments

ILs containing the ferrocene moiety, ie. (ferrocenylmethyl)imidazolium and (ferrocenylmethyl)triazolium, have been prepared.[32] Through adjustment of anion, an IL with melting point of 86°C can be obtained (Chart 1.6).

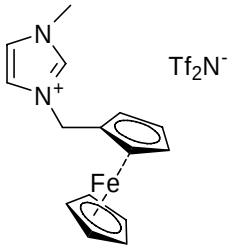

Chart 1.6 An IL containing ferrocene

1.3.1.4 N,N-bis(functionalized)-imidazolium ILs (double armed)

Many of the above mentioned functionalized ILs were mono-functionalized, however, *N,N*-bisfunctionalized-imidazolium ILs can also be obtained using two general methods. Firstly, the deprotonation of imidazole by NaH followed by addition of two equivalents of the functionalized alkyl halide precursor usually gives high yield of *N,N*-bisfunctionalized-imidazolium ILs.[33] However this method requires stronger inorganic base, thus it cannot be applied to functional groups which are sensitive to base (Scheme 1.5 left).

R = alkyl with functionality
X = I, Br, or Cl

Method 1

R = alkyl with functionality
X = I, Br, or Cl

Method 2

Scheme 1.5 Synthetic routes N,N-bisfunctionalized-imidazolium salts

The second method employs 1-trimethylsilyimidazole as a precursor. Heating a mixture of 1-trimethylsilyimidazole and two equivalent of functionalized alkyl halide gives the desired 1,3-bisfunctionalized-imidazolium in high yield (Scheme 1.5 right).[34] The $SiMe_3Cl$ by-product can be easily removed by distillation. Because no strong base agent is need for the process, this method can be applied to a wide range of precursors.

1.3.1.5 Alternative methods

It is well know that the imidazolium halides usually have high melting points and are solid at room temperature. To obtain low melting point ILs anion-exchange with imidazolium halides is required. The drawback of such process is the difficulty to prevent halide contamination, which requires repeated extraction/washing water is often used.

Since it has been demonstrated recently that the presence of halide in ILs can drastically change the physical properties of ILs,[35] and may result in catalyst poisoning and deactivation if used as solvents for catalytic reactions,[36] a halide-free route has been developed for synthesizing ILs with the $[BF_4]^-$ anion, in which trimethyloxonium tetrafluoroborate is used to react directly with *N*-alkylimidazole.[37]

Another method to prepare ILs is by neutralization of a methanol solution of 1-ethyl-3-methylimidazolium methylcarbonate ($MeOCO_2^-$) with acids containing the corresponding anions as shown in Scheme 1.6, where MeOH and CO_2 are the only by-products.[38]

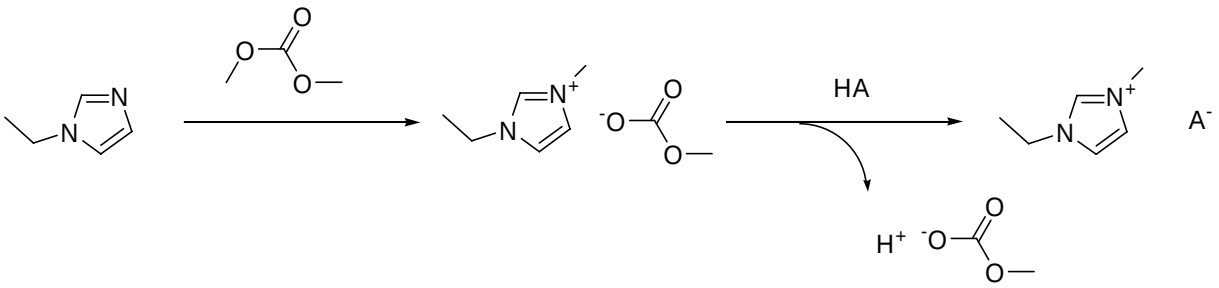

Scheme 1.6 Synthesis halide free IL with the $MeOCO_2^-$ anion

Transformation of imidazolium based zwitterions can also give halide free ILs. For example, imidazolium zwitterions with carboxylate groups can be converted into IL bearing the carboxylic acid functionality (Scheme 1.7 up). A similar process can be used to convert the sulfonate group into an alkanesulfonic acid.[39] (Scheme 1.7 down).

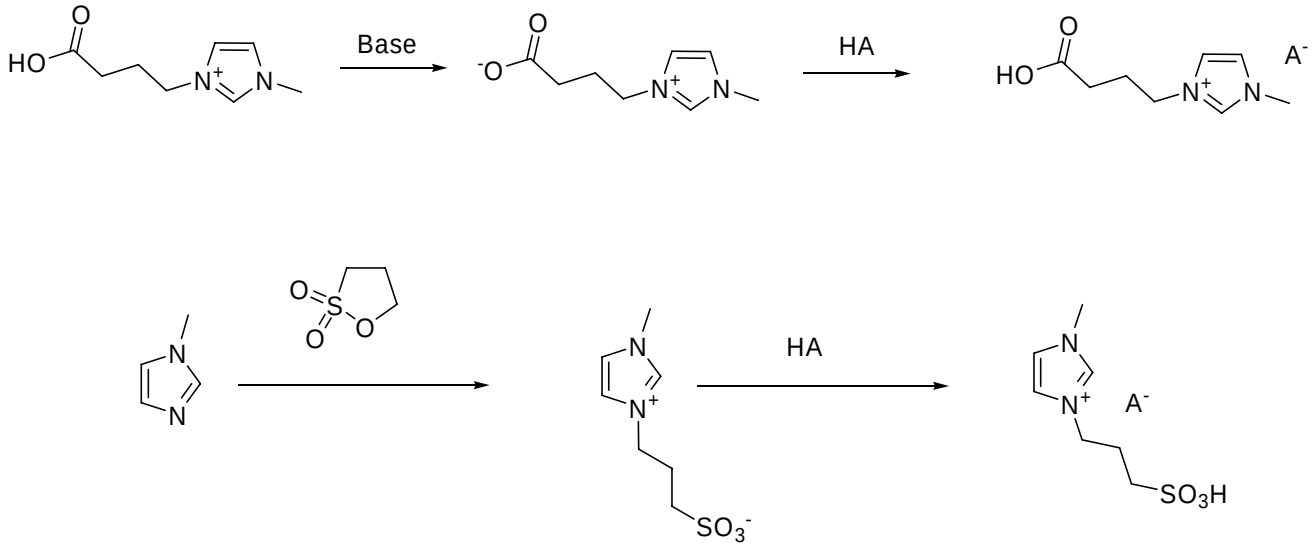

Scheme 1.7 Preparation of ILs containing carboxyl acid group (up) and sulfonic acid (down)

1.3.2 Non-imidazolium based functionalized ILs

Pyridinium functionalized ILs have received less attention than imidazolium systems, but they have been successfully functionalized with the nitrile[40] and $(CH_2)_m(CF_2)_nCF_3$ functionalities (Chart 1.7).[41]

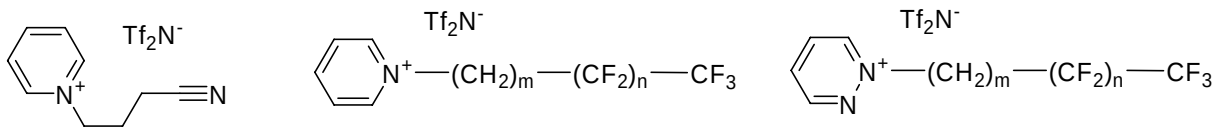

Chart 1.7 Functionalized ILs based on pyridinium and pyridazinum cations

It has also been reported that a series of 1,2,4-substitute-triazolium salts form ILs, prepared via a multi-step route (Scheme 1.9).[42]

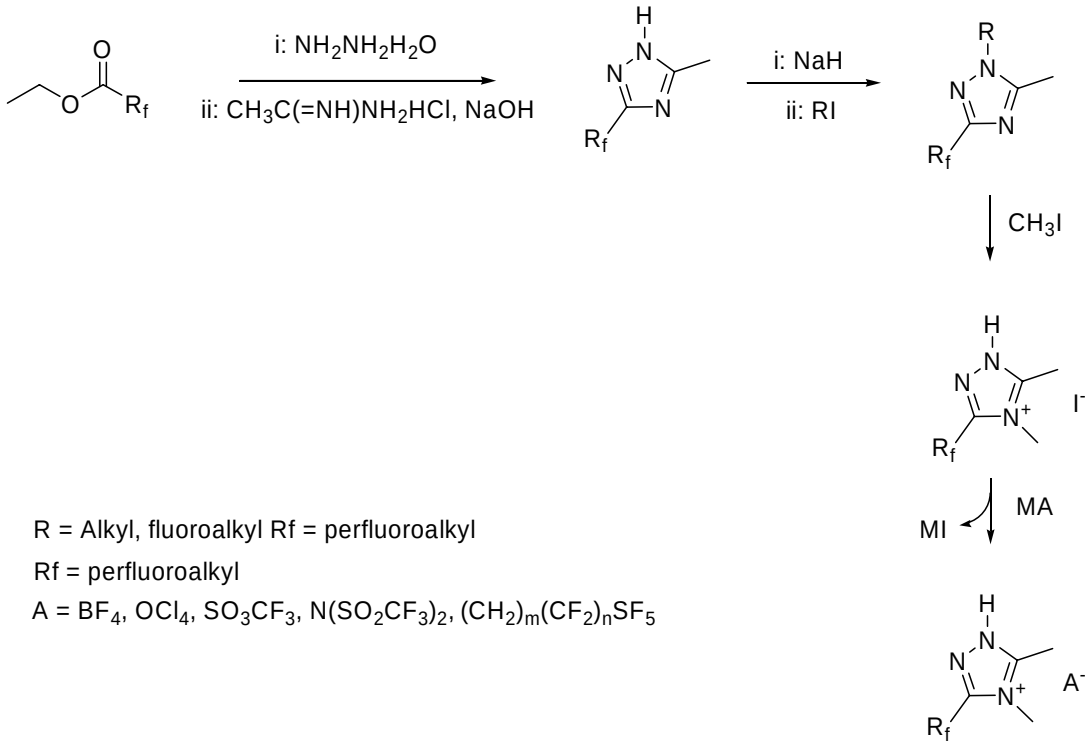

Scheme 1.9 Preparation of triazolium based functionalized ILs

Low melting N-4-functionalized-1-alkyl or polyfluoroalkyl-1,2,4-triazolium salts have also been prepared from zwiterions (Scheme 1.10). [43, 44]

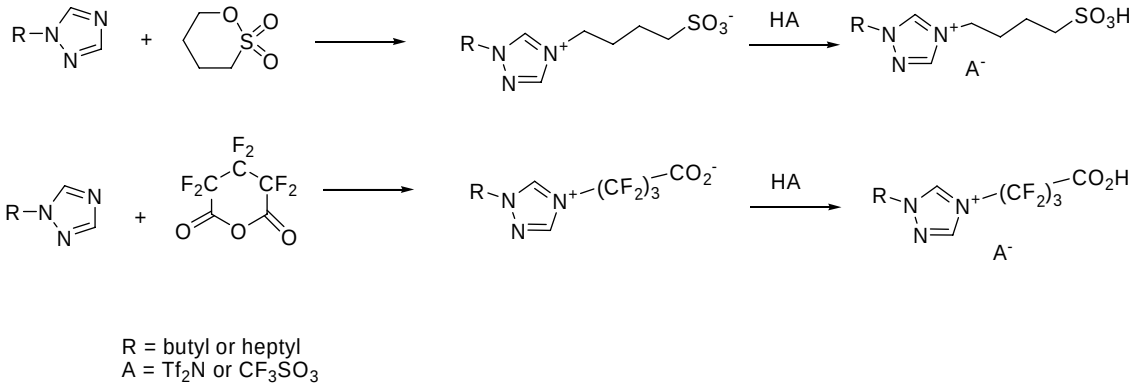

Scheme 1.10 Preparation of functionalized triazolium ILs

Low melting salts with alkyl, fluoroalkyl, alkyl ether, and fluoroalkyl ether oxazolidine and morpholine cations have been reported (Chart 1.8).[45]

Oxazolidine and morpholine based ionic liquids

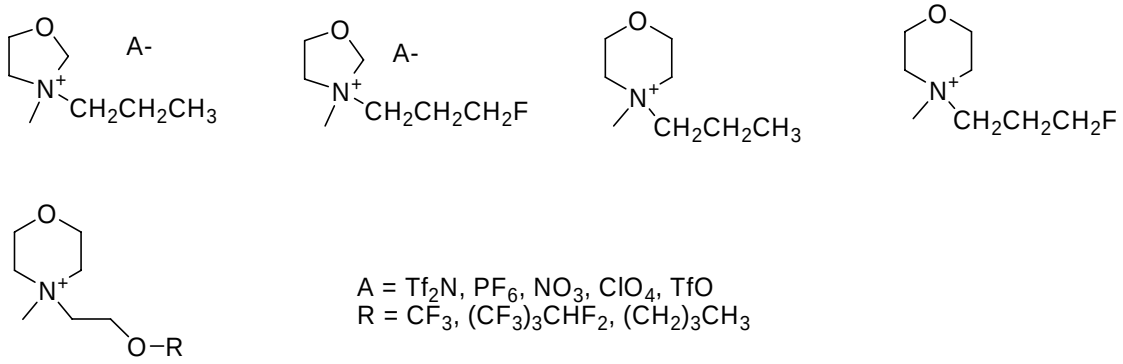

Triazine-based ionic liquids

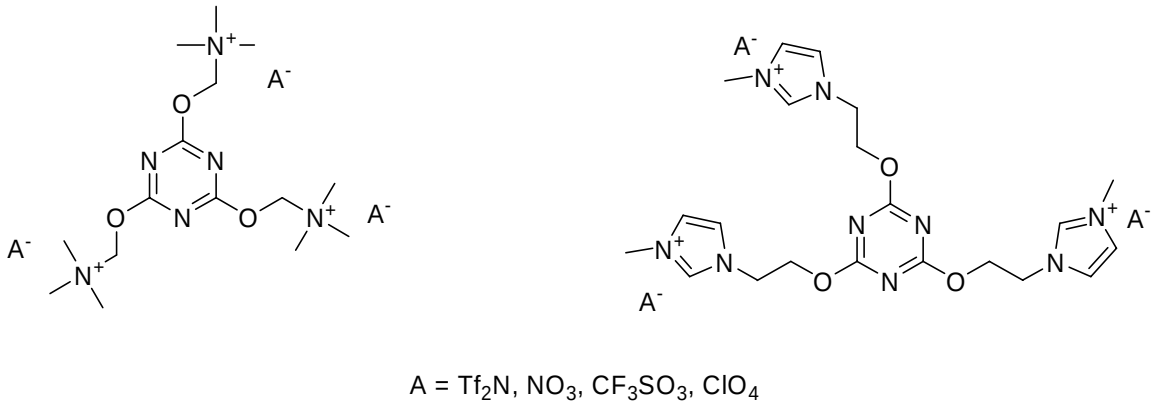

Chart 1.8 Oxazolidine, morpholine and triazine based ILs

Triazine-based polyfluorinated triquaternary liquid salts were also prepared and tested in hydrophormylation reactions (Chart 1.8).[46] Phosphazene-based ILs were also prepared and show application potentials as lubricant additives (Chart 1.9).[47]

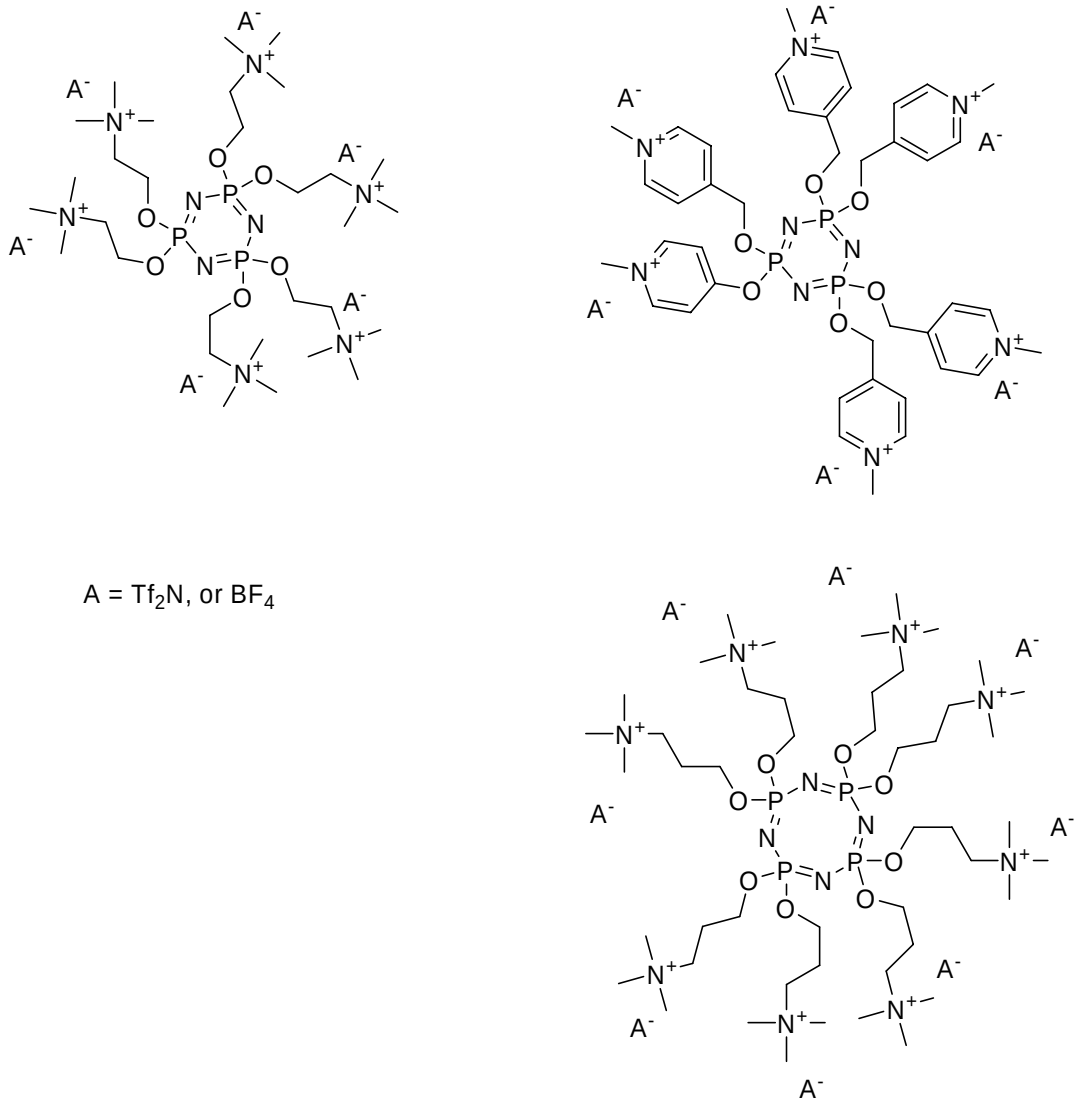

Chart 1.9 Phosphazene-based ILs

Quaternization of pyrazine, pyridazine, and pyrimidine with alkyl and polyfluoroalkyl halides to form low melting salts has also been reported.[48] Functionalized ammonium ILs, for example, ammonium salts with ether groups have been synthesized. All these quaternary ammonium salts exhibit improved cathodic and anodic stability, such as larger electrochemical window than that of the corresponding 1,3-dialkyimidazolium salts.[49] Quaternary trialkyl(polyfluoroalkyl)ammonium salts have been prepared and their physical properties were found to be mainly determined by the type of anion, regardless of substituents on the cation.[50] Low melting and low viscosity ILs prepared via protonation of trialkylamines by perfluoroalkyl β-diketones have been reported (Scheme 1.11).[51] The viscosities of this kind of IL, claimed by the authors, were as low as 3.4 cp.

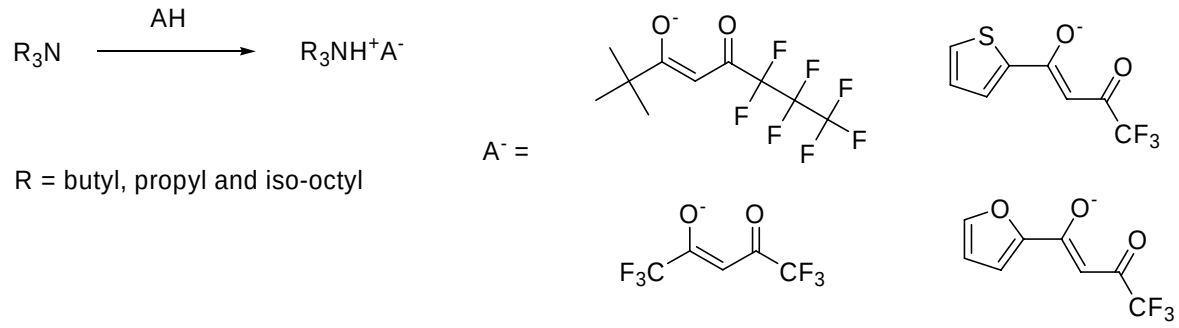

Scheme 1.11 Protonated ammonium ILs with perfluoroalkyl ß-diketonate anions

Pyrrolidinonium ILs, with the vinyl substituent, have been synthesized; their intended use is as liquid electrolytes.[52] Phosphonium ILs represent another important member in the IL family. These ILs have been used as media for degradation of phenol,[53] electrolytes for super capacitors,[54] and solvents for use in highly basic environments.[55]

1.4 References

[1] P. Walden, *Bull. Acad. Imp.Sci.* St. Petersbourg, **1914**, 1800.

[2] F. H. Hurley, P. Thomas, J. Wier, *J. Electrochem. Soc*. **1951**, *98*, 203.

[3] J. S. Wilkes, J. A. Levisky, R. A. Wilson, C. L. Hussey, *Inorg. Chem*. **1982**, *21*, 1263.

[4] For examples, see: (a) R. J. C. Brown, P. J. Dyson, D. J. Ellis, T. Welton, *Chem. Commun.* **2001**, 1862; (b) P. J. Dyson, J. S. McIndoe, D. Zhao, *Chem. Commun.* **2003**, 508; (c) A. S. Larsen, J. D. Holbrey, F. S. Tham, C. A. Reed, *J. Am. Chem. Soc.* **2000**, *122*, 7264. (d) Z.-B. Zhou, H. Matsumoto, K. Tatsumi, *Chem. Eur. J.* **2004**, *10*, 6581.

[5] A. Horváth, *Synthesis* **1995**, 1183.

[6] L. C. Branco, J. N. Rosa, R. J. J. Moura C. A. M. Alfonso, *Chem. Eur. J*. **2002**, *8*, 3671.

[7](a) J. Fraga-Dubreuil, J. P. Bazureau, *Tetrahedron Letters* **2001**, *42*, 6097; (b) J. D. Holbrey, W. M. Reichert, I. Tkatchenko, E. Bouajila, O. Walter, I. Tommasi, *Chem.Commun.* **2003**, 28.

[8] K.-S. Kim, D. Demberelnyamba, H. Lee, *Langmuir* **2004**, *20*, 556.

[9] H. Schottenberger, K. Wurst, U. E. I. Horvath, S. Cronje, J. Lukasser, J. Polin, J. M. McKenzie, H. G. Raubenheimer, *Dalton Trans.* **2003**, 4275.

[10] D. Zhao, Z. Fei, T. J. Geldbach, R. Scopelliti, G. Laurenczy, P. J. Dyson, *Helv. Chim. Acta* **2005**, *88*, 665.

[11] T. J. Geldbach, P. J. Dyson, *J. Am. Chem. Soc.* **2004**, *126*, 8114.

[12] T. L. Merrigan, E. D. Bates, S. C. Dorman, J. H. Davis Jr. *Chem. Commun.* **2000**, 2051.

[13] (a) R. P. Singh, S. Manandhar, J. M. Shreeve, *Synthesis* **2003**, *10*, 1579. (b) R. P. Singh, S. Manandhar, J. M. Shreeve, *Tetrahedron Lett.* **2002**, *43*, 9497.

[14] G. Song, Y. Cai, Y. Peng, *J. Combin. Chem.* **2005**, *7*, 561.

[15] K.-M. Lee, Y.-T. Lee, J. B. Lin, *J. Mater. Chem*. **2003**, *13*, 1079.

[16] D. J. Brauer, K. Kottsieper, C. Liek, O. Stelzer, H. Waffenschmidt, P. Wasserscheid, *J. Organomet. Chem.* **2001**, *630*, 177.

[17] A. E. Visser, R. P. Swatloski, W. M. Reichert, R. Mayton, S. Sheff, A. Wierzbicki, J. H. Davis Jr, R. D. Rogers, *Chem. Commun.* **2001**, 135.

[18] W. Bao, Z. Wang, Y. Li, *J. Org. Chem*. **2003**, *68*, 591.

[19] Z. Fei, D. Zhao, T. J. Geldbach, R. Scopelliti, P. J. Dyson, *Chem. Eur. J.* **2004**, *10*, 4886.

[20] H. Itoh, K. Naka, Y. Chujo, *J. Am. Chem. Soc.* **2004**, *126*, 3026.

[21] Z. Fei, D. Zhao, R. Scopelliti, P. J. Dyson, *Organometallics* **2004**, *23*, 1622.

[22] T. Mizumo, E. Marwanta, N. Matsumi, H. Ohno, *Chem. Lett.* **2004**, *33*, 1360.

[23] C. Ye, J. M. Shreeve, *J. Org. Chem*. **2004**, *69*, 8561.

[24] Z. Fei, D. Zhao, T. J. Geldbach, R. Scopelliti, P. J. Dyson, S. Antonijevic, G. Bodenhausen, *Angew. Chem. Int. Ed.* **2005**, *44*, 5720.

[25] C. P. Mehnert, *Chem. Eur. J.* **2005**, *11*, 50.

[26] M. H. Valkenberg, C. deCastro, W. F. Hçlderich, *Top. Catal.* **2001**, *14*, 139.

[27] A. C. Cole, J. L. Jensen, I. Ntai, K. L. Tran, K. J. Weaver, D. C. Forbes, J. H. Davis, Jr. *J. Am. Chem. Soc*. **2002**, *124*, 5962.

[28] S. T. Liddle, P. L. Arnold, *Organometallics* **2005**, *24*, 2597.

[29] (a) L. D. Field, B. A. Messerle, K. Q. Vuong, P. Turner, *Organometallics* **2005**, *24*, 4241; (b) W. A. Herrmann, C. Koecher, L. J. Goossen, G. R. J. Artus, *Chem. Eur. J.* **1996**, *2*, 1627.

[30] K. W. Kottsieper, O. Stelzer, P. Wasserscheid, *J. Mol. Catal. A. Chem.* **2001**, *175*, 285.

[31] Z. Mu, W. Liu, S. Zhang, F. Zhou, *Chem. Lett.* **2004**, *33*, 524.

[32] Y. Gao, B. Twamley, J. M. Shreeve, *Inorg. Chem*. **2004**, *43*, 3406.

[33] S. V. Dzyuba, R. A. Bartsch, *Chem. Commun*. **2001**, 1466.

[34] K. J. Harlow, A. F. Hill, T. Welton, *Synthesis* **1996**, 697.

[35] M. J. Muldoon, C. M. Gordon, I. R. Dunkin, *J. Chem. Soc., Perkin Trans.* **2001**, *2*, 433.

[36] V. Gallo, P. Mastrorilli, C. F. Nobile, G. Romanazzi, G. P. Suranna, *J. Chem. Soc., Dalton Trans*. **2002**, 4339.

[37] P. J. Dyson, D. J. Ellis, W. Henderson, G. Laurenczy, *Adv. Syn. Catal*. **2003**, *345*, 216.

[38] Z.-B. Zhou, M. Takeda, M. Ue, *J. Flourine. Chem.*, **2004**, *125*, 471.

[39] (a) S. Mori, K. Ida, M. Ue, *US Patent 4892944,* **1990**; (b) A. C. Cole, J. L. Jensen, I. Ntai, K. L. T. Tran, K. J. Weaver, D. C. Forbes, J. H. Davis, Jr. *J. Am. Chem. Soc*. **2002**, *124*, 5962.

[40] D. Zhao, Z. Fei, T. Geldbach, R. Scopelletti, P. J. Dyson, *J. Am. Chem. Soc*. **2004**, *126*, 15876.

[41] R. P. Singh, R. W. Winter, G. L. Gard, Y. Gao, J. M. Shreeve, *Inorg. Chem*. **2003**, *42*, 6142.

[42] H. Xue, B. Twamley, J. M. Shreeve, *J. Org. Chem*. **2004**, *69*, 1397.

[43] Y. R. Mirzaei, J. M. Shreeve, *Synthesis* **2003**, *1*, 24.

[44] Y. R. Mirzaei, H. Xue, J. M. Shreeve, *Inorg. Chem.* **2004**, *43*, 361.

[45] J. Kim, R. P. Singh, J. M. Shreeve, *Inorg. Chem*. **2004**, *43*, 2960.

[46] B. A. Omotowa, J. M. Shreeve, *Organometallics* **2004**, *23*, 783.

[47] B. A. Omotowa, B. S. Phillips, J. S. Zabinski, J. M. Shreeve, *Inorg. Chem*. **2004**, *43*, 5466.

[48] Y. Gao, J. M. Shreeve, *Synthesis* **2004**, *7*, 1072.

[49] Z.-B. Zhou, H. Matsumoto, K. Tatsumi, *Chem. Lett*. **2004**, 886.

[50] O. D. Gupta, P. D. Armstrong, J. M. Shreeve, *Tetrahedron Lett.* **2003**, *44*, 9367.

[51] O. D. Gupta, B. Twamley, J. M. Shreeve, *Tetrahedron Lett.* **2004**, *45*, 1733.

[52] D. Demberelnyamba, B. K. Shin, H. Lee, *Chem. Commun.* **2002**, 1538.

[53] M. D. Baumann, A. J. Daugulis, P. G. Jessop, *Appl. Micro. Biotech*. **2005**, *67*, 131.

[54] E. Frackowiak, G. Lota, J. Pernak, *Appl. Phys. Lett.* **2005**, *86*, 164104.

[55] T. Ramnial, D. D. Ino, J. A. C. Clyburne, *Chem. Commun.* **2005**, *3*, 325.

2

Synthesis and Characterization of Imidazolium ILs Incorporating the Nitrile Functionality

2.1 Introduction

If ILs are to be used to immobilize catalysts in multiphasic reactions, then the design and synthesis of F-ILs could be extremely important. Many different reactions have been catalyzed using ILs as immobilization solvents including hydrogenation,[1] hydroformylation [2] and C-C coupling reactions.[3] While the non-nucleophilic nature of many ILs seems to be advantageous, providing a protective environment for the catalyst which can extend its lifetime, it has also emerged that ILs that incorporate a coordination centre might be extremely useful, such that the IL serves as both immobilization solvent and ligand to the catalyst. Wasserscheid *et al* first described this concept by introducing a diphenylphosphine group at the 2-position of an imidazolium cation.[4] However, the resulting salt is a not a room temperature IL and must therefore be dissolved in another IL for effective use in biphasic catalysis.[5] The ligand, by virtue of being a salt, is highly soluble in ILs and is strongly retained during product extraction. Groups such as NH_2 and OH have also been successfully introduced into the imidazolium cation moieties, but their ability to coordinate to transition metals to give catalytically useful complexes is somewhat limited. More sophisticated functional groups such as thioureas and thioethers have been tethered to imidazolium based ILs and they have been shown to extract toxic metal ions from aqueous solution.[9]

This chapter describes the synthesis and characterization of imidazolium salts in which a nitrile group is attached to the alkyl side chain (single-armed as well as double-armed). The nitrile group was chosen as it is a promising donor to main group metals such as lithium and potassium, and transition metals such as palladium and platinum. The physicochemical properties of these new ILs will be described and it will be shown how the length of the alkyl unit linking the imidazolium ring to the CN group influences the melting point of the IL.

2.2 Results and Discussion

2.2.1 Single armed imidazolium ILs bearing nitrile functionality

The synthetic route used to prepare 1-alkylnitrile-3-methylimidazolium and 1-alkylnitrile-2,3-dimethylimidazolium salts is depicted in Scheme 2.1. The imidazolium chlorides $[C_nCNmim]Cl$ ($C_n = (CH_2)_n$, n = 1 **1a**, n = 2 **2a**, n = 3 **3a** and n = 4 **4a**) are prepared in high yield from 1-methylimidazole and the appropriate chloroalkyl nitrile $Cl(CH_2)_nCN$ in a modification to the

literature procedure for the related 1-alkyl-3-methylimidazolium chlorides.[6] The 1-alkylnitrile-2,3-dimethylimidazolium salt [C_3CNdimim]Cl **5a** is prepared similarly from 1,2-dimethylimidazole and $Cl(CH_2)_3CN$. The synthesis of **1a** has been described previously using a somewhat more complicated method.[7] The relatively strong electron withdrawing effect of the nitrile group activates chloromethylacetonitrile, $ClCH_2CN$, to such an extent that it reacts smoothly with 1-methylimidazole in the absence of solvent to give **1a**. However, as the alkyl chain in the chloroalkyl nitrile $Cl(CH_2)_nCN$ precursor increases in length, the temperature required to complete the reaction also increases.

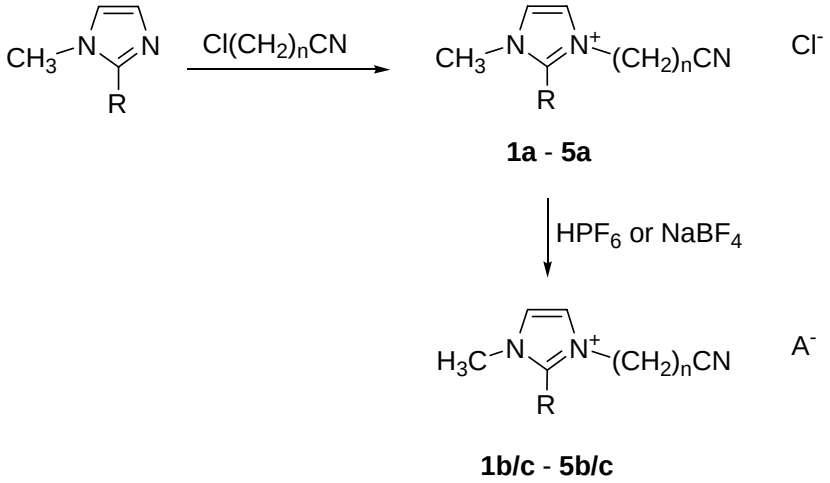

Scheme 2.1 Synthesis of ILs 1 – 5: **1a** n = 1, R = H; **2a** n = 2, R = H; **3a** n = 3, R = H; **4a** n = 4, R = H; **5a** n = 3, R = CH_3; **1b** n = 1, R = H, A = PF_6; **1c** n = 1, R = H, A = BF_4; **2b** n = 2, R = H, A = PF_6; **2c** n = 2, R = H, A = BF_4; **3b** n = 3, R = H, A = PF_6; **3c** n = 3, R = H, A = BF_4; **4b** n = 4, R = H, A = PF_6; **4c** n = 4, R = H, A = BF_4; **5b** n = 3, R = CH_3, A = PF_6; **5c** n = 3, R = CH_3, A = BF_4.

Reaction of **1a** – **4a** with a molecular equivalent of HPF_6 or $NaBF_4$ affords the imidazolium salts [C_nCNmim][PF_6] (n = 1 – 4) **1b** – **4b** and [C_nCNmim][BF_4] (n = 1 – 4) **1c** – **4c**, respectively. The imidazolium salts [C_3CNdimim][PF_6] **5b** and [C_3CNdimim][BF_4] **5c** are prepared from **5a** using an analogous method. For **1b** – **5b** the salts were washed with water in order to remove the hydrogen chloride formed during the anion exchange reaction, whereas THF and diethyl ether were used to wash **1c** – **5c**. The salts were then dried under vacuum for 1 – 2 days. The salts **2c**, **3c**, **4a**, **4b** and **3c** are liquid at room temperature and were further purified by filtration through silica and left under vacuum at 40 – 50°C for several days. All the imidazolium salts were obtained in medium to high yield. They are stable in air and showed no signs of decomposition up to 150°C.

The imidazolium salts were characterized using IR, ^{1}H and ^{13}C NMR spectroscopy, electrospray ionization mass spectrometry (ESI-MS) and elemental analysis. Electrospray ionization mass spectrometry was used to characterize the imidazolium cations diluted in methanol and in all cases strong peaks indicative of the parent ion were observed. The main feature in the IR spectra is the characteristic C≡N vibrations. The C≡N vibrations decrease in wave number as the length of the alkyl chain increases, i.e. from 2261 cm^{-1} in **1a** to 2241 cm^{-1} in **4a**, with similar trends for the other salts such that **1** >> **2** > **3** ≈ **4** ≈ **5**. The IR spectra exhibit C-H bond stretches between 3150-2950 cm^{-1} and weaker C-H bond stretches between 2850-2460 cm^{-1}, possibly arising from the formation of hydrogen bonds with the anion. The most noteworthy feature of the ^{1}H NMR spectra of the imidazolium salts is the characteristic resonance for the acidic proton in the 2-position.[8] In compounds **1** – **4** this proton is observed between 9.99 ppm (for **4a**) and 8.45 ppm (for **4b**), but no clear trends are present. It is noteworthy that H-D exchange takes place at the acidic 2-position in all the ILs described, and is fastest for **1a** where the alkyl chain is shortest and the protons interact most strongly with the anion (see below). The alkyl protons adjacent to the nitrile group also exchange with deuterium in **1a**, but at a considerably slower rate.

2.2.1.1 Structural characterisation of 1a, 3a, 3b and 5b in the solid state

Crystals suitable for analysis by single crystal X-ray diffraction were obtained from acetonitrile-diethyl ether solutions at -20°C. Structural details for the compounds are listed in Table 2.1 and the structures of **1a**, **3a**, **3b** and **5b** are illustrated in Figures 2.1 – 2.4, respectively, with key bond parameters are listed in Table 2.2 for comparison purposes.

Table 2.1 Crystal Data and Details of the Structure Determination for: 1a, 3a, 3b and 5b.

	1a	**3a**	**3b**	**5b**
Chemical formula	$C_6H_8ClN_3$	$C_8H_{12}ClN_3$	$C_8H_{12}F_6N_3P$	$C_9H_{14}F_6N_3P$
Formula weight	157.60	185.66	295.18	309.20
Crystal system	Orthorhombic	Monoclinic	Triclinic	Triclinic
Space group	*Pnma*	$P2_1/c$	*P*-1	*P*-1
a (Å)	15.0177(17)	8.737(3)	8.022(4)	8.6472(17)
b (Å)	6.2979(7)	11.015(3)	8.161(5)	8.9312(13)
c (Å)	7.8712(5)	10.4099(13)	9.460(2)	9.616(2)
α (°)	90	90	88.12(3)	74.891(15)
β (°)	90	102.503(18)	87.01(3)	65.92(2)
γ (°)	90	90	74.95(5)	78.351(14)
Volume (Å^3)	744.46(13)	978.1(4)	597.1(5)	650.7(2)
Z	4	4	2	2
D_{calc} (g cm^{-3})	1.406	1.261	1.642	1.578
F(000)	328	392	300	316
μ (mm^{-1})	0.436	0.342	0.294	0.274
Temp (K)	140	140	140	140
Wavelength (Å)	0.71073	0.71070	0.71070	0.71073
Measured reflections	4173	5812	3890	3818
Unique reflections	689	1720	1985	2017
Unique reflections [$I > 2\sigma(I)$]	616	1569	1362	1663
Data / parameters	689 / 61	1720 / 110	1985 / 164	2017 / 173
R^a [$I > 2\sigma(I)$]	0.0273	0.0525	0.0579	0.0501
wR2^a (all data)	0.0753	0.1259	0.1794	0.1467
GoF^b	1.084	1.146	0.990	1.054

^{a} $R = \Sigma| |F_o| - |F_c| |/\Sigma|F_o|$, $wR2 = \{\Sigma[w(F_o^2-F_c^2)^2]/\Sigma[w(F_o^2)^2]\}^{1/2}$; ^{b} GoF $= \{\Sigma[w(F_o^2-F_c^2)^2]/(n-p)\}^{1/2}$ where *n* is the number of data and *p* is the number of parameters refined.

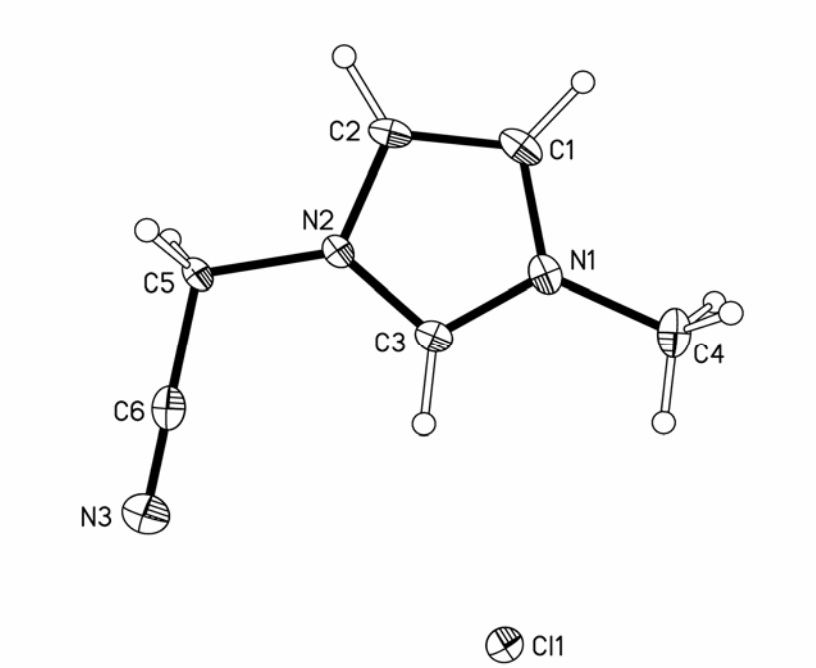

Figure 2.1 Ortep representation of the crystal structure of 1a, ellipsoids are drawn at the 50% probability level.

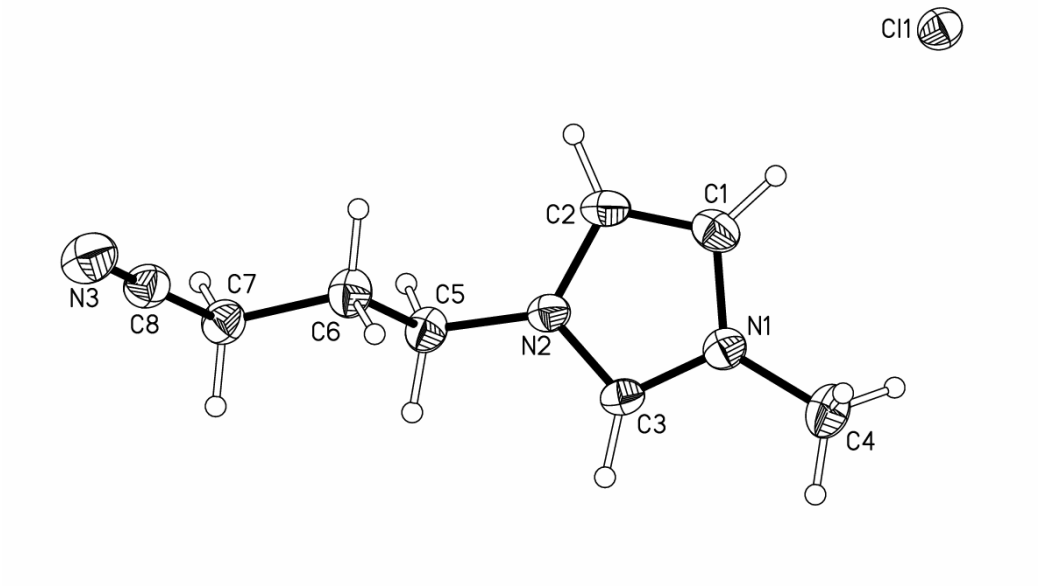

Figure 2.2 Ortep representation of the crystal structure of 3a, ellipsoids are drawn at the 50% probability level.

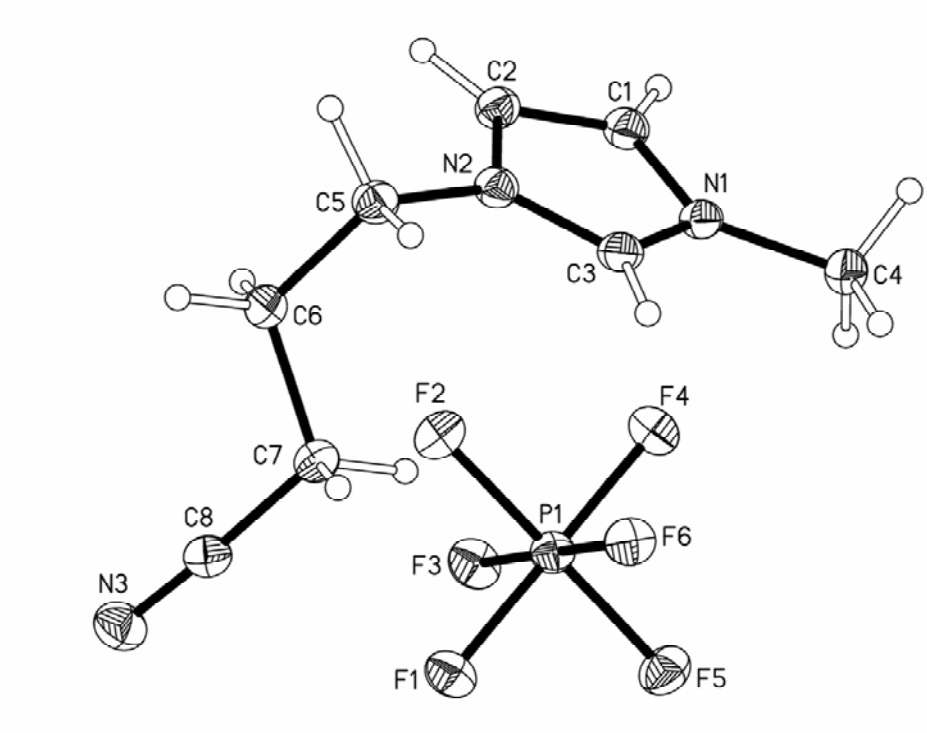

Figure 2.3 Ortep representation of the crystal structure of 3b, ellipsoids are drawn at the 50% probability level.

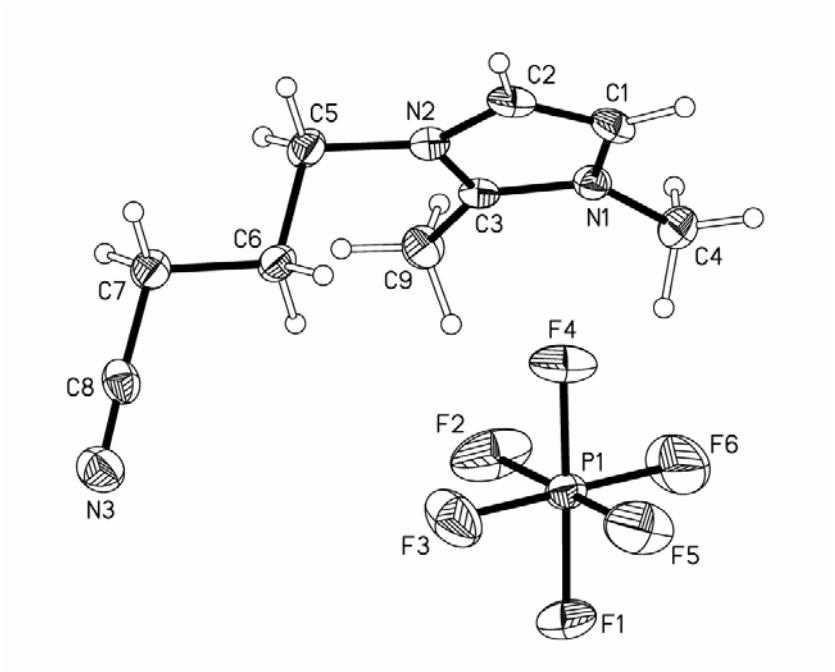

Figure 2.4 Ortep representation of the crystal structure of 5b, ellipsoids are drawn at the 50% probability level.

Table 2.2 Selected bond length (Å) for 1a, 3a, 3b and 5b.

	1a	**3a**	**3b**	**5b**
N1-C1	1.384(3)	1.377(2)	1.377(4)	1.392(3)
C1-C2	1.361(3)	1.349(3)	1.350(5)	1.349(3)
C2-N2	1.377(3)	1.379(2)	1.392(5)	1.387(3)
N2-C3	1.348(3)	1.334(2)	1.320(4)	1.356(3)
C3-N1	1.336(3)	1.331(2)	1.322(5)	1.358(3)
N1-C4	1.478(3)	1.462(2)	1.470(4)	1.473(3)
N2-C5	1.477(3)	1.461(2)	1.469(5)	1.486(3)

In the solid state structures of **1a**, **3a**, **3b** and **5b** the parameters of the atoms in the side-chains are generally very close despite the differences of their lengths and the presence of different anions. The C≡N bond lengths are also essentially the same [1.139(5) - 1.149(3) Å] in the four compounds. The imidazolium rings are all planar, however, slight differences between the imidazolium rings can be appreciated by a comparison of **1a** with **3a**. The distances of the N2-C5 and N2-C3 bonds in **1a** [1.477(3) Å and 1.348(3) Å] are both slightly longer than in **3a** [1.461(2) Å and 1.334(2) Å]. More significant is the difference of the C=C bond lengths. In **1a**, the value is 1.361(3) Å, while in **3a** the value of 1.348(3) Å – remarkably shorter! The N2-C2 distance in **3a** [1.379(2) Å] is significantly shorter than in **3b** [1.392(5) Å], while the N2-C3 bond in **3a** [1.334(2) Å] is significant longer than in **3b** [1.320(4) Å]. Slight changes in **5b** at the C3 position, compared to **3a** and **3b** [mean 1.36 Å *versus* 1.33 and 1.32] may be attributed to the presence of the methyl group in **5b**, both the N1-C3 and N2-C3 distances are longer than in **3a** and **3b**, and as a result, **5b** shows the smallest N1-C3-N2 angle [**3a**, 108.19(15)°; **3b**, 109.9(3)°; **5b**, 106.5(2)°].

It is possible that the slight differences in the molecular geometry is caused by the different hydrogen bond networks arising from the different anions and different side-chains. Hydrogen bonds in imidazolium salts have been a focus of many reports including NMR studies [9] and single crystal X-ray analysis.[10] Hydrogen bonds between the hydrogen bond acceptor usually from the counter anions and the H atoms in the imidazolium ring are the most frequently observed interactions, and in most cases they are the strongest. However, the strength of the hydrogen bond is largely dependent on the nature of the counter anion. In many cases, only small variation in the

molecular structure will give rise to significant changes in the crystal structure.[11] The introduction of the CN group in the side chain of the IL completely changes the architecture of the hydrogen bonding network. For **1a**, **3a** and **3b** the hydrogen atom at the 2-position of the imidazolium ring form one of the strongest (shortest) C-H…X (X = Cl, F) hydrogen bond which occur in the solid state [**1a**, H3…Cl1, 2.49 Å; **3a**, H3…Cl1, 2.71 Å; **3b**, H3…F1, 2.43 Å]. Other weaker (longer) C-H…X interactions involve the remaining hydrogens of the imidazolium and the methylene hydrogens of the side-chains. Interactions between the π-system and the anions also appear to be important in certain structures (see Figure 2.5). In the case of compound **3a** the chloride anion is surrounded by hydrogens and it does not interact with the π-system of the imidazolium ring; instead, it interacts with the nitrile group [3.102 Å]. However, in **3b** and **5b** the larger hexafluorophosphate interacts with the π-system [**3b**, F2…ring, 3.297 Å; **5b**, F4…ring, 3.131 Å]. This may explain why in these two cases no interactions occur with the terminal CN group. If the side-chain is smaller as in **1a** CN moieties may have weak hydrogen bond interactions [H2…N3, 2.56 Å]. Presumably the interaction of the π-system with the anion is weaker than conventional hydrogen bonds, and since it reduces the number of hydrogen bonds between the anion and cation the melting point is also lowered.

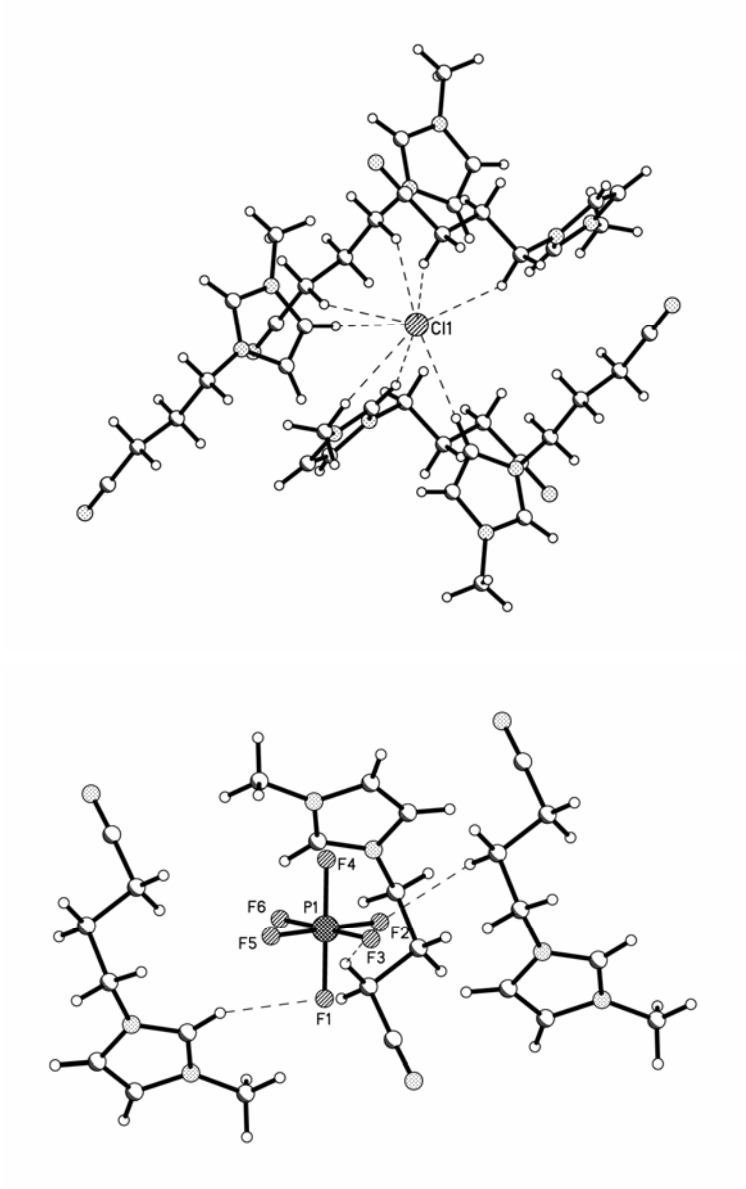

Figure 2.5 Anion-cation interactions for (top) 3a and (bottom) 3b showing the C-H…X interactions around the two different anions.

2.2.1.2 Physical properties of the ILs

The relationship between molecular structure and melting point of ILs has been investigated previously,[12] and from a theoretical perspective, the melting point is determined by the strength of a crystal lattice, which in turn, is controlled by three main factors, viz. intermolecular forces, molecular symmetry, and the conformational degrees of the freedom of a molecule.[13] Unlike hydrogen bond-free molecules, of which the melting points are somewhat predictable using different approaches,[14] the melting points of imidazolium salts are more complicated and less predictable. It was suggested that packing efficiency and disorder are key factors in keeping some

imidazolium salts as low temperature liquids.[15] However, the exact reason why many imidazolium salts are low melting liquids remains unknown, and only slight variations in the molecular structure may result in very different crystal structures, which in turn leads to very different physical properties.

A graph showing how the melting points of compounds **1 – 4** vary is presented in Figure 2.6. Of the 15 nitrile functionalised imidazolium salts reported, only four salts have melting points above 100°C, which by the most widely used definition do not constitute ILs.[1c] The salts **2c**, **3c**, **4a**, **4b** and **3c** are liquid around room temperature and of these three have very low melting points (-60°C and below). From Figure 2.6 it is clear that both the anion and the cation significantly influences the melting point of the imidazolium salt. For each cation, the melting point follows the trend Cl > PF_6 > BF_4, which is in keeping with related salts with alkyl-substituted imidazolium cations.

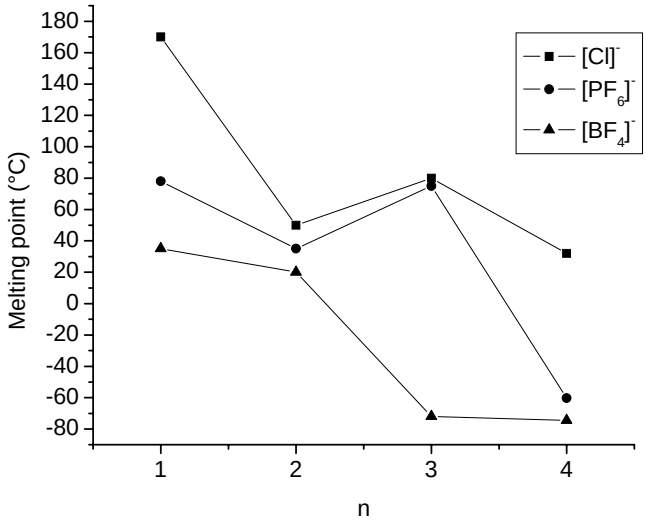

Figure 2.6: Melting point data for 1 – 4

From Figure 2.6 it is also clear that the length of the alkyl group also strongly influences the melting point, with the longer more flexible groups resulting in lower the melting points. Again, such a trend has been observed previously with related salts, although as the alkyl chain increases beyond a certain length the melting point begins to increase.[16] Both **3b** and **3c** have higher melting points than the unfunctionalized analogues [C_4mim][PF_6] and [C_4mim][BF_4] (C_4mim = 1-butyl-3-methylimidazolium). The increased melting point could be due to the more rigid nature of the cation imposed by the CN group and/or due to the possibility of increased H-bonding interactions (see

above). In general, replacement of the proton in the 2-positon by a methyl group increases the melting point of the salt,[37] and as expected, [C_3CNdimim]Cl **5a** has a higher melting point than [C_3CNmim]Cl **3a** (105 *versus* 80°C).

The density, viscosity and solubility data of the five salts that are liquid at ambient temperature are listed in Table 2.3 together with the related data for [C_4mim][PF_6] and [C_4mim][BF_4] for comparison purposes.

Table 2.3 Density, viscosity and solubility data of the room temperature ILs.

Ionic Liquid	Density[a] ($g.ml^{-1}$)	Viscosity[b] (mpa.s)	Solubility in common solvents				
			H_2O	Et_2O	EtOH	Acetone	Hexane
[C_2CNmim][BF_4] **2c**	2.15	65.5	miscible	immiscible	miscible	miscible	immiscible
[C_3CNmim][BF_4] **3c**	1.87	230	miscible	immiscible	immiscible	miscible	immiscible
[C_4CNmim][Cl] **4a**	1.61	5222	miscible	immiscible	miscible	immiscible	immiscible
[C_4CNmim][PF_6] **4b**	1.99	2181	partly miscible	immiscible	immiscible	miscible	immiscible
[C_4CNmim][BF_4] **4c**	1.71	552.9	miscible	immiscible	immiscible	miscible	immiscible
[C_4mim][PF_6]	1.37	320.3[c]	partly miscible	immiscible	partly miscible	miscible	immiscible
[C_4mim][BF_4]	1.14	115.2[d]	miscible	immiscible	immiscible	miscible	immiscible

a. Determined at 20°C.

b. Determined at 25°C.

c. Literature values 308.3 (at 20°C) [28] and 371.0 (at 20°C).[12]

d. Literature values 154.0 (at 20°C) [28] and 104.9 (at 20°C).[12]

The density of the nitrile functionalized IL deceases as the alkyl chain increases in length. For example, a comparison of the densities of the tetrafluoroborate salts shows a decrease in the order **2c** (2.15 $g.ml^{-1}$) > **3c** (1.87 $g.ml^{-1}$) > **4c** (1.71 $g.ml^{-1}$). In all cases the densities of the alkylnitrile ILs are higher than those of the non-functionalized analogues. Incorporation of the nitrile group serves to increase the density of the IL, which may result in improved separation with other solvents when used in biphasic catalysis.

It has been shown that the viscosity of imidazolium salts is influenced by their hydrogen bonding ability and by the strength of their van der Waals interactions, which in turn is strongly dependent of the type of anion present.[17] The viscosity of the ILs varies considerably, and while it is not easy to draw any firm conclusions, it would appear from the three tetrafluoroborate salts examined, that there is a steady increase in viscosity with the length of the alkyl chain, presumably as a result of the increased van der Waals interactions.

The solubility data of the new ILs is similar to that of the related non-functionalized ILs $[C_4mim][PF_6]$ and $[C_4mim][BF_4]$ (see Table 2.3). The new ILs are immiscible with non-polar solvents, such as diethyl ether and hexane, whereas with polar solvents such as ethanol and acetone, the solubility depends upon the anion as has been described elsewhere.

2.2.2 Double armed imidazolium ILs bearing nitrile functionality

A series of imidazolium salts incorporating the nitrile group on both arms of imidazolium cation, namely "double-armed" nitrile-functionalized ILs (shown as **6 — 8** in Scheme 2.2) have been also prepared.

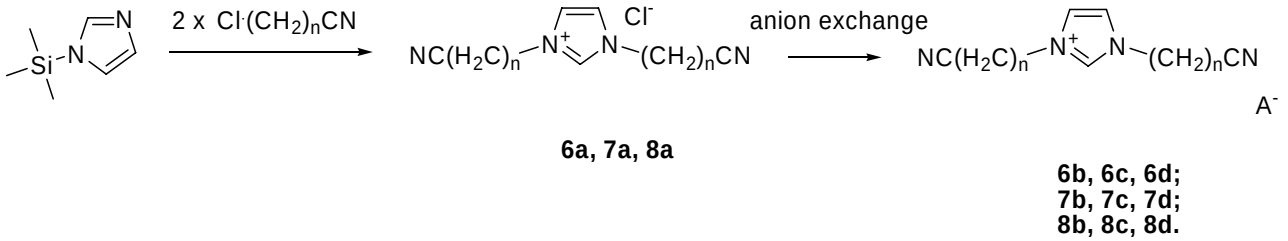

Scheme 2.2 Synthesis of ILs 6 – 8: **6a** n = 1; **7a** n = 3; **8a** n = 4; **6b** n = 1, A = PF_6; **6c** n = 1, A = BF_4; **6d** n = 2, A = Tf_2N; **7b** n = 3, A = PF_6; **7c** n = 3, A = BF_4; **7d** n = 3, A = Tf_2N; **8b** n = 4, A = PF_6; **8c** n = 4, A = BF_4; **8d** n = 4, A = Tf_2N.

Ionic liquids **6 — 8** were prepared from the direct reaction of trimethylsilyimidazole with 1-chloroalkylnitriles. Salts **6a** $[(CCN)_2im]Cl$ ($[(CCN)_2im]$ = 1,3-di-methylnitrile-imidazolium) and **7a** $[(C_3CN)_2im]Cl$ ($[(C_3CN)_2im]$ = 1,3-di-butyllnitrile-imidazolium) are solids whereas **8a** $[(C_4CN)_2im]Cl$ ($[(C_3CN)_2im]$ = 1,3-di-pentylnitrile-imidazolium) is a light brown viscous liquid.

The chloride anion has been exchanged for other anions by reaction with HPF_6, $NaBF_4$ or Lithium bis(trifluoromethylsulfonyl)amide ($Li[Tf_2N]$) affording $[(C_nCN)_2im][PF_6]$ (n = 1, 3 and 4) **6b - 8b**, $[(C_nCN)_2im][BF_4]$ (n = 1, 3 and 4) **6c - 8c** and $[(C_nCN)_2im][Tf_2N]$ (n = 1, 3 and 4) **6d - 8d** respectively. For the hydrophobic ILs, i. e. those with $[PF_6]^-$ and $[Tf_2N]^-$ anions, the salts were washed with water in order to remove the hydrogen chloride or lithium chloride formed during the anion exchange reaction. The tetrafluoroborate salts were washed with THF and diethyl ether in order to remove impurities. The salts were then dried under vacuum for 1 - 2 days. Salts **6d**, **7c**, **7d**, **8c** and **8d** are liquid at room temperature and were dried further under vacuum at 40 - 50 °C for several days. All the imidazolium salts were obtained in medium to high yields; and they are stable in air without showing any signs of decomposition at temperatures up to 150 °C.

All the imidazolium salts were characterized using electrospray ionization mass spectrometry (ESI-MS), IR, ^1H and ^{13}C NMR spectroscopy, and elemental analysis. EI-MS was used to characterize the imidazolium cations and anions following dilution in methanol or water using conditions described previously.[18] In all cases strong peaks indicative of the parent cation and anion were observed. Anion-cation aggregation can be observed when the IL sample is diluted only moderately, whereas at low concentration only the isolated parent ions are observed. The C≡N vibration in the IR spectra of **6 - 8** increase in wavenumber as the length of the alkyl chain decreases, i.e., from 2245 cm^{-1} in **8a** to 2263 cm^{-1} in **6a**. Similar trends are observed for the other salts with $[BF_4]^-$, $[PF_6]^-$ and $[Tf_2N]^-$ anions. The ^1H NMR spectra of **6 — 8** exhibit the characteristic resonance at high field due to the acidic proton in the 2-position of imidazolium ring. The proton is easily exchanged by deuterium since the spectra are recorded in D_2O. The rate of exchange is fastest for **6a,** in which the alkyl chain is the shortest, and hence the proton most acidic due to the electron withdrawing effect of the nitrile-functionality. Similar trends were described for the "single-armed" nitrile functionalized ILs.

Of the twelve "double-armed" nitrile-functionalized imidazolium salts reported herein, eight salts have melting points below 100 °C. Salts **7c**, **7d**, **8a**, **8b**, **8c** and **8d** are liquids around room temperature, with both the anion and the cation significantly influencing the melting point of the imidazolium salt. In general, it appears that as the length of the alkyl chain between the imidazolium cation and nitrile functionality increases, the melting point decreases. In comparison to

the single-armed nitrile-functionalized ILs, of which their melting points follow the trend Cl^- > $[PF_6]^-$ > $[BF_4]^-$, which is also typical of salts with alkyl-substituted imidazolium cations, the "double-armed" nitrile functionalized ILs of **3** series show a different trend, *viz*. $[PF_6]^-$ > Cl^- > $[BF_4]^-$.

The viscosities of the liquid samples of **6 — 7** have also been determined and show the following trend Cl^- > $[PF_6]^-$ > $[BF_4]^-$ > $[Tf_2N]^-$. Moreover, the "double-armed" nitrile functionalized ILs have much higher viscosities compared with the "single-armed" salts.

2.2.2.1 Solid state structures of 6a, 6b, 6c, 7a and 7b

Single crystals of **6a-6c**, **7a** and **7b** were obtained from acetonitrile solutions following slow diffusion of diethyl ether, and their molecular structures have been determined by X-ray diffraction methods. The structures of **6c** and **7b** are depicted in Figure 2.7 and Figure 2.8, respectively, and key bond lengths and angles for all five structures are listed in Table 2.4. All are very similar and differ mainly with respect to the orientation of the nitrile-chain relative to the imidazolium ring, as shown in Figure 2.9. In all five structures, the imidazolium ring is almost perfectly planar, bond angles in the rings range from 106.3(5) to 109.8(2) and distances from 1.313(7) to 1.406(6) Å. The -CH_2-C≡N moiety is essentially linear with the C≡N distance, 1.129(5) to 1.171(7) Å being found in the expected range.[19] In **6a**, one -CH_2-C≡N is parallel, the other perpendicular relative to the plane of the imidazolium ring, while in **6b** and **6c**, both nitriles moieties are perpendicular, pointing in opposite directions. In **7a**, both nitriles groups are perpendicular with respect to the imidazolium ring, pointing in the same direction, whereas in **7b**, both nitriles moieties are parallel, but on different sides relative to the plane of the imidazolium ring.

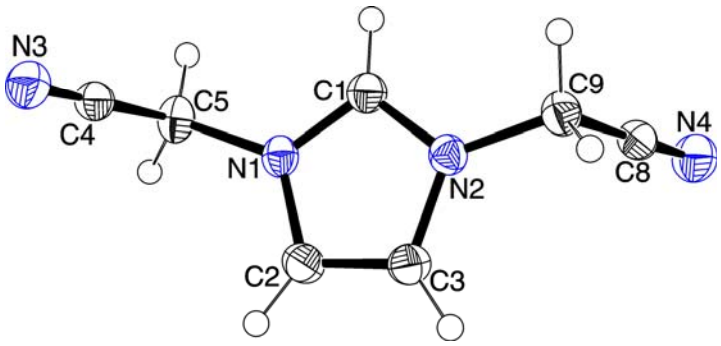

Figure 2.7 ORTEP-plot of the cationic part of 6c, ellipsoids are drawn at the 50% probability level

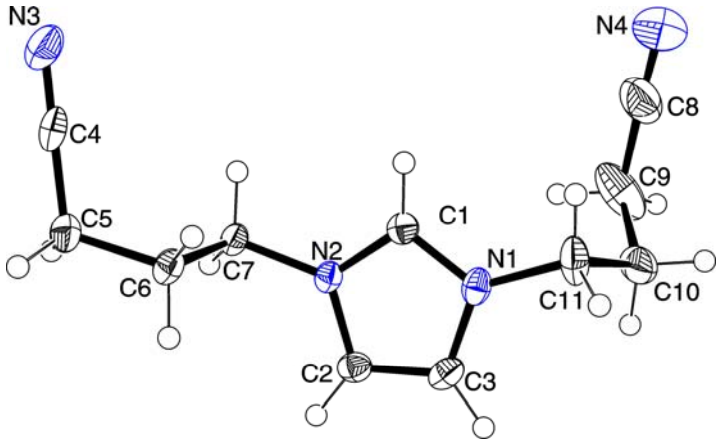

Figure 2.8 ORTEP-plot of the cationic part of 7b, ellipsoids are drawn at the 50% probability level

These crystal packing effects are probably triggered by the different hydrogen-bond accepting properties of the three different anions. There is extensive hydrogen bonding in all structures and is interesting to note that, in agreement with the observed melting points, much stronger hydrogen bond are found in the $[PF_6]^-$ salts **6b** and **7b** than in the corresponding chloride salts. In **6a** there are four hydrogen contacts to the chloride below 3 Å, ranging from 2.535 to 2.907 Å while there are 13 hydrogen contacts to the fluoride atoms below 3 Å in **6b**, ranging from 2.280 to 2.903 Å. Clearly, the correlation of melting point to the number and distance of H···X bonds alone has its limitations as otherwise one would also expect a higher melting point for the $[BF_4]^-$ derivative **6c**, as in this case, more and shorter hydrogen bonds are observed (11 contacts from 2.322 to 2.806) than in **6a**.

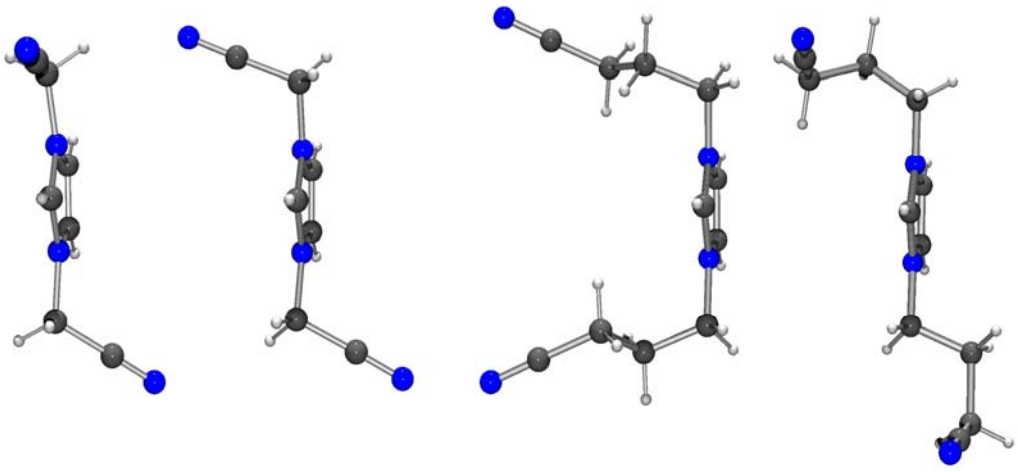

Figure 2.9 Ball-and-stick representation of 6a, 6b, 7a and 7b, showing the different orientation of the alkyl chains in the crystal lattice.

Table 2.4 Selected bond lengths (Å) and angles (°) for compounds 6a, 6b, 6c, 7a and 7b

	6a	**6b**	**6c**	**7a**	**7b**
C1-N1	1.337(8)	1.327(4)	1.333(2)	1.313(7)	1.335(3)
C1-N2	1.337(8)	1.340(4)	1.330(2)	1.337(7)	1.331(3)
C2-N1	1.401(8)	1.384(4)	1.380(2)	1.406(6)	1.374(3)
C3-N2	1.398(8)	1.378(4)	1.388(2)	1.382(7)	1.379(3)
C2-C3	1.349(9)	1.351(4)	1.346(3)	1.356(8)	1.349(3)
N3-C4	1.137(10)	1.147(4)	1.143(2)	1.171(7)	1.145(3)
N4-C8	1.134(9)	1.145(4)	1.144(2)	1.155(7)	1.129(5)
N3-C4-C5	179.8(8)	178.0(3)	178.3(2)	178.4(7)	178.9(3)
N4-C8-C9	178.7(7)	178.7(3)	178.3(2)	179.4(6)	177.4(4)
N1-C1-N2	109.9(5)	107.1(3)	107.9(2)	109.6(5)	108.5(2)

2.2.4 Concluding remarks

A series of imidazolium salts with the nitrile group attached to the alkyl side-chain, both on the single side and double side of imidazolium backbone, have been prepared and characterized using spectroscopic methods. The majority of the nitrile-functionalized imidazolium salts can be classified as ILs since they melt below 100°C. Nine of the imidazolium salts have been characterized in the solid state using single crystal X-ray diffraction analysis, to reveal an extensive series of hydrogen bonds between H-atoms on the cation and the anion. The relationship between the solid state structure and the melting point is discussed. Key physical properties (density, viscosity and solubility in common solvents) of the low melting IL have been determined and are compared with those of the related 1-alkyl-3-methylimidazolium and 1-alkyl-2,3-dimethylimidazolium ILs. The results show that the incorporation of nitrile functionality affects the physical properties of the ILs, however, the ILs still retain low melting points and viscosities, which enables them qualified to be used as reaction media.

2.2.5 Experimental

1-methylimidazole, 1,2-dimethylimidazole and the chloronitriles were purchased from Fluka, HPF_6 and $NaBF_4$ were purchased from Aldrich and were used as received without further purification. The synthesis of the imidazolium salts **1a** – **8a** was performed under an inert atmosphere of dry

nitrogen using standard Schlenk techniques in solvents dried using the appropriate reagents and distilled prior to use. All other compounds were made without precautions to exclude air or moisture. IR spectra were recorded on a Perkin-Elmer FT-IR 2000 system. NMR spectra were measured on a Bruker DMX 400, using $SiMe_4$ for ^1H, 85% H_3PO_4 for ^{31}P, as external standards at 20°C. Electrospray ionization mass spectra (ESI-MS) were recorded on a ThermoFinnigan LCQ™ Deca XP Plus quadrupole ion trap instrument on sample diluted in methanol.[19] Samples were infused directly into the source at 5 μL min^{-1} using a syringe pump and the spray voltage was set at 5 kV and the capillary temperature at 50°C. Elemental analysis was carried out at the Institute of Molecular and Biological Chemistry at the EPFL. Samples **2c**, **3c**, **4a**, **4b** and **4c** were purified by filtration through silica and left under vacuum (*ca*. 0.1 mm Hg) at 40 – 50°C in order to remove traces of salt impurities and volatile components. Differential scanning calorimetry was performed with a SETARAM DSC 131. Density was determined with a picometer at room temperature (20 ± 1°C) on 1.0 ml of sample. The measurements were repeated three times and average values were used. Viscosities were measured with a Brookfield DV-II+ viscometer on 0.50 ml of sample. The temperature of the samples was maintained to 20 ± 1°C by means of an external temperature controller. The measurements were performed in duplicate.

Synthesis of [CCNmim]Cl ***1a***

A mixture of 1-methylimidazole (8.21 g, 0.10 mol) and $ClCH_2CN$ (9.06 g, 0.12 mol) was stirred at r.t. for 24 h, during which time the reaction mixture turned to a solid. The solid was washed with diethyl ether (3 × 30 ml) and dried under vacuum for 24 h, yield: 14.5 g, 92%; M.p. 170°C. Crystals suitable for X-ray diffraction were obtained by slow diffusion of diethyl ether into an acetonitrile solution of the compound at r.t. ESI-MS (CH_3OH): positive ion: 122 [CCNmim], negative ion: 35 [Cl]. ^1H NMR (D_2O): δ = 9.06 (s, 1H), 7.72 (s, 1H), 7.61 (s, 1H), 4.65 (s, 2H), 3.96 (s, 3H). ^{13}C NMR (D_2O): δ = 140.40, 127.65, 125.52, 117.02, 74.82, 39.54. IR (cm^{-1}): 3177, 3126, 3033 ($\nu_{C\text{-}H}$ aromatic), 2979, 2909, 2838, 2771 ($\nu_{C\text{-}H}$ aliphatic), 2261 ($\nu_{C\equiv N}$), 1769 ($\nu_{C=N}$). Anal. Calcd for $C_6H_8ClN_3$ (%): C 45.73, H 5.12, N 22.66; Found: C 45.86, H 5.26, N 22.58.

Synthesis of [CCNmim]PF_6 ***1b***

To a solution of **1a** (4.73 g, 0.03 mol) in water (50 ml), HPF_6 (8.03 g, 60 wt%, 0.033 mol) was added at r.t. After 10 minutes the solid that had formed was collected by filtration and washed with

ice-water (3 × 15 ml) and then dried under vacuum. Yield: 5.61 g, 70%; M.p. 78°C. ESI-MS (CH_3OH): positive ion: 122 [CCNmim], negative ion: 145 [PF_6]. ^1H NMR (CD_3CN): δ = 8.59 (s, 1H), 7.53 (s, 1H), 7.44 (s, 1H), 5.41 (s, 2H), 3.86 (s, 3H). ^{13}C NMR (CD_3CN): δ = 139.9, 127.6, 125.5, 120.5, 40.0, 39.3. ^{31}P NMR (CD_3CN): -145.25 (hept). IR (cm^{-1}): 3180, 3133, 3027 (ν_{C-H} aromatic), 2983, 2938 (ν_{C-H} aliphatic), 2274 ($\nu_{C\equiv N}$), 1602 ($\nu_{C=N}$). Anal. Calcd for $C_6H_8N_3F_6P$ (%): C 26.98, H 3.02, N 15.73; Found: C 27.02, H 3.09, N 15.66.

Synthesis of [CCNmim]BF_4 ***1c***

A mixture of **1a** (4.73 g, 0.03 mol) and $NaBF_4$ (3.62 g, 0.033 mol) in acetone (80 ml) was stirred at room temperature for 48 h. After filtration and removal of the solvents the resulting pale yellow waxy solid was washed with thf and diethyl ether to give the product. Yield: 5.76 g, 92%; M.p. 35°C. ESI-MS (CH_3OH): positive ion: 122 [CCNmim], negative ion: 87 [BF_4]. ^1H NMR (CD_3CN): δ = 8.67 (s, 1H), 7.56 (s, 1H), 7.47 (s, 1H), 5.26 (s, 2H), 3.87 (s, 3H). ^{13}C NMR ($CDCl_3$): δ = 140.35, 127.57, 125.46, 116.76, 39.79, 39.21. IR (cm^{-1}): 3171, 3124, 3015 (ν_{C-H} aromatic), 2977, 2845 (ν_{C-H} aliphatic), 2253 ($\nu_{C\equiv N}$), 1588 ($\nu_{C=N}$). Anal. Calcd for $C_6H_8BF_4N_3$(%): C 34.48, H 3.86, N 20.11; Found: C 34.52, H 3.82, N 20.26.

Synthesis of [C_2CNmim]Cl ***2a***

A mixture of 1-methylimidazole (8.21g, 0.10 mmol) and $Cl(CH_2)_2CN$ (10.74 g, 0.12 mol) was stirred in toluene (20 ml) at 70°C for 24 h. The resulting white solid was washed with diethyl ether (5 × 30 ml). The product was then dried in vacuum for 24 h. Yield: 15.5g, 82%; M.p. 50°C. ESI-MS (CH_3OH): Positive ion: 136 [C_2CNmim], negative ion: 35 [Cl]. ^1H NMR (D_2O): δ = 8.73 (s, 1H), 7.48 (s, 1H), 7.46 (s, 1H), 4.64 (t, *J*(H, H) = 6.8 Hz, 2H), 3.94 (s, 3H), 3.03 (t, *J*(H, H) = 6.8 Hz, 2H); ^{13}C NMR (D_2O): δ = 139.58, 138.05, 126.16, 122.53, 47.86, 42.12, 38.83. IR (cm^{-1}): 3244 (ν_{C-H} aromatic), 2916, 2788, 2700 (ν_{C-H} aliphatic), 2250 ($\nu_{C\equiv N}$), 1720 ($\nu_{C=N}$). Anal. Calcd for $C_7H_{10}ClN_3$ (%): C 48.99, H 5.87, N 24.48; Found: C 50.02, H 5.75, N 24.71.

Synthesis of [C_2CNmim]PF_6 ***2b***

The same procedure was followed as that described above for **1b**, except **2a** (5.15 g, 0.03 mol) and HPF_6 (8.03 g, 60wt%, 0.033 mol) were used, and the product was obtained as a white solid. Yield: 6.83g, 81%; M.p. 35°C. ESI-MS (CH_3OH): Positive ion: 136 [C_2CNmim], negative ion: 145 [PF_6].

^{1}H NMR (CD_3CN): δ = 8.64 (s, 1H) 7.50 (s, 1H), 7.43 (s, 1H), 4.46 (t, *J*(H, H) = 6.49 Hz, 2H), 3.89 (s, 3H), 3.03 (t, *J*(H, H) = 6.49 Hz, 2H). ^{13}C NMR (CD_3CN): δ = 139.36, 127.13, 125.34, 120.49, 47.87, 39.01, 21.92. ^{31}P NMR (CD_3CN): -142.90 (hept). IR (cm^{-1}): 3168, 3126, 3101 (ν_{C-H} aromatic), 2964 (ν_{C-H} aliphatic), 2255 ($\nu_{C\equiv N}$), 1704 ($\nu_{C=N}$). Anal. Calcd for $C_7H_{10}F_6N_3P$ (%): C 29.90, H 3.58, N 14.95; Found: C 29.95, H 3.62, N 14.88.

Synthesis of [C_2CNmim]BF_4 ***2c***

The same procedure was followed as that described above for **1c**, except **2a** (5.15 g, 0.03 mol) was used instead of **1a**. The product was obtained as pale yellow liquid at room temperature. Yield: 5.69 g, 85%; M.p. 20°C. ESI-MS (CH_3OH): Positive ion: 136 [C_2CNmim], negative ion: 87 [BF_4]. ^{1}H NMR (CD_3CN,): δ = 8.56 (s, 1H), 7.41 (s, 1H), 7.37 (s, 1H), 4.48 (brs, 2H), 3.88 (s, 3H), 3.05 (brs, 2H). ^{13}C NMR (CD_3CN): δ = 138.33, 126.22, 122.56, 121.04, 47.81, 38.54, 21.81. IR (cm^{-1}): 3165 and 3124 (ν_{C-H} aromatic), 2955 and 2855 (ν_{C-H} aliphatic), 2251 ($\nu_{C\equiv N}$), 1736 ($\nu_{C=N}$). Anal. Calcd for $C_7H_{10}N_3BF_4$ (%): C 37.70, H 4.52, N 18.84; Found: C 37.52, H 4.65, N 19.05.

Synthesis of [C_3CNmim]Cl ***3a***

A mixture of 1-methylimidazole (8.21g, 0.10 mmol) and $Cl(CH_2)_3CN$ (12.43g, 0.12 mol) was stirred at 80°C for 24 h. The resulting white solid was washed with diethyl ether (3 × 30 ml). The product was dried in vacuum for 24 h. Yield: 17.6 g, 95%; M.p. 80°C. ESI-MS (CH_3OH): Positive ion: 150 [C_3CNmim], negative ion: 35 [Cl]. ^{1}H NMR ($CDCl_3$): δ = 8.73 (s, 1H), 7.45 (s, 1H), 7.39 (s, 1H), 4.27 (t, *J*(H, H) = 6.8 Hz, 2H), 3.82 (s, 3H), 2.50 (t, *J*(H, H) = 6.8 Hz, 2H), 2.20 (t, *J*(H, H) = 6.8 Hz, 2H). ^{13}C NMR ($CDCl_3$): δ = 134.11, 130.49, 120.01, 116.19, 44.01, 30.87, 21.21, 9.87. IR (cm^{-1}): 3373, 3244, 3055 (ν_{C-H} aromatic), 3029, 2974, 2949, 2927 (ν_{C-H} aliphatic), 2243 ($\nu_{C\equiv N}$), 1692 ($\nu_{C=N}$). Anal. Calcd for $C_8H_{12}ClN_3$ (%): C, 51.76, H, 6.51, N, 22.63; Found: C 51.72, H 6.55, N 22.71.

Synthesis of [C_3CNmim]PF_6 ***3b***

The same procedure was followed as that described above for **1b**, except **3a** (5.57 g, 0.03 mol) was used instead of **1a**. The product was obtained as white solid. Yield: 6.90 g, 78%; M.p. 75°C. ESI-MS (CH_3OH): Positive ion: 150 [C_3CNmim], negative ion: 145 [PF_6]. ^{1}H NMR ($CDCl_3$): δ = 8.63 (s, 1H), 7.59 (s, 1H), 7.55 (s, 1H), 4.42 (t, *J*(H, H) = 7.0 Hz, 2H), 4.03 (s, 3H), 2.66 (t, *J*(H, H) = 7.0

Hz, 2H), 2.33 (m, 2H). ^{13}C NMR ($CDCl_3$): δ = 135.50, 131.80, 120.10, 116.50, 44.25, 33.30, 22.50, 9.98. ^{31}P NMR ($CDCl_3$): -145.90 (hept). IR (cm^{-1}): 3171, 3158, 3128 (ν_{C-H} aromatic), 2980, 2807 (ν_{C-H} aliphatic), 2246 ($\nu_{C\equiv N}$), 1696 (($\nu_{C=N}$). Anal. Calcd for $C_8H_{12}F_6N_3P$ (%): C 32.55, H 4.10, N 14.24; Found: C 32.59, H 4.11, N 14.30.

Synthesis of [C_3CNmim]BF_4 ***3c***

The same procedure was followed as that described above for **1c**, except **3a** (5.57 g, 0.03 mol) was used instead of **1a**. Yield: 6.4 g, 90%; M. p. -71.9°C. ESI-MS (CH_3OH): Positive ion: 150 [C_3CNmim], negative ion: 87 [BF_4]. ^{1}H NMR ($CDCl_3$): δ = 9.32 (s, 1H), 8.18 (s, 1H), 8.14 (s, 1H), 4.96 (brs, 2H), 4.54 (s, 3H), 3.20 (brs, 2H), 2.85 (brs, 2H). ^{13}C NMR ($CDCl_3$): δ = 135.03, 131.17, 120.69, 116.71, 44.69, 33.78, 22.01, 10.15. IR (cm^{-1}): 3161, 3121 (ν_{C-H} aromatic), 2971 (ν_{C-H} aliphatic), 2249 ($\nu_{C\equiv N}$), 1712 ($\nu_{C=N}$). Anal. Calcd for $C_8F_4BH_{12}N_3$ (%): C 40.54, H 5.10, N 17.73; Found: C 40.58, H 5.13, N 17.69.

Synthesis of [C_4CNmim]Cl ***4a***

A mixture of 1-methylimidazole (8.21g, 0.10 mmol) and $Cl(CH_2)_4CN$ (14.1g, 0.12 mol) was stirred at 80°C for 4 h. The temperature was then increased to 110°C and the reaction mixture was stirred at for further 2 h. After cooling, the reaction mixture was washed with diethyl ether (3 ×15 ml) and dried under vacuum for 24 h. The product is obtained as viscous brownish liquid. Yield: 17.9 g, 90%; M.p. 32°C. ESI-MS (CH_3OH): Positive ion: 164 [C_4CNmim], negative ion: 35 [Cl]. ^{1}H NMR (CD_3CN): δ = 9.99 (s, 1H), 7.75 (s, 1H), 7.70 (s, 1H), 4.41 (t, *J*(H, H) = 7.2 Hz, 2H), 3.94 (s, 3H), 2.57 (t, *J*(H, H) = 7.0 Hz, 2H), 2.07 (m, *J*(H, H) = 6.8 Hz, 2H), 1.64 (m, *J*(H, H) = 6.8 Hz, 2H). ^{13}C NMR (CD_3CN): δ = 134.22, 129.29, 127.97, 125.81, 123.18, 41.50, 34.43, 27.47, 21.77. IR (cm^{-1}): 3138, 3088, 3082 (ν_{C-H} aromatic), 2948 (ν_{C-H} aliphatic), 2241 ($\nu_{C\equiv N}$), 1701 (($\nu_{C=N}$). Anal. Calcd for $C_9H_{14}ClN_3$ (%): C 54.13, H 7.07, N, 21.04; Found: C 54.21, H 7.09, N, 21.09.

Synthesis of [C_3CNmim]PF_6 ***4b***

The same procedure was followed as that described above for **1b**, except **4a** (5.99 g, 0.03 mol) was used instead of **1a**. The product was obtained as brown liquid at room temperature. Yield: 7.6 g, 82%; M.p. -60.3°C. ESI-MS (CH_3OH): positive ion: 164 [C_3CNmim], negative ion: 145 [PF_6]. ^{1}H NMR (CD_3CN): δ = 8.45 (s, 1H), 7.38 (s, 1H), 7.35 (s, 1H), 4.15 (t, *J*(H, H) = 7.17 Hz, 2H), 3.83 (s,

3H), 2.44 (t, *J*(H, H) = 7.17 Hz, 2H), 1.93 (m, *J*(H, H) = 7.17, 2H), 1.64 (m, *J*(H, H) = 7.17, 2H). ^{13}C NMR (CD_3CN): δ = 138.95, 126.72, 125.16, 122.85, 120.80, 38.78, 31.61, 24.74, 18.93. ^{31}P NMR ($CDCl_3$): -140.80 (hept). IR (cm^{-1}): 3168, 3123 (ν_{C-H} aromatic), 2972, 2901 (ν_{C-H} aliphatic), 2250 ($\nu_{C\equiv N}$), 1577 (($\nu_{C=N}$). Anal. Calcd for $C_9F_6H_{14}N_3P$ (%): C 34.96, H 4.56, N 13.59; Found: C 35.05, H 4.41, N 13.64.

Synthesis of [C_3CNmim]BF_4 ***4c***

The same procedure was followed as that described above for **1c**, except **4a** (5.99 g, 0.03 mol) was used instead of **1a**. The product was obtained as brown liquid at room temperature. Yield: 6.4 g, 85%; M.p. -71.9°C. ESI-MS (CH_3OH): Positive ion: 164 [C_3CNmim], negative ion: 87 [BF_4]. ^{1}H NMR (CD_3CN): δ = 8.54 (s, 1H), 7.43 (s, 1H), 7.39 (s, 1H), 4.17 (brs, 2H), 3.83 (s, 3H), 2.44 (brs, 2H), 1.92 (brs, 2H), 1.60 (brs, 2H). ^{13}C NMR (CD_3CN): δ = 139.24, 131.19, 128.02, 126.68, 123.72, 38.69, 31.64, 24.70, 18.64. IR (cm^{-1}): 3161, 3120 (ν_{C-H} aromatic), 2955, 2876 (ν_{C-H} aliphatic), 2247 ($\nu_{C\equiv N}$), 1575 ($\nu_{C=N}$). Anal. Calcd for $C_9H_{14}N_3BF_4$ (%): C 43.06, H 5.62, N 16.74; Found: C 43.12, H 5.53, N 16.70.

Synthesis of [C_3CNdimim]Cl ***5a***

A mixture of 1,2-dimethylimidazole (9.61 g, 0.10 mol) and $Cl(CH_2)_3CN$ (12.43 g, 0.12 mol) was stirred at 100°C for 24 h. Two phases were formed at the end of the reaction. The upper phase was decanted and the lower phase was washed with diethyl ether (3 × 30 ml). A pale yellow solid was formed during the washing and the product was dried in vacuum for 24 h at r.t.. Yield: 18.6 g, 93%; M.p. 105°C. × (CH_3OH): Positive ion: 164 [C_3CNdimim], negative ion: 35 [Cl]. ^{1}H NMR (CD_3CN): δ = 7.50 (s, 1H), 7.31 (s, 1H), 4.14 (t, *J*(H, H) = 7.17 Hz, 2H), 3.71 (s, 3H), 2.53 (s, 3H), 2.46 (t, *J*(H, H) = 7.17 Hz, 2H), 2.11 (m, *J*(H, H) = 7.17 Hz, 2H). ^{13}C NMR (CD_3CN): δ = 125.52, 123.70, 122.32, 120.73, 49.47, 37.66, 28.12, 16.50, 11.92. IR (cm^{-1}): 3182, 3098, 3046 (ν_{C-H} aromatic), 2989, 2898, 2834 (ν_{C-H} aliphatic), 2240 ($\nu_{C\equiv N}$), 1631 ($\nu_{C=N}$). Anal. Calcd for $C_9H_{14}ClN_3$ (%): C 54.13, H 7.07, N 21.04; Found: C 54.18, H 7.17, N 20.92.

Synthesis of [C_3CNdimim]PF_6 ***5b***

The same procedure was followed as that described above for **1b**, except **5a** (5.99 g, 0.03 mol) was used instead of **1a**. The product was obtained as white solid at room temperature. Yield: 7.33 g,

79%; M.p. 85°C. ESI-MS (CH_3OH): Positive ion: 164 [C_3CNdimim], negative ion: 145 [PF_6]. ^{1}H NMR (CD_3CN): δ = 7.34 (s, 1H), 7.32 (s, 1H), 4.18 (t, *J*(H, H) = 7.17 Hz, 2H), 3.75 (s, 3H), 2.55 (s, 3H), 2.51 (t, *J*(H, H) = 7.17 Hz, 2H), 2.14 (m, *J*(H, H) = 7.17, 2H). ^{13}C NMR (CD_3CN): δ = 144.91, 122.87, 120.99, 120.59, 46.85, 35.08, 25.02, 14.09, 9.37. ^{31}P NMR (CD_3CN): -140.80 (hept). IR (cm^{-1}): 3150 (ν_{C-H} aromatic), 2966 (ν_{C-H} aliphatic), 2249 ($\nu_{C\equiv N}$), 1628 ($\nu_{C=N}$). Anal. Calcd for $C_9F_6H_{14}N_3P$ (%): C 34.96, H 4.56, N 13.59; Found: C 35.02, H 4.52, N 13.61.

Synthesis of [C_3CNdimim]BF_4 ***5c***

The same procedure was followed as that described above for **1c**, except **5a** (5.99 g, 0.03 mol) was used instead of **1a**. The product was obtained as white waxy solid at room temperature. Yield: 6.77 g, 90%; M.p. 40°C. ESI-MS (CH_3OH): Positive ion: 164 [C_3CNdimim], negative ion: 87 [BF_4]. ^{1}H NMR (CD_3CN): δ = 7.31 (s, 1H), 7.30 (s, 1H), 4.15 (t, *J*(H, H) = 6.84 Hz, 2H), 3.72 (s, 3H), 2.59 (s, 3H), 2.47 (t, *J*(H, H) = 6.84, 2H), 2.13 (m, *J*(H, H) = 6.84, 2H). ^{13}C NMR (CD_3CN): δ = 125.54, 123.70, 122.08, 120.52, 49.51, 37.71, 28.04, 16.59, 11.98. IR (cm^{-1}) 3185, 3145 (ν_{C-H} aromatic), 2966 (ν_{C-H} aliphatic), 2244 ($\nu_{C\equiv N}$), 1701 (($\nu_{C=N}$). Anal. Calcd for $C_9H_{14}BF_4N_3$ (%): C 43.06, H 5.62, N 16.74; Found: C 42.85, H 5.75, N 16.68.

Synthesis of [$(CCN)_2$im][Cl] ***6a***

A mixture of trimethylsilyimidazole (14.03 g, 0.10 mol) and $ClCH_2CN$ (15.10 g, 0.20 mol) was stirred at room temperature for 24 h, during which time the reaction mixture turned into a solid. This white solid was washed with diethyl ether (3 × 30 ml). The solid product was dried in vacuum for 24 h. Yield: 17.3 g, 95%; m. p.: 176°C. ESI-MS (H_2O, *m/z*): positive ion, 147 [$(CCN)_2$im]$^+$; negative ion, 35, 37 [Cl]$^-$; ^{1}H NMR (D_2O): δ 9.35 (s, 1H), 7.81 (s, 2H), 5.54 (s, 4H); ^{13}C NMR (D_2O): 138.2, 123.5, 113.4, 37.5. IR (cm^{-1}): $\nu_{C\equiv N}$, 2263; Anal. Calcd. for $C_7H_7ClN_4$ (%): C 46.04, H 3.86, N 30.68; Found: C 46.08, H 3.82, N 30.65.

Synthesis of [$(CCN)_2$im][PF_6] ***6b***

Salt **6a** (18.2 g, 0.1 mol) was dissolved in water (50 ml) and HPF_6 (24.3 g, 60wt% aqueous solution, 0.10 mol) was added at room temperature. The resulting white hydrophobic solid was washed with cold water (3 × 10.0 ml). The product was dried in vacuum for 24 h. Yield: 19.8 g, 68%; M.p.: 208°C; ESI-MS (Methanol, *m/z*): Positive ion: 147 [$(CCN)_2$im]$^+$, negative ion: 145 [PF_6]$^-$; ^{1}H NMR

(Aceton-D6): δ = 9.62 (s, 1H), 8.15 (s, 2H), 5.80 (s, 4H); ^{13}C NMR (Aceton-D6): δ = 131.1, 123.9, 113.2, 37.5; IR (cm^{-1}): $\nu_{C\equiv N}$, 2262; Anal. Calcd for $C_7H_7F_6N_4P$ (%): C 28.78, H 2.42, N 19.18; Found: C 28.75, H 2.55, N 19.16.

Synthesis of [(CCN)$_2$im][BF$_4$] ***6c***

Salt **6a** (18.2 g, 0.1 mol) was mixed with $NaBF_4$ (10.98 g, 0.10 mol) in acetone and stirred at room temperature for 24 h. After filtration and removal of the solvent, the resulting pale yellow solid was washed with THF (2 ×10 ml) and diethyl ether (3 × 10ml) to give the product. It was recrystallised from acetonitrile to give coulorless crystals which were collected by filtration. Yield: 14.9 g, 64%; M.p.: 110°C; ESI-MS (Methanol, *m/z*): Positive ion: 147 $[(CCN)_2im]^+$, negative ion: 87 $[BF_4]^-$; ^{1}H NMR (Aceton-D6): δ = 9.29 (s, 1H), 7.77 (s, 2H), 5.48 (s, 4H); ^{13}C NMR (Aceton-D6): δ = 131.1, 123.5, 113.3, 37.4; IR (cm^{-1}): $\nu_{C\equiv N}$, 2258; Anal. Calcd. for $C_7H_7BF_4N_4$ (%): C 35.94, H 3.02, N 23.95; Found: C 35.99, H 3.05, N 23.86.

Synthesis of [(CCN)$_2$im][Tf$_2$N] ***6d***

Salt **6a** (18.2 g, 0.1 mol) was dissolved in water (50 ml) and Li[Tf_2N] (28.7 g, 0.10 mol) was added at room temperature. The resulting white hydrophobic solid was washed with water (3 × 10 ml). The product was dried in vacuum for 24 h. Yield: 19.8 g, 68%; M.p.: 68°C; ESI-MS (Methanol, *m/z*): Positive ion: 147 $[(CCN)_2im]^+$, negative ion: 280 $[Tf_2N]^-$; ^{1}H NMR (Aceton-D6): δ = 9.59 (s, 1H), 8.14 (s, 1H), 5.87 (s, 4H); ^{13}C NMR (Aceton-D6): δ = 131.1, 123.8, 113.2, 36.8; IR (cm^{-1}): $\nu_{C\equiv N}$, 2262; Anal. Calcd. for $C_9H_7F_6N_5O_4S_2$ (%): C 25.30, H 1.65, N 16.39; Found: C 25.28, H 1.70, N 16.36.

Synthesis of [(CCN)$_2$im][Cl] ***7a***

A mixture of (trimethysily)imidazole (14.03 g, 0.10 mmol) and $Cl(CH_2)_3CN$ (24.86 g, 0.24 mol) was stirred at 80°C for 24 h. The resulting white solid was washed with diethyl ether (3 x 30 mL). The product was dried in a vacuum for 24 h. Yield: 22.4 g, 94%; m. p.: 100°C. ESI-MS (H_2O, *m/z*): positive ion, 203 $[Di(CH_2)_3C\equiv Nim]^+$; negative ion, 35, 37 $[Cl]^-$; ^{1}H NMR (D_2O): δ 8.56 (s, 1H), 7.52 (s, 2H), 4.48 (t, 4H, ^1J(H, H) = 7.15 Hz), 2.66 (m, 4H), 2.35 (t, 4H, ^1J(H, H) = 7.15 Hz); ^{13}C NMR (D_2O): 137.08, 123.44, 119.25, 48.37, 29.33, 25.17. IR (cm^{-1}): 3148, 3115, 2967, 2247, 1567; Anal. Calcd for $C_{11}H_{15}ClN_4$ (%): C 55.35, H 6.33, N 23.47. Found: C 54.98, H 6.08, N 23.55.

Synthesis of [$(C_3CN)_2$im][PF_6] ***7b***

Salt **7a** (23.87 g, 0.1 mol) was dissolved in water (50 ml) and HPF_6 (24.3 g, 60wt% aqueous solution, 0.10 mol) was added at room temperature. The resulting white hydrophobic solid was washed with water (3 × 10 ml). The product was dried in vacuum for 24 h. Yield: 20.2 g, 58%; M.p.: 79°C; ESI-MS (Methanol, *m/z*): Positive ion: 203 $[(C_3CN)_2im]^+$, negative ion: 145 $[PF_6]^-$; ^{1}H NMR (Aceton-D6): δ = 9.18 (s, 1H), 7.86 (s, 2H), 4.53 (t, ^1J(H,H) = 7.51 Hz, 4H), 2.68 (t, ^1J(H, H) = 7.51 Hz, 4H), 2.38 (p, ^1J(H, H) = 7.51 Hz, 4H); ^{13}C NMR (Aceton-D6): δ = 136.6, 123.1, 111.5, 48.5, 25.7, 13.5; IR (cm^{-1}): $\nu_{C\equiv N}$, 2250; Anal. Calcd. for $C_{11}H_{15}F_6N_4P$ (%): C 37.94, H 4.34, N 16.09; Found: C 37.99, H 4.38, N 16.12.

Synthesis of [$(C_3CN)_2$im][BF_4] ***7c***

Salt **7a** (23.87 g, 0.1 mol) mixed with Na[BF_4] (10.98 g, 0.10 mol) in acetone and stirred at room temperature for 24 h. After filtration and removal of the solvent the resulting pale yellow liquid was washed with THF (3 × 30 ml) and diethyl ether (3 × 30 ml) to give the product. The product was dried in vacuum for 24 h. Yield: 21.5 g, 74%; M.p.: -55.2 °C; ESI-MS (Methanol, *m/z*): Positive ion: 203 $[(C_3CN)_2im]^+$, negative ion: 87 $[BF_4]^-$; ^{1}H NMR (Aceton-D6): δ = 9.12 (s, 1H), 7.83 (s, 2H), 4.49 (t, ^1J(H,H) = 7.51 Hz, 4H), 2.65 (t, ^1J(H, H) = 7.51 Hz, 4H), 2.35 (p, ^1J(H, H) = 7.51 Hz, 4H); ^{13}C NMR (Aceton-D6): δ = 136.6, 123.01, 118.5, 48.4, 25.8, 13.5; IR (cm^{-1}): $\nu_{C\equiv N}$, 2248; Anal. Calcd. for $C_{11}H_{15}BF_4N_4$ (%): C 45.55, H 5.21, N 19.32; Found: C 45.66, H 5.24, N 19.28.

Synthesis of [$(C_3CN)_2$im][Tf_2N] ***7d***

Salt **7a** (23.87 g, 0.1 mol) was dissolved in water (50 ml) and Li[Tf_2N] (28.7 g, 0.10 mol) was added at room temperature. The resulting pale yellow hydrophobic liquid was washed with water (3 × 30 ml). The product was dried in vacuum for 24 h. Yield: 32.9 g, 68%; M.p.: -58.6°C; ESI-MS (Methanol, *m/z*): Positive ion: 203 $[(C_3CN)_2im]^+$, negative ion: 280 $[Tf_2N]^-$; ^{1}H NMR (Aceton-D6): δ = 9.17 (s, 1H), 7.82 (s, 2H), 4.50 (t, ^1J(H,H) = 7.51 Hz, 4H), 2.65 (t, ^1J(H, H) = 7.51 Hz, 4H), 2.38 (p, ^1J(H, H) = 7.51 Hz, 4H); ^{13}C NMR (Aceton-D6): δ = 136.4, 123.0, 121.6, 48.5, 25.7, 13.6; IR (cm^{-1}): $\nu_{C\equiv N}$, 2250; Anal. Calcd. for $C_{13}H_{15}F_6N_5O_4S_2$ (%): C 32.30, H 3.13, N 14.49; Found: C 32.29, H 3.18, N 14.42.

Synthesis of [$(C_4CN)_2$im][Cl] ***8a***

A mixture of (trimethysily)imidazole (14.03 g, 0.10 mol) and $Cl(CH_2)_4CN$ (23.40 g, 0.20 mol) was refluxed at 80 °C for 24 h, during which time the reaction mixture turned into a waxy liquid. The liquid was washed with diethyl ether (3 × 30 ml). The product was dried in a vacuum for 24 h. Yield: 26.07 g, 98%; m. p.: -19.8°C. ESI-MS (H_2O, *m/z*): positive ion, 231 $[(C_4CN)_2im]^+$; negative ion, 35, 37 $[Cl]^-$; ^{1}H NMR (D_2O): δ = 8.89 (s, 1H), 7.57 (s, 2H), 4.28 (t, ^1J(H,H) = 6.83 Hz, 4H), 2.56 (p, ^1J(H,H) = 7.51 Hz, 4H), 2.02 (p, ^1J(H,H) = 6.83 Hz, 4H), 1.69 (p, ^1J(H,H) = 7.51 Hz, 4H); ^{13}C NMR (D_2O): 135.5, 122.6, 121.4, 48,8, 28.5, 21.6, 16.1; IR (cm^{-1}): $\nu_{C\equiv N}$, 2245; Anal. Calcd. for $C_{13}H_{19}ClN_4$ (%): C 58.53, H 7.18, N 21.00; Found: C 58.57, H 7.14, N 20.94.

Synthesis of [$(C_4CN)_2$im] [PF_6] ***8b***

Salt **8a** (26.67 g, 0.1 mol) was dissolved in water (50 ml) and HPF_6 60wt% solution (24.3 g, 0.10 mol) was added at room temperature. The resulting pale yellow hydrophobic liquid was washed with water (3 × 30 ml).The was washed with water (3 × 30 ml). The product was dried in a vacuum for 24 h. Yield: 28.2 g, 75%; m. p.: -44.81°C. ESI-MS (H_2O, *m/z*): positive ion, 231 $[(C_4CN)_2im]^+$; negative ion, 145 $[PF_6]^-$; ^{1}H NMR (Aceton-D6) 9.08 (s, 1H), 7.81 (s, 2H), 4.45 (t, ^1J(H,H) = 6.83 Hz, 4H), 2.58 (t, ^1J(H, H) = 7.51 Hz, 4H), 2.11 (p, ^1J(H, H) = 6.83 Hz, 4H), 1.74 (p, ^1J(H, H) = 7.51 Hz, 4H); ^{13}C NMR (Aceton-D6): δ = 136.0, 122.8, 119.4, 48.9, 28.8, 22.0, 15.8; IR (cm^{-1}): $\nu_{C\equiv N}$, 2247; Anal. Calcd. for $C_{13}H_{19}F_6N_4P$ (%): C 41.50, H 5.09, N 14.89; Found: C 41.47, H 5.12, N 14.92.

Synthesis of [$(C_4CN)_2$im] [BF_4] ***8c***

Salt **8a** (26.67 g, 0.1 mol) mixed with Na[BF_4] (10.98 g, 0.10 mol) in acetone and stirred at room temperature for 48 h. After filtration and removal of the solvent the resulting pale yellow liquid was washed with THF (3 × 15) and diethyl ether (3 × 30) to give the product. The product was dried in vacuum for 24 h. Yield: 29.90 g, 94%; M.p.: -58.94 °C; ESI-MS (Methanol, *m/z*): Positive ion: 231 $[(C_4CN)_2im]^+$, negative ion: 87 $[BF_4]^-$; ^{1}H NMR (Aceton-D6): δ = 8.80 (s, 1H), 7.55 (s, 2H), 4.28 (t, ^1J(H,H) = 6.83 Hz, 4H), 2.56 (t, ^1J(H, H) = 7.51 Hz, 4H), 2.03 (p, ^1J(H, H) = 6.83 Hz, 4H), 1.70 (t, ^1J(H, H) = 7.51 Hz, 4H); ^{13}C NMR (Aceton-D6): δ = 135.39, 122.55, 121.40, 48.83, 28.47, 21.73, 16.04; IR (cm^{-1}): $\nu_{C\equiv N}$, 2247; Anal. Calcd. for $C_{13}H_{19}BF_4N_4$ (%): C 49.08, H 6.02, N 17.61; Found: C 49.01, H 5.59, N 17.48.

Synthesis of [$(C_4CN)_2$im][Tf_2N] ***8d***

Salt **8a** (26.67 g, 0.1 mol) was dissolved in water (50 ml) and Li[Tf_2N] (28.7 g, 0.10 mol) was added at room temperature. The resulting pale yellow hydrophobic liquid was washed with water (3 × 30 ml). The product was dried in vacuum for 24 h. Yield: 37.3 g, 73%; m. p.:-63.0 °C. ESI-MS (H_2O, *m/z*): positive ion, 231, $[(C_4CN)_2im]^+$; negative ion, 280 $[Tf_2N]^-$; ^{1}H NMR (Aceton-D6) 9.15 (s, 1H), 7.80 (s, 2H), 4.42 (t, ^1J(H,H) = 6.85 Hz, 4H), 2.54 (t, ^1J(H, H) = 7.51 Hz, 4H), 2.08 (p, ^1J(H, H) = 6.83 Hz, 4H), 1.73 (p, ^1J(H, H) = 7.51 Hz, 4H); ^{13}C NMR (Aceton-D6): δ = 136.1, 123.8, 122.8, 118.4, 48.8, 29.3, 22.0, 15.8; IR (cm^{-1}): $\nu_{C\equiv N}$, 2249; Anal. Calcd. for $C_{15}H_{19}F_6N_5O_4S_2$ (%): C 35.22, H 3.74, N 13.69; Found: C 35.27, H 3.78, N 13.61.

X-ray structure determination

Data collections were performed at 140 K on a 4-circle kappa goniometer equipped with an Oxford Diffraction KM4 Sapphire CCD for compound **1a** and **5b**. Diffraction data for **3a** and **3b** were measured at 140 K on a marresearch mar345 IPDS. Data reduction was carried out with CrysAlis RED, release 1.6.9.[20] Absorption correction [21] has been applied to data sets belonging to **3b**. Structure solution and refinement as well as molecular graphics and geometrical calculations were performed for all structures with the SHELXTL software package, release 5.1.[22] The structures were refined using the full-matrix least-squares on F^2 with all non-H atoms anisotropically defined. H atoms were placed in calculated positions using the 'riding model'.

2.3 References

[1] For example see: (a) Y. Chauvin, H. Olivier-Bourbigou, *Chemtech.* **1995**, *25*, 26. (b) P. J. Dyson, D. J. Ellis, D. G. Parker, T. Welton, *Chem Commun*. **1999**, 25. (c) P. A. Z. Suarez, J. E. L. Dullius, S. Einloft, R. F. de Souza, J. Dupont, *Polyhedron* **1996**, *15*, 1217. (d) L. A. Müller, J. Dupont, R. F. de Souza, *Macromol. Rapid Commun*. **1998**, *19*, 409 . (e) P. J. Dyson, D. J. Ellis, T. Welton, *Canadian J. Chem*. **2001**, *79,* 705. (f) S. Steines, P. Wasserscheid, B. Drieβen-Hölscher, *J. Prakt. Chem*. **2000**, *342*, 348.

[2] For example see: (a) K. W. Kottsieper, O. Stelzer, P. Wasserscheid, *J. Mol. Catal. A: Chem.* **2001**, *175*, 285. (b) F. Favre, H. Olivier-Bourbigou, D. Commereuc, L. Saussine, *Chem. Commun.* **2001**,

1360. (c) C. C. Brasse, U. Englert, A. Salzer, H. Waffenschmidt, P. Wasserscheid, *Organometallics* **2000**, *19*, 3818. (d) M. F. Sellin, P. B. Webb, D. J. Cole-Hamilton, *Chem. Commun.* **2001**, 781. (e) O. Stenzel, H. G. Raubenheimer, C. Esterhuysen, *J. Chem. Soc., Dalton Trans.* **2002**, 1132.

[3] (a) L. Xu, W. Chen, J. Xiao, *Organometallics* **2000**, *19*, 1123. (b) C. J. Mathews, P. J. Smith, T. Welton, A. J. P. White, D. J. Williams, *Organometallics* **2001**, *20*, 3848 (c) A. J. Carmichael, M. J. Earle, J. D. Holbrey, P. B. McCormac, K. R. Seddon, *Org. Lett.* **1999**, *1*, 997. (d) C. J. Mathews, P. J. Smith, T. Welton, *Chem. Commun.* **2000**, 1249. (e) S. T. Handy, X. Zhang, *Org. Lett.* **2001**, *3*, 233.

[4] D. J. Brauer, K. Kottsieper, C. Liek, O. Stelzer, H. Waffenschmidt, P. Wasserscheid, *J. Organomet. Chem.* **2001**, *630*, 177.

[5] (a) K. Kottsieper, O. Stelzer, P. Wasserscheid, *J. Mol. Catal. A: Chem.* **2001**, *175*, 285. (b) J. Sirieix, M. Ossberger, B. Betzemeier, P. Knochel, P. *Synlett.* **2000**, *11*, 1613.

[6] P. B. Hitchcock, K. R. Seddon, T. Welton, *J. Chem. Soc. Dalton Trans.* **1993**, 2639.

[7] W. A. Herrmann, L. J. Goossen, M. Spiegler, *Organometallics* **1998**, *17*, 2162.

[8] K. R. Seddon, A. Stark, M. J. Torres, *Pure Appl. Chem.* **2000**, *72*, 2275.

[9] J.-F. Huang, P.-Y. Chen, I.-W. Sun, S. P. Wan, *Inorg. Chim. Acta* **2000**, *320*, 7.

[10] (a) A. G. Avent, P. A. Chaloner, M. P. Day, K. R. Seddon, T. Welton, *J. Chem. Soc. Dalton Trans*. **1994**, 3405. (b) A. Elaiwi, P. B. Hitchcock, K. R. Seddon, N. Srinivasan, Y.-M. Tan, T. Welton, J. A. Zora, *J. Chem. Soc. Dalton Trans*. **1995**, 3467.

[11] J. Dupont, P. A. Z. Suarez, R. F. de Souza, R. A. Burrow, J.-P. Kintzinger, *Chem. Eur. J.* **2000**, *6*, 2377.

[12] A. R. Katritzky, R. Jain, A. Lomaka, R. Petrukhin, U. Maran, M. Karelson, *Crystal. Growth & Design* **2001**, *1*, 261.

[13] J. C. Dearden, *Sci. Total. Environ.* **1991**, *109/110*, 59.

[14] W. J. Lyman, W. F. Reehl, In *Handbook of Chemical Property Estimation Methods*, Rosenblatt, D. H. McGraw-Hill Book Company, New York, **1982**.

[15] A. S. Larsen, J. D. Holbrey, F. S. Tham, C. A. Reed, *J. Am. Chem. Soc.* **2000**, *122*, 7264.

[16] J. D. Holbrey, K. R. Seddon, *J. Chem. Soc., Dalton Trans*. **1999**, 2133.

[17] P. Bonhôte, A.-P. Dias, N. Papageorgiou, K. Kalyanasundaram, M. Graetzel, *Inorg. Chem.* **1996**, 35, 1168.

[18] P. J. Dyson, J. S. McIndoe, D. Zhao, *Chem. Commun.* **2003**, 508.

[19] F. H. Allen, O. Kennard, D. G. Watson, L. Brammer, G. Orpen, R. Taylor, *J. Chem. Soc., Perkin Trans 2.* **1987**, S1.

[20] Oxford Diffraction Ltd., Abingdon, Oxfordshire, UK, **2002**.

[21] DELABS, N. Walker, D. Stuart, *Acta Crystallogr*., *Sect A* **1983**, 39, 158.

[22] G. M. Sheldrick, University of Göttingen, Germany, **1997**; Bruker AXS, Inc., Madison, Wisconsin, 53719, USA, **1997**.

3

Palladium Complexes of Nitrile Functionalized Imidazolium ILs and their Applications in Catalysis

3.1 Introduction

In this chapter palladium complexation with the nitrile-functionalized imidazolium ILs, and their application in C-C coupling and hydrogenation reactions will be described.

3.2 Results and Discussion

3.2.1 Reaction of Nitrile Functionalized Ionic Liquids with $PdCl_2$

Acetonitrile solutions of the imidazolium chloride salts **3a**, **5a**, and 7**a** were treated with $PdCl_2$, affording the corresponding $[PdCl_4]^{2-}$ salts **9a-11a**, as outlined in (Scheme 3.1). Dichloromethane can also be used as a solvent, but the reaction is very slow at room temperature and requires several days to reach completion, probably due to the low solubility of the imidazolium salts in this solvent. Despite the competition between the nitrile group and the chloride anion, in the reaction environment, the preference is for reaction with the latter.

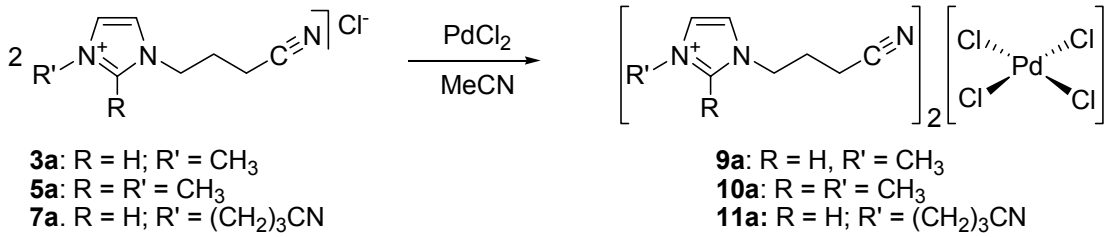

3a: R = H; R' = CH_3
5a: R = R' = CH_3
7a. R = H; R' = $(CH_2)_3CN$

9a: R = H, R' = CH_3
10a: R = R' = CH_3
11a: R = H; R' = $(CH_2)_3CN$

Scheme 3.1 Synthesis of complexes 9a, 10a and 11a

In contrast to the chloride salts, the ILs **3b-3d** and **5b-5d** react with $PdCl_2$ in dichloromethane at room temperature to form $[(C_3CNmim)_2PdCl_2][PF_6]_2$ **9b**, $[(C_3CNmim)_2PdCl_2][BF_4]_2$ **9c**, $[(C_3CNmim)_2PdCl_2][Tf_2N]_2$ **9d**, $[(C_3CNdmim)_2PdCl_2][PF_6]_2$ **10b**, and $[(C_3CNdmim)_2PdCl_2][BF_4]_2$ **10c** $[(C_3CNdmim)_2PdCl_2][Tf_2N]_2$ **10d** (Scheme 3.2). In these reactions, acetonitrile cannot be used.

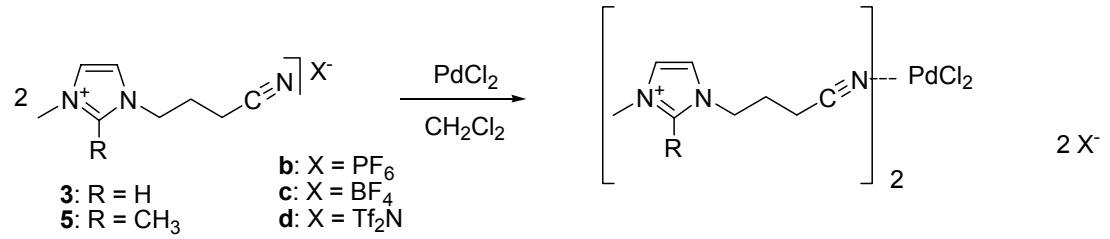

3: R = H
5: R = CH_3

b: X = PF_6
c: X = BF_4
d: X = Tf_2N

9: R = H
10: R = CH_3

b: X = PF_6
c: X = BF_4
d: X = Tf_2N

Scheme 1.2 Synthesis of complexes 9b-9d and 10b-10d

Compounds $[C_3CNmim]_2[PdCl_4]$ **9a** and $[C_3CNdmim]_2[PdCl_4]$ **10a** react with further $PdCl_2$ in dichloromethane to form salts which can be viewed as hybrids of the two types described above, viz. $[PdCl_2(C_3CNmim)_2][PdCl_4]$ **11b** and $[PdCl_2(C_3CNdmim)_2][PdCl_4]$ **12b**. At the start of the reaction, the starting materials form an orange suspension in dichloromethane, but on continued stirring the color of the reaction becomes orange-yellow, and after 5 days, only a pale yellow powder is present which is soluble in DMSO.

All of the new palladium salts have been characterised by ^{1}H and ^{13}C NMR although it provided only limited information because signals from the imidazolium moiety can only be identified. The IR spectra, however, were very informative. The stretching vibration of the C≡N group remains essentially unchanged in **9a-10a**, relative to the imidazolium precursors. Yet, in those complexes where the nitrile moiety coordinates to the palladium centre, namely **9b** – **10d** and **9b** – **10d**, the νC≡N stretching band is shifted to higher wave number, and similar trends were observed for **11b** (νC≡N 2300 cm-1) and **12b** (νC≡N 2309 cm-1). However, electrospray ionization mass spectrometry was not very informative.

Salts **9** – **10** are air stable and do not decompose on washing with water or alcohols at room temperature, although they are unstable in water or in alcohols over prolonged time or on heating. They are scarcely soluble in chlorinated solvents such as chloroform or dichloromethane. In acetonitrile, **9a** and **10a** are soluble and may be crystallized by addition of diethyl ether. In contrast, complexes **9b**, **10b**, **9c** and **10c** are unstable and convert to **3b**, **3b**, **5c** and **5c** with the concomitant formation of $Pd(CH_3CN)_2Cl_2$. Salts **11b** and **12b** also revert back to **3a** and **5a** and $Pd(CH_3CN)_2Cl_2$ in acetonitrile.

Crystals of **9a**, **10a** and **11a**, suitable for X-ray diffraction, were obtained from diffusion of diethyl ether into acetonitrile solutions and their structures are shown in Figure 3.1 - 3.3, and selected bond lengths and angles are listed in Table 3.1 and table of X-ray details. The structures of the cations do not change significantly upon reaction of the imidazolium chloride with $PdCl_2$ and are comparable to those described above. In all three structures, the palladium atom resides at a centre of inversion, and similar structures have been reported previously. The anion $[PdCl_4]^{2-}$ has a regular square planar geometry with Cl-Pd-Cl angles ranging between 88.67(2) and 91.33(2)°. The coordination plane of the $[PdCl_4]^{2-}$ anion in **9a**, **10a** and **11a**, is tilted by 123.0°, 74.4° and 123.6°, respectively, relative to the mean plane of the imidazolium rings.

Although there are numerous interactions between the hydrogen atoms and the chloride ligands, these are, as expected, generally much weaker than those in the presence of perfluorated anions. The shortest hydrogen bond is found in **11a**, stemming from H2 to Cl1, 2.564 Å. Yet, in **9a** and **10a** there are additional close contacts from hydrogen atoms to the metal centre, H5B···Pd1 2.671 Å in **9a** and H12C···Pd1 2.763 Å in **10a**.

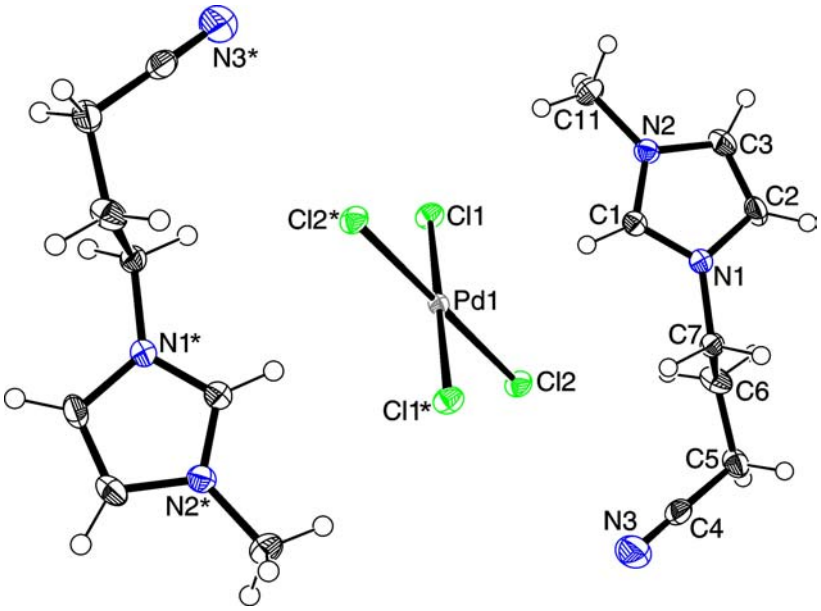

Figure 3.1 ORTEP-plot of 9a, ellipsoids are drawn at the 50% probability level; the starred atoms are obtained by the symmetry operation –x+2, -y+2, -z+1.

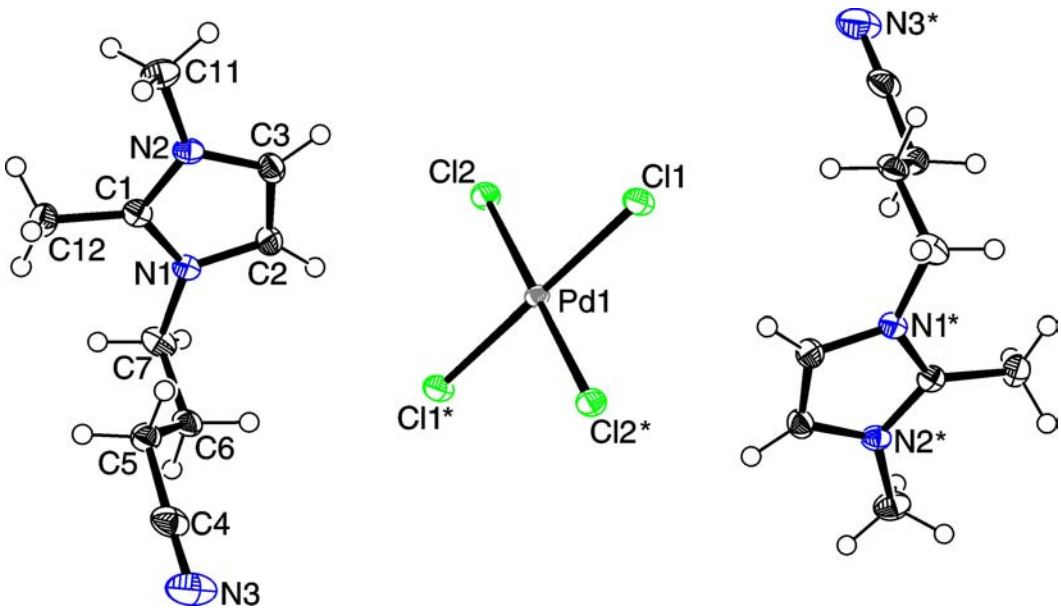

Figure 3.2 ORTEP-plot of 10a, ellipsoids is drawn at the 50% probability level; the starred atoms are obtained by the symmetry operation –x, -y, -z.

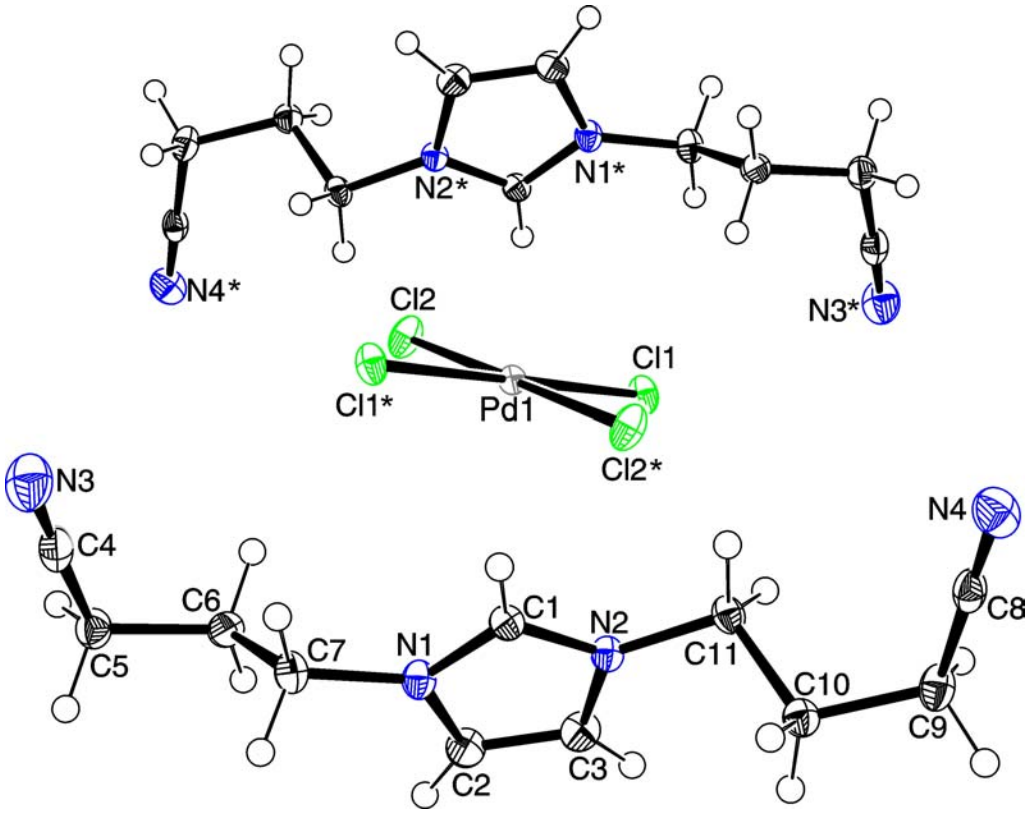

Figure 3.3 ORTEP-plot of 11a, ellipsoids are drawn at the 50% probability level; the starred atoms are obtained by the symmetry operation –x, -y, -z+2.

Table 3.1 Selected bond lengths (Å) and angles (°) for compounds 9a, 10a and 11a

	9a	10a	11a
Pd1-Cl1	2.3147(6)	2.3229(5)	2.3113(6)
Pd1-Cl2	2.3113(6)	2.3177(5)	2.3205(7)
C1-N1	1.335(3)	1.351(3)	1.333(3)
C1-N2	1.333(3)	1.336(3)	1.339(3)
C2-N1	1.384(3)	1.387(3)	1.384(3)
C3-N2	1.385(3)	1.383(3)	1.380(3)
C2-C3	1.349(4)	1.349(3)	1.356(4)
N3-C4	1.141(3)	1.148(3)	1.143(4)
N4-C8			1.143(4)
N3-C4-C5	178.9(3)	177.8(3)	177.9(3)
N4-C8-C9			179.4(3)
N1-C1-N2	108.5(2)	107.2(2)	108.7(2)

The main incentive for studying the reactions of the nitrile functionalised ILs with $PdCl_2$ was to characterise the way in which the liquids interact with the metal as it was envisaged that the resulting systems might find applications in catalysis. As mentioned above, 1-alkyl-3-methylimidazolium chloride react with palladium chloride to form $[C_nmim]_2PdCl_4$,[1] which has been dissolved in ILs and used as catalyst in 1,3-butadiene hydrodimerization.[2] More generally, palladium(II) compounds are widely used as catalyst precursors for a wide range of different reactions, notably C-C coupling reactions[3], and with this in mind the catalytic activity of these palladium complexes was investigated in Suzuki, Heck and Stille C-C coupling reactions as well as in hydrogenation reactions.

3.2.2 Carbon-Carbon coupling reactions

Suzuki cross-coupling reactions in $[C_4mim][BF_4]$ using $Pd(PPh_3)_4$ as the catalyst have been reported previously, and a number of benefits have been noted compared to using organic solvents including increased reaction rates, higher selectivity, as well as operating under milder conditions and giving rise to catalyst recycling and reuse.[4] Palladium (II) complexes such as $Pd(OAc)_2$ and $PdCl_2$ have been used as precatalysts in Suzuki reactions.[5] Quantitative data concerning the retention of the palladium(0) or palladium(II) catalyst was not reported. It is not unreasonable to assume that loss to the organic phase takes place. With this in mind, the palladium complexes **9** and **10**, were evaluated in $[C_4mim][BF_4]$ and some nitrile F-ILs.

The results from the Suzuki coupling reaction between iodobenzene and phenylboronic acid to afford biphenyl are summarized in Table 3.2.

Table 3.2 Suzuki cross-coupling reaction in ILs catalyzed by palladium complexes[a]

Entry	Catalyst Precursor	Ionic Liquid	Yield (%)[b]	Pd loss
1	**9a**	$[C_3CNmim][BF_4]$	100	5
2	**9b**	$[C_3CNmim][BF_4]$	100	5
3	**9c**	$[C_3CNmim][BF_4]$	< 99	5
4	**9a**	$[C_4mim][BF_4]$	100	116
5	**9b**	$[C_4mim][BF_4]$	100	86
6	**9c**	$[C_4mim][BF_4]$	100	96
7	$PdCl_2$	$[C_3CNmim][BF_4]$	100	5
8	$PdCl_2$	$[C_4mim][BF_4]$	100	84
9	**10c**	$[C_3CNmim][BF_4]$	100	< 1
10	**10c**	$[C_4mim][BF_4]$	< 99	86
11	**9a**	$[C_3CNmim][Tf_2N]$	100	2
12	**9a**	$[(C_3CN)_2im][Tf_2N]$	100	< 1

[a]

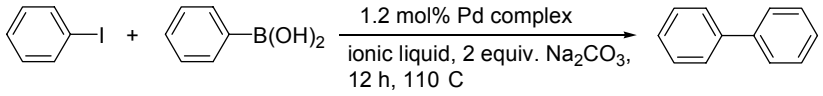

[b] Conversion determined by GC

Figure 3.4 Comparison of reactions after catalysis in the CN-IL, (left) $[C_3CNmim][BF_4]$ and $[C_4mim][BF_4]$ (right)

It can be seen from Table 3.2 that all the complexes are active catalysts for Suzuki coupling in both $[C_4mim][BF_4]$ and the nitrile-functionalized ILs. In all cases, essentially quantitative conversion to

biphenyl was observed. Comparable activities were also observed when $PdCl_2$ was used (entries 7 and 8 in Table 3.2). The most notable difference observed between the common and the F-IL is the extent of palladium leaching, which is always considerably higher for $[C_4mim][BF_4]$ than for the ILs bearing nitrile functionalities. The advantage of using nitrile functionalised IL can also be appreciated from Figure 3.4. In $[C_4mim][BF_4]$, the precipitation of palladium black is observed, whereas in $[C_3CNmim][BF_4]$ no such precipitation occurs.

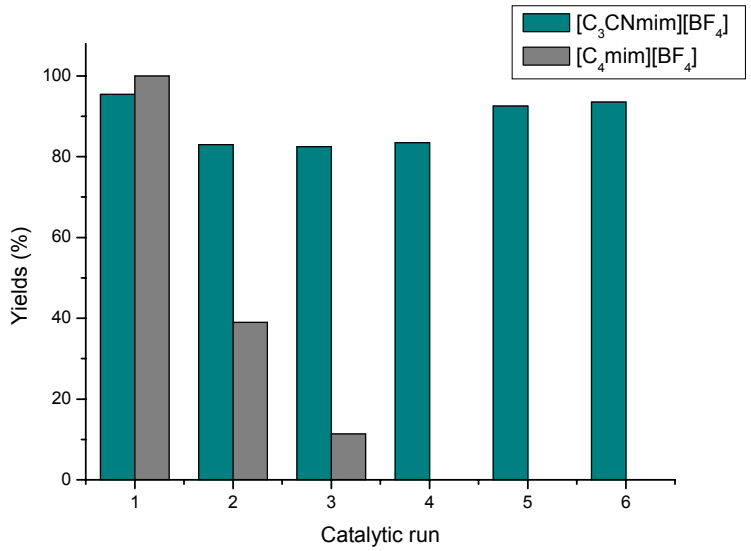

Figure 3.5 Comparison of recycling for the Suzuki reaction of nitrile F-IL and conventional IL (using 9a as catalyst).

Heck reactions have also been investigated in ILs[6] and carbene complexes derived from the imidazolium based ILs have been implicated in catalysis,[7,8] The Heck coupling of iodobenzene and ethyl acrylate to give ethyl cinnamate has been undertaken using our system and the results are collected in Table 3.3.

Table 3.3 Heck coupling of iodobenzene with ethyl acrylate.[a]

Entry	Catalyst Precursor	Ionic liquid	Yield (%)[b]	Selectivity (%)[c]	Pd loss
1	**9a**	$[C_4mim][BF_4]$	25	100	75
2	**9b**	$[C_4mim][BF_4]$	26	100	60
3	**9c**	$[C_4mim][BF_4]$	23	100	75
4	**9a**	$[C_3CNmim][BF_4]$	26	100	10
5	**9b**	$[C_3CNmim][BF_4]$	26	100	9
6	**9c**	$[C_3CNmim][BF_4]$	27	100	9
7	**9a**	$[C_3CNmim][Tf_2N]$	26	100	10
8	**9a**	$[(C_3CN)_2mim][Tf_2N]$	28	100	9
9	$PdCl_2$	$[C_3CNmim][BF_4]$	43	100	1
10	$PdCl_2$	$[C_4mim][BF_4]$	51	100	111

a

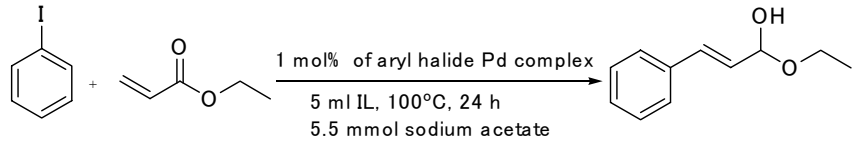

[b] conversion determined by GC

[c] selectivity of trans-ethyl cinnamate

All the complexes are active in the Heck reaction studied, affording trans-ethyl cinnamate as the only product. $PdCl_2$ is a more effective catalyst precursor in both nitrile-functionalised and conventional ILs compared to the pre-coordinated palladium species evaluated. In all cases, superior catalyst retention was observed in the nitrile-functionalized IL with typical leaching of around 10 ppm.

Table 3.4 Stille coupling of iodobenzene with tributylvinyl tin[a]

Entry	Catalyst Precursor	Ionic liquid	Yield (%)[b]	Pd loss
1	**9a**	$[C_4mim][BF_4]$	58	6
2	**9a**	$[C_3CNmim][BF_4]$	80	< 1
3	**9b**	$[C_3CNmim][BF_4]$	81	< 1
4	**9c**	$[C_3CNmim][BF_4]$	84	< 1
5	**9a**	$[C_3CNmim][BF_4]$	83	< 1
6	**9a**	$[C_3CNmim][Tf_2N]$	63	< 1
7	**9a**	$[(C_3CN)_2im][Tf_2N]$	68	< 1
8	$PdCl_2$	$[(C_3CN)_2im][BF_4]$	96	< 1
9	$PdCl_2$	$[C_4mim][BF_4]$	84	13

[a]

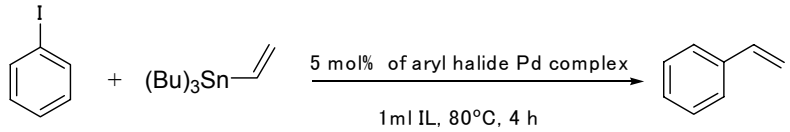

[b]conversion determined by GC

The Stille C-C coupling reaction,[9] has also been reported in ILs with benefits such as elimiation of toxic co-catalysts, enhanced activities and recyclibility.[10] The Stille coupling reaction of vinylstannane with iodobenzene has been investigated and the data is summarized in Table 3.4. In keeping with previous observations inhibition of palladium leaching is accomplished in the nitrile-functionalized ILs, however, in addition, significantly superior activities are also observed in the nitrile-functionalized ILs. There is also an anion effect in that $[Tf_2N]^-$ based systems are less effective than the equivilant $[BF_4]^-$ ILs.

Figure 3.6 shows the reaction mixtures after catalysis in $[C_4mim][BF_4]$, **3c**, **3d** and **7d**. It is clear that in the non-F-IL, $[C_4mim][BF_4]$, palladium precipitates are observed. In the nitrile-F-ILs, $[C_3CNmim][BF_4]$, however, such particle aggregation is not observed. Nevertheless, for the nitrile F-IL $[C_3CNmim][BF_4]$ (Figure 3.6-B), the catalytic system shows an apparent reddish homogeneous state; for nitrile F-IL of $[Tf_2N]$ anion, minor aggregation is observed, which appears to be evenly dispersed in IL phase (Figure 3.6-C and D). There is also a difference between the "single-armed" and "double-armed" ILs. In the "single-armed" IL, only palladium particles can be found (Figure 3.6-D); whereas in "double-armed" one both the catalyst particles and reddish appearance are presented (Figure 3.6-D). Such phenomena might be related to the coordinating ability of nitrile group to the palladium catalyst. The nucleophilic nature of the $[Tf_2N]^-$ anion might

also favours catalyst reduction to Pd(0) nanoparticles. It is not unreasonable to propose that these differences contribute to the differences in catalytic activity, i.e. F-IL with the $[BF_4]^-$ anion catalyzes the reaction in a "homogeneous" manner by the nitrile group coordinating to catalyst, whereas "single-armed" F-IL with $[Tf_2N]^-$ afford nanoparticles that are less active. The "double-armed" F-IL $[(C_3CN)_2im][Tf_2N]$ shows intermediate behaviour, and results in a slightly enhanced catalytic activity over that of the "single-armed" analogue.

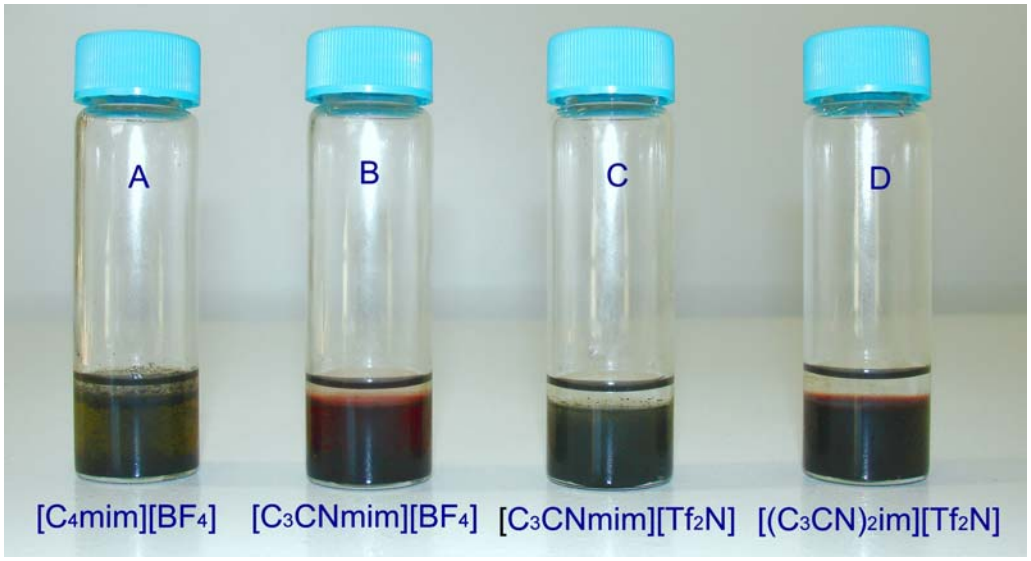

Figure 3.6 Comparison of different catalytic systems for the Stille reaction (9a was used as catalyst precursor)

Transition electron microscopy (TEM) has been extensively used to analyze for nanoparticles in ILs. The preparation and application of transition-metal nanoparticles immobilized in ILs has also been reported. The first example is the iridium nanoparticles prepared in $[C_4C_1im][PF_6]$, which is active for alkene hydrogenation.[11] Other nanoparticles composed of rhodium,[12] platinum,[13] and gold[14] have also been published. Evidence has accumulated to show that many C-C coupling reactions involve palladium nanoparticles, especially when simple metal salts, for example, palladium (II) halides, are used as the catalyst precursors.[15, 10(d)]. Palladium nanoparticles were also isolated from $[C_4mim][BF_4]$ and $[C_3CNmim][BF_4]$ following the Stille reaction and they are analyzed by TEM. As shown in Figure 3.7, the nanoparticles obtained from $[C_4mim][BF_4]$ have a diameter of ~20 nm, whereas the nanoparticles obtained from $[C_3CNmim][Tf_2N]$ exhibit a diameter of ~5 nm.

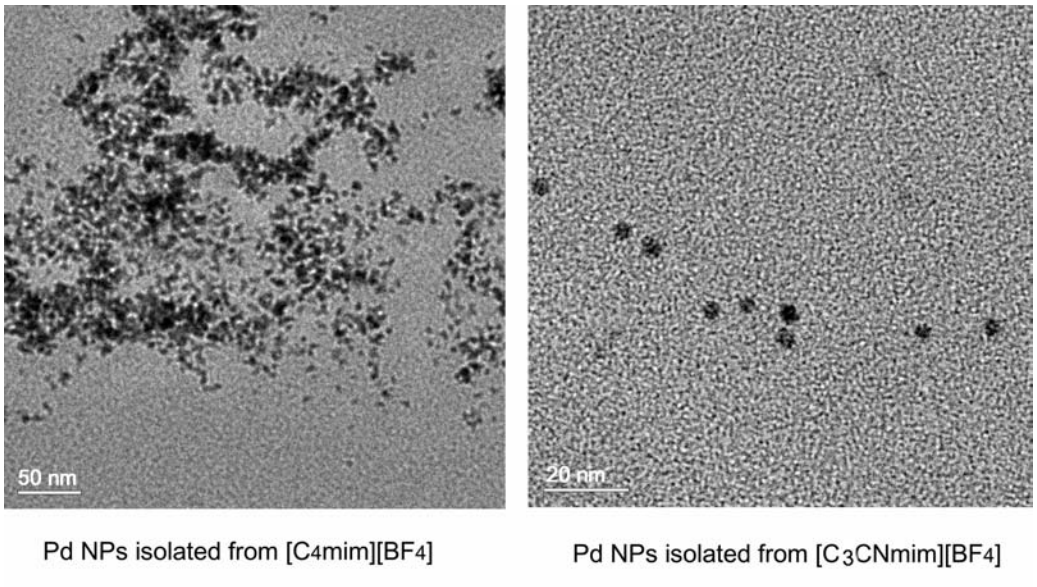

Figure 3.7 Comparison of TEM images of the Pd NPs in different ILs

It is plausible that the nitrile functionality weakly coordinates to the palladium nanoparticle surface and therefore stabilizing the nanoparticles, preventing nanoparticle agglomeration into bigger particles such that, catalyst activity is maintained.

Palladium leaching into the organic extract was also analyzed by the ICP. Similarly to the Suzuki and Heck reactions, the palladium detected in the extract from non-functioanlized IL, $[C_4mim][BF_4]$, is about 10 times greater than that from nitrile functionalized ILs, which again, demonstrates the excellent catalyst retention capacity of the nitrile F-ILs.

To further demonstrate the catalyst stabilizing advantage of the nitrile F-ILs, the recyclability of the Stille reaction in nitrile F-ILs was evaluated compared and with non-F-IL. It is shown in Figure 3.8 that the yield of the Stille product can be maintained around 90% in nitrile-F-IL, $[C_3CNmim][BF_4]$, after six runs, whilst in non-F-IL $[C_4mim][BF_4]$ the yield decreased after the first run and continues to drop after each recyle.

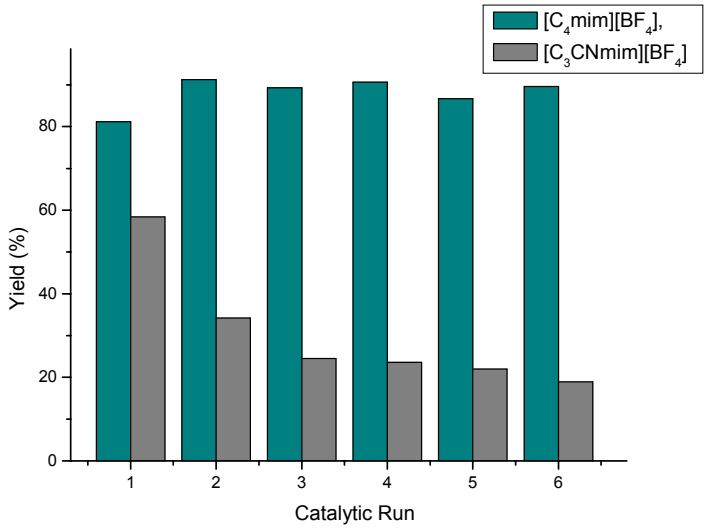

Figure 3.8 Comparison of the catalytic recycling in the Stille reaction of the nitrile functionalized IL and non-functionalized IL

3.2.3 Hydrogenation of cyclohexadiene

Hydrogenation reactions catalysed by transition metal complexes have previously been carried out in ILs,[16] and therefore the catalytic activity of **9a, 9b** and **9c** were evaluated in $[C_4mim][BF_4]$ and $[C_3CNmim][BF_4]$ under biphasic condition. Using cyclohexa-1,3-diene as the substrate it was found that both high conversion and high selectivity to the partially hydrogenated product, cyclohexene, was possibile. Selective hydrogenation of cyclohexa-1,3-diene using palladium and platinum complexes with chiral ferrocenylamine sulfide and selenide ligands have been reported previously.[40] However, the advantage of our palladium ILs system is that the use of other expensive chiral ligands is not necessary.

As illustrated in Table 3.5, biphasic hydrogenation proceeded with high conversions and excellent selectivity by using complexes **9a**, **9b**, **9c** and $PdCl_2$ in $[C_4mim][BF_4]$ and $[C_3CNmim][BF_4]$.

Table 3.5 Hydrogenation of cyclohexa-1,3-diene by complexes 9a, 9b, and 9c[a]

Entry	Catalytic precursor	Ionic liquid	Conversion (%)	Selectivity (%)[b]	Pd loss
1	**9a**	$[C_4mim][BF_4]$	99	99	39
2	**9b**	$[C_4mim][BF_4]$	99	99	39
3	**9c**	$[C_4mim][BF_4]$	93	98	58
4	**9a**	$[C_3CNmim][BF_4]$	96	96	5
5	**9b**	$[C_3CNmim][BF_4]$	95	98	5
6	**9c**	$[C_3CNmim][BF_4]$	93	99	4
7	$PdCl_2$	$[C_4mim][BF_4]$	84	99	96
8	$PdCl_2$	$[C_3CNmim][BF_4]$	93	100	10

a

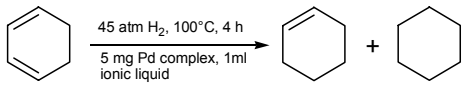

[b] selectivity to cyclohexene.

ICP analysis also shows superior catalyst retention in the nitrile functionalised IL than in $[C_4mim][BF_4]$.

3.3 Concluding remarks

The palladium complexes of CN functionalized imidazolium salts, among which **9b**, **9c**, **9d**, **10b**, **10c** and **10d** are among the first examples of transition metal complexes using the imidazolium cation as carrier for coordination center, i.e. nitrile functionality. The bimetallic complexes **11b** and **12b** containing both Pd atom in the anions and cations are highly novel considering both transition metals centers can be easily varied. The complexes are active catalyst precusors for Suzuki, Heck and Stille C-C coupling reaction as well as for hydrogenation. The most significant advantage of the Pd/CN-functionalised catalytic system, however, is the superior catalyst retetion and improved stabilizing ability (evidenced by TEM observation), by which a highly recyclable solvent/catalyst system is developed.

3.4 Experimental

Trimethylsilyimidazole, sodium tetrafluoroborate, hexafluorophosphoric acid, lithium bis(trifluoromethylsulfonyl)amide and palladium dichloride were purchased from Aldrich Chemical Co. Synthesis of imidazolium salts and palladium complexes was performed under an inert atmosphere of dry nitrogen using standard Schlenk techniques. Solvents were dried using the

appropriate reagents and distilled prior to use. NMR spectra were obtained at 20°C with a Bruker DMX 400 instrument using $SiMe_4$ for ^1H, ^{13}C as external standards. IR spectra were recorded on a Perkin-Elmer FT-IR 2000 system. ESI-MS spectra were recorded on a ThermoFinnigan LCQ™ Deca XP Plus quadrupole ion trap instrument. Samples were infused directly into the source at 5 μL min^{-1} using a syringe pump. The spray voltage was set at 5 kV and the capillary temperature at 50°C. The MS detector was tuned automatically on the base peak, which optimized the remaining parameters. Elemental analysis was carried out by the Institute of Molecular and Biological Chemistry at the EPFL. Differential scanning calorimetry was performed with a SETARAM DSC 131. ICP-AES (inductively coupled plasma-atomic emission spectrometer). Samples were analyzed on a Perkin-Elmer Optima 3000 ICP-AE spectrometer. Intensities of spectral lines at 340.458 nm were measured in all samples and standards. The Pd level in the samples was determined by comparing the intensity of the spectral line with a Pd standard curve. Each sample was measured three times, and the average Pd concentration level of these measurements has been reported. Melting points of solid samples were measured with Büchi Schmelzpunktbestimmungs Apparat capillary melting point apparatus.

*Synthesis of complexes **9a**, **10a** and **11a***

Typical procedure: A reaction mixture of $PdCl_2$ (177 mg, 1.0 mmol) and **3a** (373 mg, 2.00 mmol) in 5 ml acetonitrile was heated at 80°C for 4 h. After removal of the solvent, the resulting orange solid was washed with dichloromethane (2 × 2.0 ml), dried under vacuum to give the product.

9a $[(C_3CNmim)_2]PdCl_4$: Yield: 99%. M.p.: 178°C. ^1H NMR (DMSO-d6): 9.37 (s, 1H), 7.87 (s, 1H), 7.79 (s, 1H), 4.32 (t, *J*(H, H) = 6.60 Hz, 2H), 3.89 (s, 3H), 2.64 (t, *J*(H, H) = 6.80 Hz 2H), 2.18 (m, 2H). ^{13}C NMR (DMSO-d6): 135.28, 131.36, 120.13, 116.18, 44.02, 31.22, 21.77, 9.99. IR (cm^{-1}): $\nu_{C\equiv N}$, 2241; Anal. Calcd. for $C_{16}H_{24}Cl_4N_6Pd$ (%): C 35.03, H 4.41, N 15.32; Found: C 35.07, H 4.44, N 15.29%.

10a $[(C_3CNdmim)_2]PdCl_4$: Yield: 96%. M.p.: 175°C. ^1H NMR (DMSO-d6): δ = 7.72 (s, 1H), 7.68 (s, 1H), 4.22 (t, *J*(H, H) = 7.16 Hz, 2H), 3.75 (s, 3H), 2.63 (t, *J*(H, H) = 7.18 Hz, 2H), 2.61 (s, 3H), 2.06 (m, 2H); ^{13}C NMR (DMSO): δ = 148.10, 125.94, 124.26, 123.24, 49.62, 38.21, 28.51, 16.88 and 12.74; IR (cm^{-1}): $\nu_{C\equiv N}$, 2244; Anal. Calcd. for $C_{18}H_{28}Cl_4N_6Pd$ (%): C 37.49, H 4.89, N 14.57; Found: C 37.52, H 4.83, N 14.64.

11a $[(C_3CN)_2mim)_2]PdCl_4$: Yield: 96%. M.p.: 125°C. ^{1}H NMR (DMSO-d6): δ = 9.43 (s, 1H), 7.78 (s, 2H), 4.27 (t, *J*(H, H) = 7.16 Hz, 2H), 2.61 (p, *J*(H, H) = 7.18 Hz, 2H), 2.15 (t, *J*(H, H) = 7.16 Hz, 2H); ^{13}C NMR (DMSO): δ = 137.2, 123.1, 120.1, 48.2, 25.6, 14.01 and 12.7; IR (cm^{-1}): $\nu_{C\equiv N}$, 2249; Anal. Calcd. for $C_{22}H_{30}C_{l4}N_8Pd$ (%): C 40.36, H 4.62, N 17.11; Found: C 40.40, H 4.58, N 17.14.

*Synthesis of Complexes **9b**, **9c**, **9d**, **10b**, **10c**, and **10d***

Typical procedure: A reaction mixture of $PdCl_2$ (177 mg, 1.0 mmol) and **3b** (590 mg, 2.00 mmol) in dichloromethane (5.0 ml) was stirred at r.t. for 4 days. The resulting yellow solid was collected by centrifugation filtration and washed with dichloromethane (2 × 2.0 ml), dried under vacuum to give the product.

9b $[(C_3CNmim)_2PdCl_2]_2[PF_6]$: Yield: 98%. M.p.: 130°C. ^{1}H NMR (DMSO-d6): 9.09 (s, 1H), 7.76 (s, 1H), 7.70 (s, 1H), 4.25 (t, *J*(H, H) = 6.90 Hz, 2H), 3.85 (s, 3H), 2.58 (t, *J*(H, H) = 7.10 Hz, 2H), 2.18 (m, 2H), ^{13}C NMR (DMSO-d6): 135.2, 131.8, 120.1, 116.0, 44.0, 31.1, 21.5, 9.9. ^{31}P NMR (DMSO-d6): -145 (hept). IR (cm^{-1}): $\nu_{C\equiv N}$, 2322; Anal. Calcd. for $C_{16}H_{24}Cl_2F_{12}N_6P_2Pd$ (%): C 25.03, H 3.15, N 10.95; Found: C 25.12, H 3.23, N 10.88.

10b $[(C_3CNdmim)_2PdCl_2]_2[PF_6]$: Yield: 95%; M. p.: 160°C; ^{1}H NMR (DMSO-d6): δ = 7.62 (s, 1H), 7.60 (s, 1H), 4.16 (t, *J*(H, H) = 7.17 Hz, 2H), 3.72 (s, 3H), 2.56 (s, 3H), 2.53 (t, *J*(H, H) = 7.18 Hz, 2H), 2.05 (m, 2H); ^{13}C NMR (DMSO-d6): δ = 148.0, 125.9, 124.2, 123.1, 49.6, 38.0, 28.3, 16.8, 12.6; IR (cm^{-1}): $\nu_{C\equiv N}$, 2324; Anal. Calcd. for $C_{18}H_{28}Cl_2F_{12}N_6P_2Pd$ (%): C 27.17, H 3.55, N 10.56; Found: C 27.25, H 3.63, N 10.64.

9c: $[(C_3CNmim)_2PdCl_2]_2[BF_4]$ Yield: 99%. M.p.: 80°C. ^{1}H NMR (DMSO-d6): 9.09 (s, 1H), 7.77 (s, 1H), 7.71 (s, 1H), 4.25 (t, *J*(H, H) = 7.00 Hz, 2H), 3.86 (s, 3H), 2.58 (t, *J*(H, H) = 7.10 Hz, 2H), 2.18 (m, 2H). ^{13}C NMR (DMSO-d6): 132.1, 120.1, 118.6, 116.0, 44.0, 33.3, 27.8, 9.8. IR (cm^{-1}): $\nu_{C\equiv N}$, 2324; Anal. Calcd. for $C_{16}H_{24}B_2Cl_2F_8N_6Pd$ (%): C 29.50, H 3.71, N 12.90; Found: C 29.62, H 3.83, N 12.88.

10c $[(C_3CNdimim)_2PdCl_2]_2[BF_4]$ Yield: 94%; M. p.: 130°C. ^{1}H NMR (DMSO-d6): δ = 7.62 (s, 1H), 7.61 (s, 1H), 4.16 (t, *J*(H, H) = 7.17 Hz, 2H), 3.72 (s, 3H), 2.57 (s, 3H), 2.56 (t, *J*(H, H) = 7.17 Hz, 2H), 2.06 (m, 2H); ^{13}C NMR (DMSO-d6): δ = 148.10, 125.91, 124.20, 123.16, 49.61, 38.09, 28.39, 16.81 and 12.60; IR (cm^{-1}): $\nu_{C\equiv N}$, 2325; Anal. Calcd. for $C_{18}H_{28}B_2Cl_2F_8N_6Pd$ (%): C 31.82, H 4.15, N 12.37; Found: C 31.88, H 4.14, N 12.34.

9d: $[(C_3CNmim)_2PdCl_2]_2[Tf_2N]$ yield: 99%. ^{1}H NMR (DMSO-d6): 9.09 (s, 1H), 7.76 (s, 1H), 7.39 (s, 1H), 4.26 (t, *J*(H, H) = 7.00 Hz, 2H), 3.83 (s, 3H), 2.56 (t, *J*(H, H) = 7.10 Hz, 2H), 2.14 (m, 2H). ^{13}C NMR (DMSO-d6): 137.2, 124.2, 122.7, 120.0, 48.0, 36.2, 25.6, 13.9; IR (cm^{-1}): $\nu_{C\equiv N}$, 2315; Anal. Calcd. for $C_{22}H_{28}Cl_2F_{12}N_8O_8PdS_4$ (%): C 24.79, H 2.65, N 10.51; Found: C 24.71, H 2.59, N 10.49.

10d $[(C_3CNdimim)_2PdCl_2]_2[Tf_2N]$ Yield: 94%; ^{1}H NMR (DMSO-d6): δ = 7.62 (s, 2H), 7.60 (s, 1H), 4.42 (t, *J*(H, H) = 7.17 Hz, 2H), 3.72 (s, 3H), 2.96 (s, 3H), 2.65 (t, *J*(H, H) = 7.17 Hz, 2H), 2.05 (p, 2H); ^{13}C NMR (DMSO-d6): δ = 145.1, 122.9, 121.5, 120.1, 46.6, 35.1, 25.4, 13.8, 9.6; IR (cm^{-1}): $\nu_{C\equiv N}$, 2290; Anal. Calcd. for $C_{22}H_{28}Cl_2F_{12}N_8O_8PdS_4$ (%): C 24.79, H 2.65, N 10.51; Found: C 24.88, H 2.52, N 10.34.

*Synthesis of **11b** and **12b***

Typical procedure: $PdCl_2$ (177 mg, 1.0 mmol) was added to a suspension of **9a** in dichloromethane (5.0 ml). The reaction mixture was stirred at room temperature for 5 days, during which time, the orange colour of the suspension disappeared and a light yellow suspension formed. The resulting yellow solid was collected by centrifugation filtration and washed with dichloromethane (2 × 2.0 ml), dried under vacuum to give the product.

11b $[(C_3CNmim)_2PdCl_2]_2[PdCl_4]$ Yield: 95%; M. p.: 153°C. ^{1}H NMR (DMSO-d6): δ = 9.11 (s, 1H), 7.77 (s, 1H), 7.71 (s, 1H), 4.24 (t, *J*(H, H) = 6.84 Hz, 2H), 3.84 (s, 3H), 2.58 (t, *J*(H, H) = 6.80 Hz , 2H), 2.11 (m, 2H); ^{13}C NMR (DMSO-d6): δ = 140.2, 127.1, 125.7, 123.0, 51.0, 39.2, 28.6, 16.9; IR (cm^{-1}): $\nu_{C\equiv N}$, 2300; Anal. Calcd. for $C_{16}H_{24}Cl_6N_6Pd_2$ (%): C 26.47, H 3.33, N 11.58; Found: C 26.51, H 3.35, N 11.57.

12b $[(C_3CNmim)_2PdCl_2]_2[PdCl_4]$ Yield: 94%; M. p.: 145°C; ^{1}H NMR (DMSO-d6): δ = 7.23 (s, 1H), 7.18 (s, 1H), 4.06 (t, *J*(H, H) = 7.17 Hz, 2H), 3.61 (s, 3H), 2.44 (s, 3H), 2.39 (t, *J*(H, H) = 7.18 Hz, 2H), 2.02 (m, 2H); ^{13}C NMR (DMSO-d6): δ = 148.0, 124.6, 122.9, 119.3, 48.7, 37.0, 27.2, 15.8, 11.4; IR (cm^{-1}): $\nu_{C\equiv N}$, 2309; Anal. Calcd. for $C_{18}H_{28}Cl_6N_6Pd_2$ (%): C 28.67, H 3.74, N 11.15; Found: C 28.71, H 3.68, N 11.14.

Crystallography

Data collection for the X-ray structure determinations were performed on a KUMA diffractometer system, except for 9b and 9c, which were measured on a mar345 IPDS, by using graphite-monochromated MoKα (0.71070 Å) radiation and a low temperature device [T = 140(2) K]. Colorless crystals of 6 and 8 suitable for X-ray diffraction, were obtained from a water-acetonitrile solution at 0 °C. Data reduction was performed by CrysAlis RED.[17] Structure solution and refinement was performed on PCs by using the SHELX97[18] software package, with the exception of 11a, which was solved with SHELX86. Graphical representations of the structures were made with ORTEP32.[19] Structures were solved by direct methods (except 3b, which was solved by Patterson methods) and successive interpretation of the difference Fourier maps, followed by full matrix least-squares refinement (against F2). An empirical absorption correction (DELABS)[20] was applied for 9b and 9c. All atoms were refined anisotropically. The contribution of the hydrogen atoms, in their calculated positions, was included in the refinement using a riding model. Compound 11a was refined using the TWIN command, implemented in SHELX97. Relevant data concerning crystallographic data, data collection and refinement details are listed in Table 3.6.

Table 3.6 Relevant crystallographic data for 9a, 10a and 11a

	9a	**11a**	**11a**
Formula	$C_{16}H_{24}Cl_4N_6Pd$	$C_{18}H_{28}Cl_4N_6Pd$	$C_{22}H_{30}Cl_4N_8Pd$
M	548.61	576.66	654.74
Crystal system	monoclinic	monoclinic	triclinic
Space group	*I*2/*a*	$P2_1/c$	*P*-1
a/*Å*	14.381(1)	8.3277(4)	8.3363(7)
b/*Å*	10.8029(8)	11.3897(8)	8.8898(6)
c/*Å*	14.586(1)	13.1294(9)	10.667(1)
α/°	90	90	90.517(8)
β/°	100.68(1)	104.847(5)	107.260(8)
γ/°	90	90	113.689(7)
V/$Å^3$	2226.8(3)	1203.8(1)	683.9(1)
Z	4	2	1
Density [Mg/m^3]	1.636	1.591	1.590
*Θ*range/°	$3.49 \leq \Theta \leq 25.02$	$3.10 \leq \Theta \leq 25.02$	$3.46 \leq \Theta \leq 25.02$
μ/mm^{-1}	1.327	1.232	1.097
Reflections measured	6508	6906	4088
Unique reflections [$I>2\sigma($.	1966 (R_{int} = 0.0373)	2085 (R_{int} = 0.0320)	2114 (R_{int} = 0.0273)
Final *R*1, *wR*2[$I>2\sigma(I)$]	0.0219, 0.0474	0.0230, 0.0632	0.0245, 0.0630

Catalysis procedures:

Suzuki coupling

Typical procedure: To a 20 ml two-necked flask fitted with a septum and reflux condenser iodo-benzene halide (2.5 mmol, 1 equiv.) was mixed with $[C_3CNmim][BF_4]$ (5 ml) under a nitrogen atmosphere. Then arylboronic acid (335mg, 2.75mmol, 1.1 equiv.), Na_2CO_3 (560 mg, 5.28 mmol, 2.1 equiv.) and 2.5 ml water followed by the palladium complex (0.03 mmol, 1.2 mol% based on iodo-benzene). The mixture was heated to 110^{o}C and stirred vigorously for 12 h. The mixture was then cooled and extracted with diethyl ether (3 x 15 ml). The combined extracts were washed with brine and water and then dried with $MgSO_4$. The biphenyl product was obtained by filtering the solution followed by evaporation to dryness, and was characterized by GC and ^{1}H NMR. The IL phase was washed with diethyl ether again and put under vacuum for overnight and be ready for catalytic recycle. The sample for ICP analysis was prepared by taking 5 ml diethyl ether extract, removing the solvent, then adding 500 ml 65% HNO_3. The mixture was stirred at room temperature for 2 days and evaporated to dryness again. The remains were dissolved by 15 ml 2% HNO_3 aqueous solution.

Heck reactions

Typical procedure: To a 20 ml two-necked flask fitted with a septum and reflux condenser iodo-benzene (5.0 mmol, 1 equiv.) was mixed with $[C_3CNmim][BF_4]$ (5 ml) under nitrogen atmosphere. Then anhydrous sodium acetate (451 mg, 5.5 mmol, 1.1 equiv.), palladium complex (0.05 mmol, 1 mol% of iodo-benzene) were added. After flushing the flask with dry nitrogen, ethyl acrylate (0.76 ml, 7.0 mmol, 1.4 equiv.) was injected through the septum. The mixture was heated to 100^{o}C at stirred vigorously for 24 h. When the reaction finished, the mixture was cooled down and extracted with ethyl acetate (3 x 30 ml). The combined extract were washed with brine and water and then dried with $MgSO_4$. The product was obtained by filtering the solution followed by evaporation to dryness, and characterized by GC and ^{1}H NMR.

Stille reactions

Typical procedure: Reactions were carried out in 5 ml two-neck flask fitted with a septum vials. To a suspension of palladium complex (0.025 mmol) in 1 ml of IL were added iodobenzene (0.5 mmol) and the tributylvinylstannane (0.6 mmol). The mixtures were stirred at 80 °C for 2 h. The products

were extracted with *n*-pentane (3 × 1 ml), the organic layers were dried over $MgSO_4$ and diluted to an exactly known volume. The product was characterised by GC and ^1H NMR.

Hydrogenation of cyclohexa-1,3-diene

The palladium complex (5.0 mg) was dissolved in the IL (1.0 ml), and the 1,3-cyclohexadiene (1.0 ml) was added. The multi-cell autoclave was pressurized with H_2 to 45 atm, sealed and heated to 100°C for 4 h. The products were identified using a combination of GC versus known standards and ^{13}C NMR spectroscopy. Turnover frequencies are quoted in number of moles of substrate converted per mole of catalyst per hour.

TEM sample preparation

A reaction mixture containing IL and catalyst was taken after the Stille catalysis, and ethanol (2.0 mL) was added. The mixture was centrifuged, and the nanoparticles were collected at the bottom of the centrifugation vessel. They were then suspended in ethanol (2 mL) and centrifuged, and the ethanol was decanted. This process was repeated four times to wash the nanoparticles. Finally, the ethanol/nanoparticle suspension was deposited on a carboncoated copper grid (500 mesh) and dried at ambient temperature. The TEM images were obtained on a PHILIPS CM 20 transmission electron microscope.

3.5 References

[1] C. Hardacre, J. D. Holbrey, P. B. McCormac, S. E. J. McMath, M. Nieuwenhuyzen, K. R. Seddon, *J. Mater. Chem.* **2001**, *11*, 346.

[2] J. E. L. Dullius, P. A. Z. Suarez, S. Einloft, R. F. de Souza J. Dupont, *Organometallics* **1998**, *17*, 815.

[3] (a) A. O. King, *Handbook of Organopalladium Chemistry for Organic Synthesis* John Wiley & Sons, Inc., **2002**, *2*, 2753. (b) A. O. King, R. D. Larsen, E. Negishi, *Handbook of Organopalladium Chemistry for Organic Synthesis*, John Wiley & Sons, Inc., **2002**, *2*, 2719-2752. (c) M. K. Lakshman, *J. Organomet. Chem*. **2002**, *653*, 234.

[4] C. J. Mathews, P. J. Smith, T. Welton, *Chem. Commun*. **2000**, 1249.

[5] Y. Deng, L. Gong, A. Mi, H. Liu, Y. Jiang, *Synthesis*, **2003**, *3*, 337.

[6] For example, see: (a) D. E. Kaufmann, M. Nouroozian, H. Henze, *Syntlett* **1996**, 1091. (b) W. A. Hermann, V. P. W. Böhm, *J. Organomet. Chem*. **1999**, 572. (c) V. P. W. Böhm, W. A. Hermann, *Chem. Eur. J*. **2000**, *6*, 1017. (d) S. Bouquillon, B. Ganchequi, B. Estrine, F. Henin, J. Muzart, *J. Organomet. Chem*. **2001**, *643*, 153. (e) V. Calo, A. Nacci, A. Monopoli, L. Lopez, A. di Cosmo, *Tetrahedron*, **2001**, *57*, 6071. (f) J. Sillberg, T. Schareina, R. Kempe, K. Wurst, M. R. Buchmeiser, *J. Organomet. Chem*. **2001**, *622*, 6. (g) L. Xu, W. Chen, J. Ross, J. Xiao, *Org. Lett*. **2001**, *3*, 295. (h) A. J. Carmichael, M. J. Earle, J. D. Holbrey, P. B. McCormac, K. R. Seddon, *Org. Lett.* **1999**, *1*, 997. (i) R. R. Deshmukh, R. Rajagopal, K. V. Srinivasan, *Chem. Commun*. **2001**, 1544. (j) H. Hagiwara, Y. Shimizu, T. Hoshi, T. Suzuki, M. Ando, K. Ohkubo, C. Yokoyama, *Tetrahedron Lett.* **2001**, *42*, 4349.

[7] L. Xu, W. Chen, J. Xiao, *Organometallics* **2000**, *19*, 1123.

[8] C. J. Mathews, P. J. Smith, T. Welton, A. J. P. White, *Organometallics* **2001**, *20*, 3848.

[9] (a) J. K. Stille, *Angew. Chem. Int. Ed. Engl.* **1986**, *25*, 508; (b) V. Farina in *Comprehensive Organometallic Chemistry II*, Vol. 12 (Eds.: E.W. Abel, F. G. A. Stone, G. Wilkinson), Pergamon, Oxford, **1995**, chap. 3.4; (c) T. N. Mitchell, *Synthesis* **1992**, 803; (d) T. N. Mitchell in *Metal-Catalyzed Cross-Coupling Reactions* (Eds.: F. Diederich, P. J. Stang), Wiley-VCH, New York, **1998**, chap. 4.

[10] (a) S. Liu, T. Fukuyama, M. Sato, I. Ryu, *Synlett* **2004**, 1814; (b) C. Chiappe, G. Imperato, E. Napolitano, D. Pieraccini, *Green Chem.* **2004**, *6*, 33; (c) S. T. Handy, X. Zhang, *Org. Lett.* **2001**, *3*, 233; (d) D. Zhao, Z. Fei, T. J. Geldbach, R. Scopelliti, P. J. Dyson, *J. Am. Chem. Soc.* **2004**, *126*, 15876.

[11] J. Dupont, G. S. Fonseca, A. P. Umpierre, P. F. P. Fichtner, *J. Am. Chem. Soc*. **2002**, *124*, 4228.

[12] G. S. Fonseca, A. P. Umpierre, P. F. P. Fichtner, S. R. Teixeira, J. Dupont, *Chem. Eur. J.* **2003**, 3264.

[13] C. W. Scheeren, G. Machado, J. Dupont, P. F. P. Fichtner, S. R. Texeira, *Inorg. Chem.* **2003**, *42*, 4738.

[14] K.-S. Kim, D. Demberelnyamba, H. Lee, *Langmuir,* **2004**, *20*, 556. (b) H. Itoh, K. Naka, Y. Chujo, *J. Am. Chem. Soc.* **2004**, *126*, 3026.

[15] S. Klingelhöfer, W. Heitz, A. Greiner, S. Oestreich, S. Forster, M. Antonietti, *J. Am. Chem. Soc.* **1997**, *119*, 10116. (b) J. Huang, T. Jiang, B. Han, H. Gao, Y. Chang, G. Zhao, W. Wu, *Chem. Commun*. **2003**, 1654.

[16] For review, see: P. J. Dyson, *Appl. Organomet. Chem*., **2002**, *16,* 495. For example, see: (a) Y. Chauvin, L. Mussmann H. Olivier-Bourbigou, *Angew. Chem., Int. Ed.* **1995**, *34*, 2698; (b) P. A. Z. Suarez, J. E. L. Dullius, S. Einloft, R. F. de Souza J. Dupont, *Polyhedron* **1996**, *15*, 1217; (c) P. J. Dyson, D. J. Ellis, D. G. Parker, T. Welton, *Chem Commun*. **1999**, 25; (d) C. J. Adams, M. J. Earle K. R. Seddon, *Chem. Commun*. **1999**, 1043; (e) F. Liu, M. B. Abrams, R. T. Baker, W. Tumas, *Chem. Commun*. **2001**, 433. (f) C. J. Boxwell, P. J. Dyson, D, J. Ellis T. Welton, *J. Am. Chem. Soc*. **2002,** *124*, 9334.

[17] Oxford Diffraction Ltd, 68 Milton Park, Abingdon, OX14 4 RX, UK, **2003**.

[18] G. M. Sheldrick, SHELX-97. Structure Solution and Refinement Package. Universität Göttingen, **1997**.

[19] L. J. Farrugia, *J. Appl. Cryst.* **1997**, *30*, 565.

[20] N. Walker, D. Stuart, *Acta Crystallogr. A* **1983**, *A39*, 158.

4

Synthesis and Characterization of Pyridinium ILs Incorporating the Nitrile Functionality and Applications in C-C Coupling Reactions

4.1 Introduction

In this chapter the synthesis of a series of nitrile F-ILs based on the *N*-butylnitrile pyridinium cation, $[C_3CNpy]^+$, and their suitability as solvents for palladium-catalyzed biphasic Suzuki and Stille coupling reactions will be described. A comparison of TEM images of nanoparticles formed *in situ* in the Stille reaction reveals that the nitrile-F-IL exerts a superior nanoparticle-stabilizing effect compared to the non-F-IL.

4.2 Results and Discussion

4.2.1 Synthesis of the ILs

The synthetic pathway leading to the *N*-butyronitrile pyridinium ILs, $[C_3CNpy][anion]$, is summarized in Scheme 4.1. Quaternization of pyridine with 4-chlorobutyronitrile results in the formation of the chloride salt $[C_3CNpy]Cl$ **13a** within 24 hours at 80 °C. Anion metathesis with either $H[PF_6]$, $Na[BF_4]$ or $Li[Tf_2N]$ ($Tf_2N = N(SO_2CF_3)_2$) affords the salts $[C_3CNpy][PF_6]$ **13b**, $[C_3CNpy][BF_4]$ **13c** and $[C_3CNpy][Tf_2N]$ **13d**, respectively, in high yield. Salts **13a**, **13b** and **13c** are solids at room temperature, but with melting points below 100°C, can nevertheless be classified as ILs. Compound **13d** is a liquid at room temperature with a melting point of -64.5°C and a relatively low viscosity (170 mPa·s at 20°C, cf. 50.1 mPa·s for $[C_4py][Tf_2N]$ at 20°C).[1]

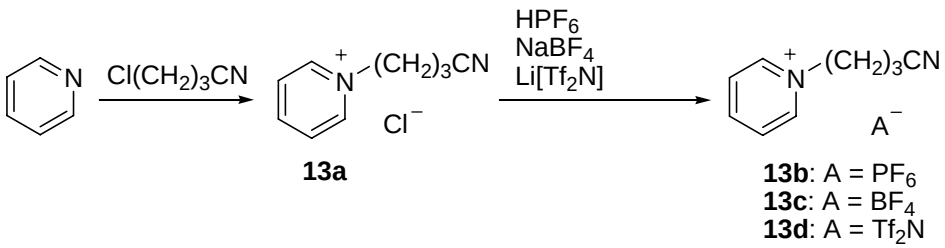

Scheme 4.1 Synthesis of the nitrile F-ILs 13a – 13d

The pyridinium salts **13a** – **13d** were characterized using electrospray ionization mass spectrometry (ESI-MS), IR, ^1H and ^{13}C NMR spectroscopy and elemental analysis. The positive ion ESI mass spectra in methanol reveal a strong parent peak at m/z 174 corresponding to the pyridinium cation $[C_3CNpy]^+$. The nature of the anion can be deduced directly from the positive ion spectra as aggregates corresponding to $[C_3CNpy]_2[anion]^+$ are observed. The negative ion spectra also confirmed the identity of the appropriate anion. The ^1H and ^{13}C NMR data of compounds **13a** – **13d** are of routine nature, with little change in the spectra with respect to the different anions present. In

the ^{13}C NMR spectra, the nitrile carbon is observed between 123.0 and 120.5 ppm. The IR spectra show characteristic C≡N vibrations between 2245 and 2246 cm^{-1}. In the case of **13a**, additional weak absorptions between 2862 and 2714 cm^{-1} are observed that can be attributed to the presence of Cl···H–C hydrogen bonds. Such hydrogen bonding is well established from X-ray crystallography (*vide infra*).

4.2.2 Reactions of 13a – 13d with palladium(II) chloride

In acetonitrile, palladium(II) chloride reacts with two equivalents of $[C_3CNpy]Cl$ **13a** to form $[C_3CNpy]_2[PdCl_4]$ **14a** (Scheme 4.2). Addition of a further equivalent of $PdCl_2$ to **14a** in dichloromethane affords $([C_3CNpy]_2[PdCl_4])_2PdCl_2$ **14e**, over a period of several days. In the absence of coordinating anions, the reaction of $PdCl_2$ with two equivalents of **13b** – **13d** in dichloromethane affords the complexes $[Pd(C_3CNpy)_2Cl_2][PF_6]_2$ **14b**, $[Pd(C_3CNpy)_2Cl_2][BF_4]_2$ **14c** and $[Pd(C_3CNpy)_2Cl_2][N(SO_2CF_3)_2]_2$ **14d**, respectively. Compounds **14b** – **14c** are yellow solids whereas **14d** can only be isolated as a highly viscous brown liquid. All of these new palladium complexes are air stable and do not decompose on washing with water or alcohols at room temperature, but decompose in water and alcohols over prolonged periods of time. They are poorly soluble in chlorinated solvents such as chloroform or dichloromethane and degrade on contact with acetonitrile in that coordination of the pyridinium cation to the metal is lost and the respective IL together with $Pd(CH_3CN)_2Cl_2$ is obtained.

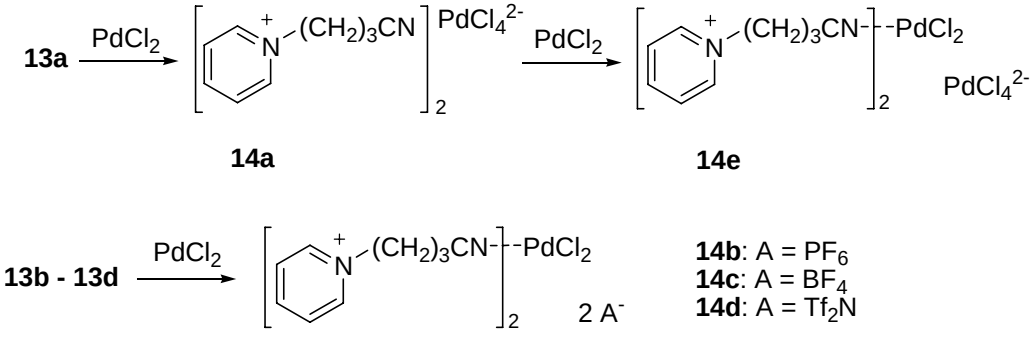

Scheme 4.2 Synthesis of palladium complexes 14a – 14e

Coordination of the nitrile to the palladium is clearly established using IR spectroscopy (it is not possible to use NMR as the few solvents which dissolve **14a** – **14d** cleave the metal-nitrile bond). Whereas the C≡N-stretching frequency of the free nitrile in the pyridinium salts **13a** – **13d/14a** is

found in the range 2244 – 2252 cm^{-1}, interaction with the metal in **14b** – **14e** leads to a marked change in the $\nu_{C\equiv N}$ bands which appear in the range 2319 – 2326 cm^{-1}.

4.2.3 Solid state structures of 13a and 14a

Single crystals of $[C_3CNpy][Cl]$ **13a** and $[C_3CNpy]_2[PdCl_4]$ **14a** were obtained from acetonitrile following slow diffusion of diethyl ether and their molecular structures were determined by X-ray diffraction methods. Their structures are depicted in Figures 4.1 and 4.2, respectively, and key bond lengths are listed in Table 4.1. The organic cations in **13a** and **14a** exhibit a geometry that is in good agreement with previously published pyridinium salts.[2] Bond angles in the pyridinium rings range from 118.1(6) to 121.5(5) and distances from 1.340(8) to 1.386(3) Å. The $-CH_2-C\equiv N$ moiety is essentially linear with the C-N distance [1.139(3) in **13a** and 1.128(7) and 1.128(8) in **14a**] being found in the expected range.[3] The nitrile moiety in **13a** lies almost in the same plane as the alkyl chain (deviation 10.5°), whereas in **14a** it is tilted out of plane by 117.1 and 118.4°, respectively. This difference is probably due to crystal packing effects such as $C\equiv N\cdots\pi$ interactions. Distances from the nitrile nitrogen atom to the centre of the pyridine ring of a nearby cation are 3.28 Å in **1** and 3.34 and 3.55 Å in **14a**. The nitrile moiety points towards the centre of the ring in **1**, but is almost parallel to the plane of the ring in **14a**. The anion $[PdCl_4]^{2-}$ in **14a** has a regular square planar geometry with Cl-Pd-Cl angles ranging between 89.62(6) and 90.43(7)°. The coordination plane of the $[PdCl_4]^{2-}$ anion is tilted by 114.7° and 118.6° relative to the mean plane of the pyridine rings. Similar structures of the type $[C_n\text{-py}][PdX_4]$, where C_n are long alkyl chains, have recently been reported and display comparable properties.[4] Furthermore, related paraquat salts of $[PdCl_4]^{2-}$ are also known.[5]

Table 4.1 Selected bond lengths (Å) and angles (º) for13a and 14a. The starred bond lengths refer to the second pyridinium cation in 14a.

	13a		**14a**	
Pd1-Cl1			2.3151(17)	
Pd1-Cl2			2.3116(17)	
Pd1-Cl3			2.3152(17)	
Pd1-Cl4			2.3145(17)	
N2-C9	1.139(3)	1.128(7)		1.128(8)*
N1-C1	1.343(3)	1.348(6)		1.354(6)*
N1-C5	1.352(3)	1.346(6)		1.353(7)*
C1-C2	1.383(3)	1.365(8)		1.359(9)*
C2-C3	1.386(3)	1.384(8)		1.385(8)*
C3-C4	1.384(3)	1.373(7)		1.375(8)*
C4-C5	1.374(3)	1.367(8)		1.340(8)*
C7-C8-C9	111.6(2)	114.0(5)		113.6(5)*
N2-C9-C8	178.1(3)	179.9(9)		179.9(9)*
C1-N1-C5	121.4(2)	121.0(5)		120.3(5)*
Cl1-Pd-Cl2			90.05(7)	
Cl2-Pd-Cl3			89.62(6)	
Cl3-Pd-Cl4			89.90(6)	
Cl4-Pd-Cl1			90.43(7)	

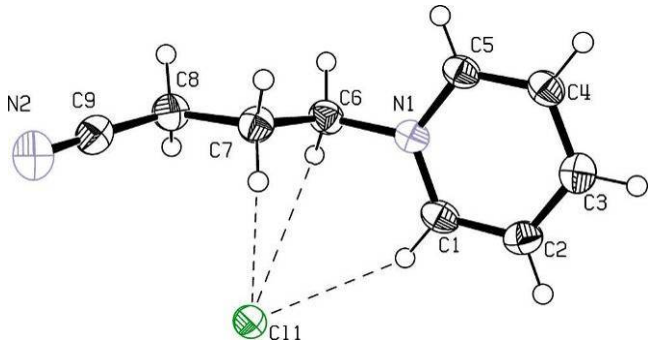

Figure 4.1 ORTEP representation of 13a showing some of the Cl-H interactions shorter than 3 Å; ellipsoids drawn at the 50 % probability level.

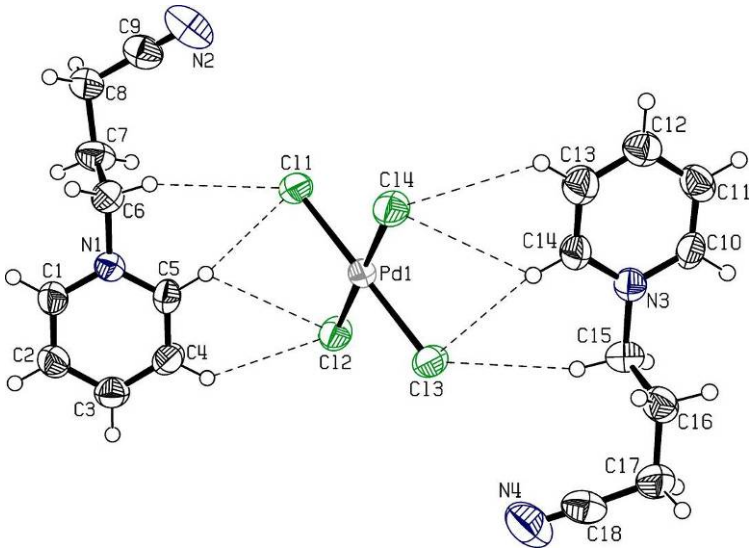

Figure 4.2 ORTEP representation of 14a showing some of the Cl-H interactions shorter than 3 Å; ellipsoids drawn at the 50 % probability level

In both structures, the organic cation and the inorganic anion are held in place by extensive C-H···Cl interactions. In **13a**, eight hydrogen contacts below 3 Å, which stem from five different cations and range between 2.609 and 2.931 Å, are observed. The $[PdCl_4]^{2-}$ anion is close to 15 hydrogen atoms belonging to six different cations, with distances between 2.708 and 2.997 Å. Such hydrogen bonding is well established from imidazolium [6] and pyridinium [2,4,5] halides and explains to some degree their markedly higher melting points relative to, for example, their BF_4^- derivatives.

4.2.4 Carbon-carbon coupling reactions

Palladium catalyzed carbon-carbon bond formation, such as in the Suzuki and Stille reactions usually take place in high yield under relatively mild conditions and tolerate a wide variety of functional groups on either coupling partner.[7] The development of biphasic (or multiphasic) systems for these types of reactions has received considerable attention [8] and both Suzuki [9,10] and Stille[11] reactions have previously been studied in ILs.

The Suzuki reaction was evaluated using the palladium complexes **14a** – **14d** and $PdCl_2$ as pre-catalysts immobilized in either $[C_3CNpy][Tf_2N]$ **13d**, or in the non-F-IL $[C_4py][Tf_2N]$, employing conditions described previously.[12] The performance of these catalyst precursors in the reaction between phenylboronic acid and iodobenzene is listed in Table 4.2.

Table 4.2 Suzuki coupling reactions conducted in 4 and [C_4py][Tf_2N].[a)]

Pre-catalyst	Ionic liquid	Aryl halide	Yield, %[b)]
14a	**13d**	PhI	86
14e	**13d**	PhI	85
14c	**13d**	PhI	88
14d	**13d**	PhI	81
14d	**13d**	PhI	85
14d	[C_4py][Tf_2N]	PhI	84
$PdCl_2$	**13d**	PhI	88

[a)] Conditions: iodobenzene (2.5 mmol), IL (5 ml), phenylboronic acid (2.75 mmol), Na_2CO_3 (5.28 mmol), water (2.5 ml), palladium complex (0.03 mmol), 110°C, 12 hours. [b)] Yield corresponds to biphenyl determined by GC.

The yields for all the reactions are high although it is worth noting that a relatively short reaction time was used; quantitative conversion can be obtained by increasing the reaction time. Clearly, the nature of the palladium source does not seem to have a major effect on the kinetics of the reaction. The difference between the reactions conducted in the nitrile-F-IL **13d** and [C_4py][Tf_2N] becomes apparent in the recycling studies, which are summarized in Figure 4.3. After nine cycles with complex **14d** as catalyst precursor in the F-IL, there is no significant decrease in activity. However, if **14d** is immobilized in [C_4py][Tf_2N], the catalyst solution rapidly loses its activity to become completely inactive after the fifth cycle.

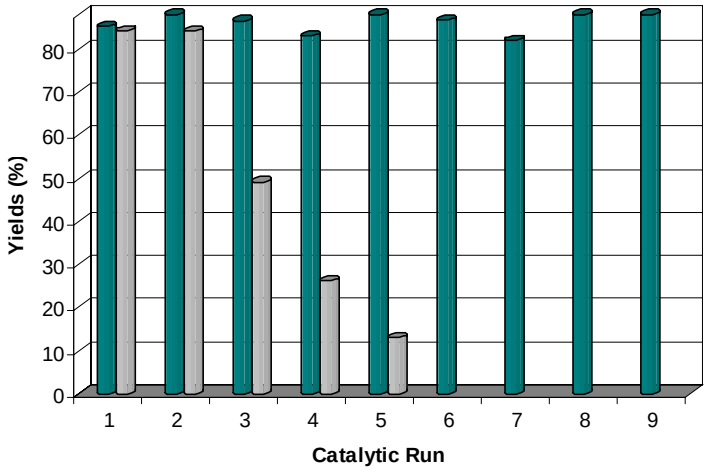

Figure 4.3 Recyclability in [C_3CNpy][Tf_2N] 13d (green) and [C_4py][Tf_2N] (grey) in the Suzuki reaction between phenylboronic acid and iodobenzene using 14d as the catalyst precursor.

The superiority of the nitrile F-IL catalyst system compared to the alkyl-pyridinium IL based one appears to be due to several factors. Inductive coupled plasma spectroscopy (ICP) was used to analyze the organic fractions after catalysis for palladium content. These analyses showed that while less than 5 ppm of palladium was lost from **13d** into the organic phase, typically 28 ppm of palladium was lost from [C_4py][Tf_2N]. These differences in palladium loss does not fully account for the differences in recycling and the catalyst in the non-F-IL must also be less stable. It is conceivable to attribute the superior retention of the palladium complex in **13d** to coordination of the palladium to the IL via the nitrile moiety resulting in higher capacity for immobilization the palladium complex. It has also been suggested that carbene complexes are the active catalytic species for the Suzuki reaction in imidazolium-based ILs,[13] but the formation of carbenes from pyridinium-based ILs is less likely. Attempts to identify the nature of the catalyst failed which prevents delineation of the role of the nitrile group. In contrast, in the Stille reaction carried out under conditions described previously, further insights could be gained. The results from the Stille coupling reaction between iodobenzene and phenyltributylstannane are compiled in Table 4.3.[14]

Table 4.3 Stille reaction catalyzed by palladium complexes in ILs [a)]

Pd-source	Ionic Liquid	Aryl halide	Yield (%) [b)]
14a	**13d**	Ph-I	62.1
14b	**13d**	Ph-I	58.3
14c	**13d**	Ph-I	43.9
14d	**13d**	Ph-I	43.7
14e	**13d**	Ph-I	48.9
14a	[C_4py][Tf_2N]	Ph-I	65.5
14e	[C_4py][Tf_2N]	Ph-I	56.0
$PdCl_2$	**13d**	Ph-I	62.6

[a)] Conditions: iodobenzene (1.0 mmol), IL (1 ml), phenyltributylstanne (1.2 mmol), palladium complex (0.05 mmol), 80^{o}C, 12 hours. [b)] Yield corresponds to biphenyl determined by GC.

The results are in keeping with the Suzuki reactions, i.e. there is little difference between the catalytic activity in **13d** or [C_4py][Tf_2N] in the first batch, however, while activity remains essentially constant in **13d** activity decreases rapidly in [C_4py][Tf_2N] as is clear from Figure 4.4.

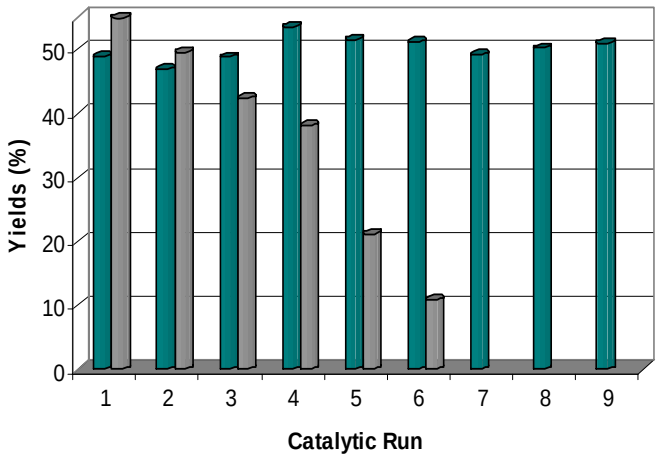

Figure 4.4 Recyclability of 9 in [C_3CNpy][Tf_2N] 13d (green) and [C_4py][Tf_2N] (grey) in the Stille reaction between phenyltributylstannane and iodobenzene using 14d as the catalyst precursor.

The catalyst recycling experiments demonstrate the advantage of using the nitrile-F-IL as the biphasic catalyst support: with **13d** as catalyst support, the product yield is essentially unchanged even in the ninth catalytic cycle while in [C_4py][Tf_2N], no activity is observed after six batches. Again, a much lower palladium content was found in the organic phase with **13d** relative to [C_4py][Tf_2N] (7 ppm versus 46 ppm), indicating that the nitrile-F-IL facilitates catalyst retention *and* stability.

In contrast to the Suzuki coupling, where no significant color change is observed in the course of the reaction, the IL-palladium complex solution rapidly turns black in the Stille reactions following addition of the phenyltributylstannane, indicative of nanoparticles formation. It proved possible to isolate the palladium nanoparticles from the Stille reactions which were subsequently analyzed using transmission electron microscopy (TEM) and the TEM images are shown in Figure 4.5.

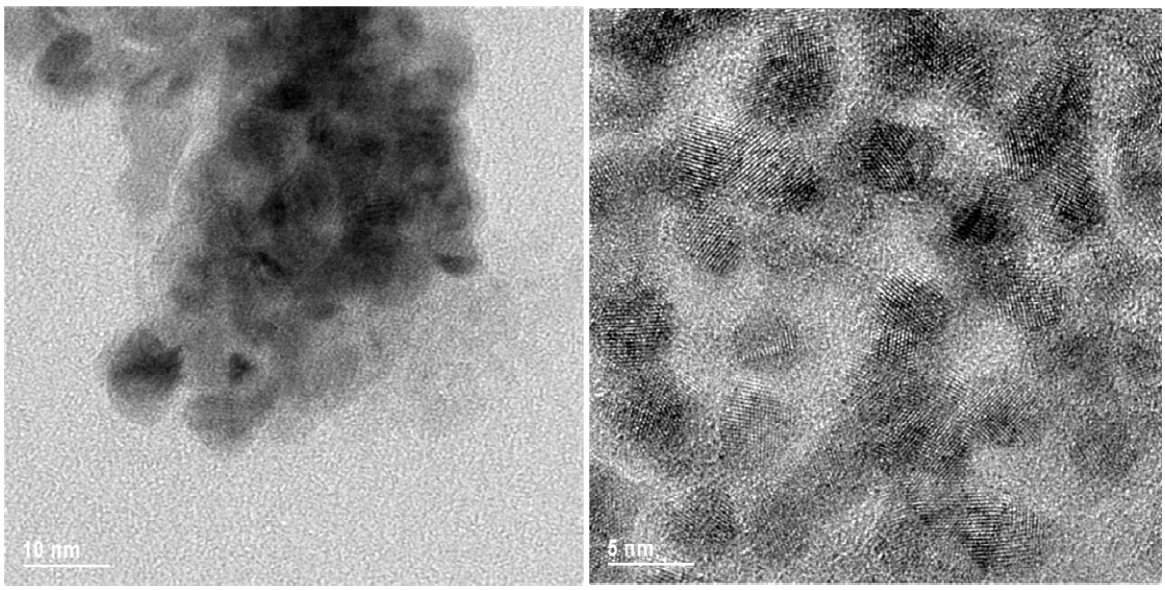

Figure 4.5 Comparison of TEM images of the palladium nanoparticles isolated after the Stille reaction from [C_4py][Tf_2N] (left) and [C_3CNpy][Tf_2N] (right).

The nanoparticles from both [C_4py][Tf_2N] and [C_3CNpy][Tf_2N] **4** have a diameter of ca. 5 nm, but they exhibit different states. Whereas those from [C_4py][Tf_2N] are aggregated, nanoparticles generated in **13d** are evenly distributed and the surface lattice can be clearly observed. Such micro dissimilarity is in accordance with the macro appearance disparity of the two IL systems. The TEM images support the hypothesis that the nitrile-F-IL stabilizes the palladium colloid. The nitrile moiety could either weakly coordinate to the surface or point away from the nanoparticles surface thereby repelling proximal neighbors. In either case agglomeration would be prevented and ultimately catalyst deactivation suppressed. The former hypothesis has been suggested previously for different systems.[15]

4.3 Concluding remarks

The nitrile-F-IL [C_3CNpy][Tf_2N], **13d**, is a considerably more effective immobilization solvent for palladium catalyzed Suzuki and Stille reactions than [C_4py][Tf_2N]. ICP analysis indicates that the nitrile F-IL markedly reduces palladium leaching compared to the non-F-IL. In addition, TEM analysis of nanoparticles extracted from the catalysis solution directly shows the stabilizing effect of the nitrile F-IL. Such task-specific ILs may well prove to be decisive in transferring ILs from the laboratory to production scale processes in C-C bond forming reactions. The [C_3CNpy][Tf_2N] IL

described herein is that it can be prepared from relatively inexpensive precursors which provides further incentive for its deployment on a larger scale.

4.4 Experimental

All manipulations were carried out under a nitrogen atmosphere using standard Schlenk techniques using dried and distilled solvents. All reagents were purchased from Aldrich and used as received. IR spectra were recorded on a Perkin-Elmer FT-IR 2000 system. NMR spectra were measured on a Bruker DMX 400 with chemical shifts given in ppm and coupling constants (*J*) in Hz. Electrospray ionization mass spectra (ESI-MS) were recorded on a ThermoFinnigan LCQ™ Deca XP Plus quadrupole ion trap instrument on samples diluted in methanol. Samples were infused directly into the source at 5 μL min^{-1} using a syringe pump and the spray voltage was set at 5 kV and the capillary temperature at 50°C as described previously.[16] Elemental analysis were carried out at the Institute of Chemical Sciences and Engineering (EPFL). Differential scanning calorimetry was performed using a SETARAM DSC 131. Inductively coupled plasma-atomic emission spectroscopy was conducted using a Perkin-Elmer Optima 3000 ICP-AE spectrometer. Intensities of spectral lines at 340.458 nm were measured in all samples and standards. The palladium level in the samples was determined by comparing the intensity of the spectral line with the palladium standard.

Table 4.4 Crystallographic data for compounds 13a and 14a.

	13a	**14a**
empirical formula	$C_9H_{11}ClN_2$	$C_{18}H_{22}Cl_4N_4Pd$
formula weight	182.65	542.60
crystal system	monoclinic	monoclinic
space group	$P2_1/c$	$P2_1/n$
a, Å	8.074(3)	14.142(7)
b, Å	12.108(4)	10.421(5)
c, Å	10.505(2)	15.367(3)
α, °	90	90
β, °	112.46(2)	104.78(3)
γ, °	90	90
V, Å^3	949.1(5)	2189.8(15)
Z	4	4
Density [Mg/m^3]	1.278	1.346
T, K	140	293
Θrange/°	$3.21 \leq \Theta \leq 25.02$	$2.99 \leq \Theta \leq 25.02$
μ/mm^{-1}	0.349	1.346
Reflections measured	5684	13420
Unique reflections [$I>2\sigma($	1626 (R_{int} = 0.0430)	3803 (R_{int} = 0.0658)
Final $R1$, $wR2[I>2\sigma(I)]$	0.0528, 0.1301	0.0436, 0.0944

Synthesis of [C_3CNpy]Cl ***13a***

A mixture of pyridine (7.90 g, 0.10 mol) and $Cl(CH_2)_3CN$ (12.42 g, 0.12 mol) was stirred at 80°C for 24 h, during which time two phases formed. The reaction mixture was cooled to room temperature, acetonitrile (100 ml) and activated carbon (3 g) were added and the mixture stirred for 30 minutes. The solution was then reheated to 80°C and filtered. The resulting product was crystallized upon cooling 0°C, washed with diethyl ether (3 × 30 ml) and dried under vacuum for 24 hours to afford **1** as colorless solid. Yield: 16.8 g, 92%; M.p.: 101°C. ESI-MS (CH_3OH): positive ion: 147 [C_3CNpy], negative ion: 35, [Cl]. ^{1}H-NMR (D_2O): δ = 8.94 (d, 2H, $^3J_{HH}$ = 5.6), 8.60 (m, 1H), 8.12 (m, 2H), 4.77 (t, 2H, $^3J_{HH}$ = 7.2), 2.68 (t, 2H, $^3J_{HH}$ = 6.8), 2.44 (m, 2H). ^{13}C-NMR (D_2O): δ = 149.3, 147.5, 131.6, 123.0, 63.1, 29.2, 16.9; IR (cm^{-1}): 3030, 3002 ($\nu_{C\text{-}H}$ aromatic), 2933, 2862, 2714 ($\nu_{C\text{-}H}$ aliphatic), 2245 ($\nu_{C\equiv N}$). Anal. Calcd for $C_9H_{11}ClN_2$ (%): C 59.18, H 6.07, N 15.34; Found: C 59.14, H 6.11, N 15.31

Synthesis of [C_3CNpy]PF_6 ***13b***

To a solution of **13a** (5.46 g, 0.03 mol) in water (50 ml), HPF_6 (8.03 g, 60 wt%, 0.033 mol) was added at RT. After 10 minutes the solid that had formed was collected by filtration, washed with ice-water (3 × 15 ml) and then dried under vacuum. Yield: 6.13 g, 70%; M.p.: 95°C. ESI-MS (CH_3OH): positive ion: 147 [C_3CNpy], negative ion: 145 [PF_6]. ^{1}H-NMR (CD_3CN): δ = 8.72 (d, 2H, $^3J_{HH}$ = 5.5), 8.53 (m, 1H), 8.07 (m, 2H), 4.60 (t, 2H, $^3J_{HH}$ = 7.2), 2.55 (t, 2H, $^3J_{HH}$ = 6.8), 2.32 (m, 2H). ^{13}C-NMR (CD_3CN): δ = 149.2, 147.6, 131.6, 120.5, 63.1, 29.4, 16.6; IR (cm^{-1}): 3143, 3102, ($\nu_{C\text{-}H}$ aromatic), 2985, 2985 ($\nu_{C\text{-}H}$ aliphatic), 2246 ($\nu_{C\equiv N}$). Anal. Calcd for $C_9H_{11}F_6N_2P$ (%): C 37.00, H 3.79, N, 9.59; Found: C 37.02, H 3.75, N 9.61.

Synthesis of [C_3CNpy]BF_4 ***13c***

A mixture of **1** (5.46 g, 0.03 mol) and $NaBF_4$ (3.62 g, 0.033 mol) in acetone (80 ml) was stirred at room temperature for 48 h. After filtration and removal of the solvents the resulting pale yellow waxy solid was washed with THF and diethyl ether to give the product. Yield: 6.45 g, 92%; M.p.: 62°C. ESI-MS (CH_3OH): positive ion: 147 [C_3CNpy], negative ion: 87 [BF_4]; ^{1}H-NMR (CD_3CN): δ = 8.77 (d, 2H, $^3J_{HH}$ = 5.5), 8.55 (m, 1H), 8.07 (m, 2H), 4.62 (t, 2H, $^3J_{HH}$ = 7.2), 2.56 (t, 2H, $^3J_{HH}$ = 6.8), 2.34 (m, 2H). ^{13}C-NMR (CD_3CN): δ = 149.2, 147.7 131.6, 120.7, 63.1, 29.5, 16.6. IR (cm^{-1}): 3142, 3079 ($\nu_{C\text{-}H}$ aromatic), 2970 ($\nu_{C\text{-}H}$ aliphatic), 2246 ($\nu_{C\equiv N}$). Anal. Calcd for $C_9H_{11}BF_4N_2$ (%): C 46.20, H 4.74, N 11.97; Found: C 46.21, H 4.75, N 12.01.

Synthesis of [C_3CNpy][$N(SO_2CF_3)_2$] ***13d***

To a solution of **1** (5.46 g, 0.03 mol) in water (50 ml), Li(N[SO_2CF_3]$_2$) (9.47 g, 0.033 mol) was added at room temperature in one portion and the reaction mixture was stirred for 10 h and then extracted with dichloromethane (200 ml) and the extract dried with $MgSO_4$ overnight. The $MgSO_4$ was removed by filtration and the solvent was removed under reduced pressure. The resulting hydrophobic liquid was washed with water (3 × 10 ml) and dried in vacuum. Yield: 9.22 g, 72%; M.p.: -64.5°C. ESI-MS (CH_3OH): positive ion: 147 [C_3CNpy], negative ion: 280 [$N(SO_2CF_3)_2$]. ^{1}H-NMR (CD_3CN): δ = 8.74 (d, 2H, $^3J_{HH}$ = 5.5), 8.56 (m, 1H), 8.09 (m, 2H), 4.64 (t, 2H, $^3J_{HH}$ = 7.2), 2.57 (t, 2H, $^3J_{HH}$ = 6.8), 2.35 (m, 2H). ^{13}C NMR (CD_3CN): δ = 146.3, 147.7, 128.7, 121.5, 117.4, 60.2, 26.5, 13.72; IR (cm^{-1}): 3139, 3074 ($\nu_{C\text{-}H}$ aromatic), 2961, ($\nu_{C\text{-}H}$ aliphatic), 2252 ($\nu_{C\equiv N}$), 1491

($\delta_{C\text{-}F}$), 1178 ($\nu_{N\text{-}SO2}$), 1133 ($\nu_{S=O}$). Anal. Calcd for $C_{11}H_{11}N_3F_6S_2O_4$ (%): C 30.92, H 2.59, N, 9.83; Found: C 31.02, H 2.55, N 9.86.

Synthesis of [(C$_3$CNpy)$_2$]PdCl$_4$ ***14a***

A reaction mixture of $PdCl_2$ (177 mg, 1.0 mmol) and **1** (364 mg, 2.00 mmol) in acetonitrile (5 ml) was heated at 80°C for 4 h. After removal of the solvent, the resulting orange solid was washed with dichloromethane (2 × 2 ml), and dried under vacuum to give the product. Yield: 536 mg, 99%. M.p.: 165°C. ^{1}H-NMR (DMSO-d6): δ = 9.16 (d, 2H, $^3J_{HH}$ = 5.6), 8.63 (m, 1H), 8.18 (m, 2H), 4.72 (t, 2H, $^3J_{HH}$ = 7.2), 2.67 (t, 2H, $^3J_{HH}$ = 6.8), 2.29 (m, 2H). ^{13}C-NMR (DMSO-d6): δ = 149.5, 148.5, 131.6, 122.9, 62.9, 29.7, 16.9. IR (cm^{-1}): 3121, 3051 ($\nu_{C\text{-}H}$ aromatic), 2988, 2972, 2926, 2901 ($\nu_{C\text{-}H}$ aliphatic), 2244 ($\nu_{C\equiv N}$). Anal. Calcd for $C_{18}H_{22}Cl_4N_4Pd$ (%): C 39.84, H 4.09, N 10.33; Found: C 39.87, H 4.04, N 10.29.

Synthesis of [(C$_3$CNpy)$_2$PdCl$_2$]PdCl$_4$ ***14e***

$PdCl_2$ (177 mg, 1.0 mmol) was added to a suspension of **14a** (543 mg, 1.0 mmol) in dichloromethane (5.0 ml). The reaction mixture was stirred at room temperature for 3 days, during which time, the orange color of the suspension disappeared and a light yellow suspension formed. The resulting yellow solid was collected by centrifugation filtration and washed with dichloromethane (2 × 2 ml), and dried under vacuum to give the product. Yield: 687 mg, 95%; M. p.: 110°C, (decomp.); ^{1}H-NMR (DMSO-d6): δ = 9.15 (d, 2H, $^3J_{HH}$ = 5.6), 8.63 (m, 1H), 8.18 (m, 2H), 4.71 (t, 2H, $^3J_{HH}$ = 7.2), 2.67 (t, 2H, $^3J_{HH}$ = 7.2), 2.29 (m, 2H). ^{13}C-NMR (DMSO-d6): δ = 149.3, 148.5. 131.6, 122.9, 62.9, 29.6, 16.9; IR (cm^{-1}): 3130, 3057 ($\nu_{C\text{-}H}$ aromatic), 2962, 2937 ($\nu_{C\text{-}H}$ aliphatic), 2319 ($\nu_{C\equiv N}$). Anal. Calcd for $C_{18}H_{22}Cl_6N_4Pd_2$ (%): C 30.03, H 3.08, N 7.78; Found: C 30.05, H 3.09, N 7.69.

Synthesis of Complexes ***14b*** *–* ***14d***

Typical procedure: A reaction mixture of $PdCl_2$ (177 mg, 1.0 mmol) and **2** (584 mg, 2.00 mmol) in dichloromethane (5.0 ml) was stirred at RT for 4 days. The resulting yellow solid was collected by centrifugation filtration and washed with dichloromethane (2 × 2 ml), and dried under vacuum to give the product. Complexes **14c** and **14d** are prepared using the same procedure.

14b $[(C_3CNpy)_2PdCl_2]2PF_6$: Yield: 98%. M.p.: 150°C. ^{1}H-NMR (DMSO-d6): δ = 9.08 (d, 2H, $^3J_{HH}$ = 5.8), 8.61 (m, 1H), 8.16 (m, 2H), 4.65 (t, 2H, $^3J_{HH}$ = 7.2), 2.64 (t, 2H, $^3J_{HH}$ = 7.2), 2.28 (m, 2H); ^{13}C-NMR (DMSO-d6): δ = 149.2, 148.4, 131.6, 122.9, 63.0, 29.5, 16.9. IR (cm^{-1}): 3138, 3098, 3071 ($\nu_{C\text{-}H}$ aromatic), 2987, 2972, 2901 ($\nu_{C\text{-}H}$ aliphatic), 2326 ($\nu_{C\equiv N}$). Anal. Calcd for $C_{18}H_{22}Cl_2F_{12}N_4P_2Pd$ (%): C 28.39, H 2.91, N 7.36; Found: C 28.42, H 2.95, N 7.29.

14c $[(C_3CNpy)_2PdCl_2]2BF_4$: Yield: 95%; M.p.: 131°C; ^{1}H-NMR (DMSO-d6): δ = 9.07 (d, 2H, $^3J_{HH}$ = 5.5), 8.61 (m, 1H), 8.16 (m, 2H), 4.65 (t, 2H, $^3J_{HH}$ = 7.2), 2.63 (t, 2H, $^3J_{HH}$ = 7.2), 2.27 (m, 2H); ^{13}C-NMR (DMSO-d6): δ = 149.2, 148.4, 131.6, 122.9, 63.0, 29.5, 16.9. IR (cm^{-1}): 3138, 3092, 3069 ($\nu_{C\text{-}H}$ aromatic), 2987, 2901 ($\nu_{C\text{-}H}$ aliphatic), 2326 ($\nu_{C\equiv N}$). Anal. Calcd for $C_{18}H_{22}B_2Cl_2F_8N_4Pd$ (%):C 33.50, H 3.44, N 8.68; Found: C 33.47, H 3.45, N 8.62

14d $[(C_3CNpy)_2PdCl_2]2(N[SO_2CF_3]_2)$ Yield: 99%. Viscous liquid. ^{1}H-NMR (DMSO-d6): δ = 8.74 (d, 2H, $^3J_{HH}$ = 5.6), 8.57 (m, 1H), 8.09 (m, 2H), 4.64 (t, 2H, $^3J_{HH}$ = 7.2), 2.57 (t, 2H, $^3J_{HH}$ = 6.8), 2.35 (m, 2H). ^{13}C-NMR (D_2O): δ = 146.3, 147.8, 128.7, 121.5, 60.2, 26.5, 13.7; IR (cm^{-1}): 3122, 3051, 3038 ($\nu_{C\text{-}H}$ aromatic), 2962, ($\nu_{C\text{-}H}$ aliphatic), 2319 ($\nu_{C\equiv N}$). 1492 ($\delta_{C\text{-}F}$), 1177 ($\nu_{N\text{-}SO2}$), 1131 ($\nu_{S=O}$). Anal. Calcd for $C_{22}H_{22}Cl_2F_{12}N_6O_8PdS_4$ (%): C 25.60, H 2.15, N, 8.14; Found: C 25.62, H 2.21, N 8.19.

Typical Suzuki C-C coupling procedure

To a 20 ml two-necked flask fitted with a septum and reflux condenser, iodobenzene (2.5 mmol, 1 equiv.) was mixed with IL (5 ml). Then phenylboronic acid (335 mg, 2.75 mmol, 1.1 equiv.), Na_2CO_3 (560 mg, 5.28 mmol, 2.1 equiv.) water (2.5 ml) and finally the appropriate palladium complex (0.03 mmol, 1.2 mol% based on iodobenzene) were added. The mixture was heated to 110^{o}C and stirred vigorously for 12 h. The mixture was cooled to RT and extracted with diethyl ether (3 × 15 ml). The combined extracts were washed with brine and water and then dried with $MgSO_4$. The biphenyl product was obtained by filtering the solution followed by removal of solvent. The product was characterized by GC and ^{1}H NMR. The IL phase was washed with diethyl ether and put under vacuum overnight prior to the next catalytic cycle. The samples for ICP analysis were prepared by evaporating diethyl ether extract (5 ml) following addition of 65% HNO_3 (500 ml)[17].

The mixture was stirred at room temperature for 2 days and evaporated to dryness again. The residue was dissolved in 15 ml 2% HNO_3 aqueous solution.

Typical Stille C-C coupling procedure

To a 20 ml two-neck flask fitted with a spetum and reflux condenser, iodobenzene (204 mg, 1.0 mmol) and the appropriate palladium complex (0.05 mmol) were mixed with IL (1.0 ml) the mixture heated to 80°C and phenyltributylstanne (0.39 ml, 1.2 mmol) added. After stirring for 12 h at 80°C the reaction mixture was allowed to cool to room temperature and the product extracted with diethyl ether (3 × 10 ml). The combined organic layers were washed with saturated aqueous potassium fluoride (3 × 30 ml) and then dried over $MgSO_4$, filtered and concentrated in vacuum. The remaining IL solution was washed with water and dried in vacuum overnight for further catalytic cycles. The ICP analysis samples are prepared in the same way to that described for the Suzuki reaction.

Crystallography

Data collection for the X-ray structure determinations were performed on a mar345 IPDS diffractometer system using graphite-monochromated $Mo_{K\alpha}$ (0.71070 Å) radiation and a low temperature device [T = 140(2) K]. Colorless crystals of **13a** and **14a** suitable for X-ray diffraction were obtained by slow diffusion of diethyl ether into an acetonitrile solution of the compound at room temperature. Data reduction was performed using CrysAlis RED.[18] Structure solution and refinement was performed using the SHELX97 software package,[19] graphical representations of the structures were made with ORTEP32.[20] Structures were solved by direct methods and successive interpretation of the difference Fourier maps, followed by full matrix least-squares refinement (against F^2). An empirical absorption correction (DELABS)[21] was applied to **14a**. All atoms were refined anisotropically. The contribution of the hydrogen atoms, in their calculated positions, was included in the refinement using a riding model. Relevant data concerning crystallographic data are compiled in Table 4.4.

TEM sample preparation

A reaction mixture containing IL **13d** or $[C_4py][N(SO_2CF_3)_2]$ (1.0 ml) was taken after the catalysis and ethanol (2.0 ml) was added. The mixture was centrifuged and the nanoparticles were collected

at the bottom of centrifugation vessel. They were then suspended in ethanol (2 ml), centrifuged, and the ethanol was decanted. This process was repeated four times. Finally the ethanol-nanoparticle suspension was deposited on a carbon coated copper grid (500 mesh) and dried at ambient temperature. The TEM images were obtained on a PHILIPS CM 300 Transmission Electron Microscope.

4.5 References

[1] S. N. Baker, G. A. Baker, M. A. Kane, F. V. Bright, *J. Phys. Chem. B.* **2001**, *105,* 9663.

[2] (a) H. H. Paradies, F. Habben, *Acta Crystallogr.* **1993**, *C49*, 744; (b) D. L. Ward, R. R. Rhinebarger, A. I. Popov, *Acta Crystallogr.* **1986,** *C42*, 1771.

[3] F. H. Allen, O. Kennard, D. G. Watson, L. Brammer, G. Orpen, R. Taylor, *J. Chem. Soc., Perkin Trans 2.* **1987**, S1.

[4] (a) F. Neve, A. Crispini, S. Armentano, O. Francescangeli, *Chem. Mat*. **1998**, *10*, 1904; (b) F. Neve, A. Crispini, *Crystal Growth & Design*, **2001**, *1*, 387.

[5] C. K. Prout, P. Murray-Rust, *J. Chem. Soc. A.* **1969**,1520.

[6] (a) B. Kratochvil, J. Ondracek, J. Velisek, J. Hasek, *Acta Crystallogr.* **1988**, *C44*(9), 1579; (b) J. D. Holbrey, W. M. Reichert, I. Tkatchenko, E. Bouajila, O. Walter, I. Tommasi, R. D. Rogers, *Chem. Commun.* **2003**, 28; (c) J. J. Golding, D. R. MacFarlaine, L. Spiccia, M. Forsyth, B. Skelton, A. H. White, *Chem. Commun.* **1998**, 1593; (d) P. B. Hitchcock, K. R. Seddon, T. Welton, *J. Chem. Soc., Dalton Trans.* **1993**, 2639.

[7] (a) J. Tsuji, *Palladium Reagents & Catalysts - Innovations in Organic Syntheses* 2ed., John Wiley and Sons Ltd, Chichester, **2004**; (b) N. Miyaura, A. Suzuki. *Chem. Rev.* **1995**, *95*, 2457; (c) K. J. Stille, *Angew. Chem. Int. Ed.* **1986**, *25*, 508.

[8] (a) M. R. Buchmeiser, S. Lubbad, M. Mayr, K. Wurst, *Inorg. Chim. Acta* **2003**, *345*, 145; (b) J. Navarro, M. Sagi, E. Sola, F. J. Lahoz, I. T. Dobrinovitch, A. Katho, F. Joo, L. A. Oro, *Adv. Synth. Catal.* **2003**, *345(1+2)*, 280; (c) C. C. Tzschucke, C. Markert, H. Glatz, W. Bannwarth, *Angew. Chem. Int. Ed*. **2002**, *41*, 4500; (d) D. E. Bergbreiter, P. L. Osburn, A. Wilson, E. M. Sink, *J. Am. Chem. Soc.* **2000**, *122*, 9058.

[9] C. J. Mathews, P. J. Smith, T. Welton, *Chem. Commun.* **2000**, 1249.

[10] (a) J. McNulty, A. Capretta, J. Wilson, J. Dyck, G. Adjabeng, A. Robertson, *Chem. Commun.* **2002**, 1986; (b) J. D. Revell, A. Ganesan, *Org. Lett.* **2002**, *4*, 3071; (c) R. Rajagopal, D. V. Jarikote, K. V. Srinivasan, *Chem. Commun.* **2002**, 616.

[11] (a) C. Chiappe, G. Imperato, E. Napolitano, D. Pieraccini, *Green Chem.* **2004**, *6*, 33; (b) S. T. Handy, X. Zhang, *Org. Lett.* **2001**, *3*, 233.

[12] N. Miyaura, T. Yanagi, A. Suzuki, *Synth. Commun*. **1981**, *11*, 513.

[13] (a) L. Xu, W. Chen, J. Xiao, *Organometallics* **2000**, *19*, 1123; (b) F. Mclachlan, C. J. Mathews, P. J. Smith, T. Welton, *Organometallics* **2003**, *22*, 5350.

[14] C. R. Johnson, J. P. Adams, M. P. Braun, C. B. W. Senanayake, *Tetrahedron Lett.* **1992**, *33*, 919.

[15] S. Bucher, J. Hormes, H. Modrow, R. Brinkmann, N. Waldöfner, H. Bönnemann, L. Beuermann, S. Krischok, W. Maus-Friedrichs, V. Kempter, *Surface Sci.* **2002**, *497*, 321.

[16] P. J. Dyson, J. S. McIndoe, *Inorg. Chim. Acta*. **2003**, *354*, 68.

[17] E. S. Beary P. J. Paulsen, *Anal. Chem.* **1995**, *67*, 3193.

[18] Oxford Diffraction Ltd, 68 Milton Park, Abingdon, OX14 4 RX, UK, 2003.

[19] G. M. Sheldrick, *SHELX-97. Structure Solution and Refinement Package*. Universität Göttingen, 1997.

[20] L. J. Farrugia, *J. Appl. Crystallogr.* **1997**, *30*, 565.

[21] N. Walker, D. Stuart, *Acta Crystallogr.* **1983**, *A39*, 158.

5

Synthesis, Characterization and Reactivity of Allyl F-ILs

5.1 Introduction

N-ally-imidazolium salts have been reported as early as 1971;[1] they are also frequently mentioned in current communications. However, a detailed study including synthesis and structural analysis has yet to be reported. The fact that all the allyimidazolium halides are liquids at room temperature maybe due to the high flexibility of the ally group, and the strong intra-hydrogen bondings between the H atoms from the imidazole ring and the counter anion. This encourages me to replace the halide anion with a more bulky and none-coordinating anion, namely BPh_4 (Crystal Engineering). In addition, introduce transition metals were introduced to the ally-F-IL, and a palladium complex of melting point as low as 58°C, which can be classified as an IL, is obtained. It is well known that the ally group is a popular functional group and can be converted to many other functional groups. Keeping this in mind, several reactions were conducted starting from the ally-F-ILs. Addition of benzene to the C=C double bond in the presence of triflic acid lead to isolation of new IL.

As mentioned above, alkene F-ILs have been reported previously.[3-5] It is interesting to note that the first liquid imidazolium-alkene (or allyl) salts were reported as early as 1971, however at that time, the liquid nature of these compounds was not appreciated and was in part attributed to their deliquescent nature. As yet, no extensive study on ILs bearing alkene functionality has been reported, although it has been shown that 1-ally-3-methylimidazolium chloride can be used as solvent for cellulose acetylation.[2] In addition, a series of allylimidazolium halides were prepared and their conductivities, viscosities and thermal properties were investigated, indicating that the introduction of ally group onto *N*-position effectively suppress their crystallization.[3]

In this chapter the synthesis and characterization of a series of ILs incorporating the allyl functionality and some nascent reactions that they undergo, indicating that they are useful precursor to a wide range of other F-ILs, will be described.

5.2 Results and discussion

5.2.1 Synthesis and characterization of allyl F-ILs and their reactivity with palladium chloride

The synthetic route used to prepare the allyl functionalised imidazolium salts **15a** – **18a** is illustrated in Scheme 5.1. Allyl bromide and 1-methylimidazole or 1-allylimidazole are diluted in methanol and stirred at room temperature, to afford **15a** and **16a**, respectively.[1] Metathesis of **15a** or **16a** with Na[BF_4] or Na[BPh_4] in acetone using standard methods [4]affords **15b**, **15c**, **16b** and **16c.** Compound **15c** can also be prepared by a halide-free strategy by methylation of 1-allylimidazole with trimethyloxonium tetrafluoroborate.[5] Spectroscopic data for **15c** prepared using the different routes is the same, but the IL prepared via the halide-free route has a higher liquid transition point [-55.4 versus -81.1°C]. Salts **15a**, **16a**, **15c** and **16c** are liquid at room temperature with melting points or glass transition temperature of -52.5, -26.5, -81.1/-55.4 and -46.8 °C, respectively, determined using DSC in repeated heating mode. All the other salts are solids at ambient temperatures. The bis-functionalised ILs **16a** and **16c** have higher melting points than the mono-functionalised ILs **15a** and **15c**. Presumably due to their higher symmetry, which is in keeping with previous observations.[6]

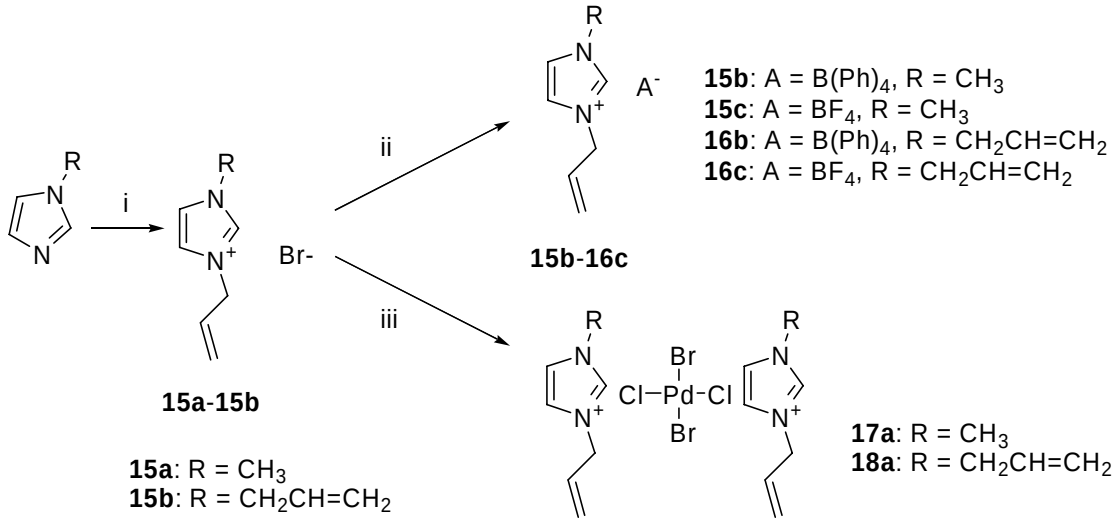

Scheme 5.1 Synthesis of ally functionalized imidazolium salts. Reagents and conditions: (i) 1 equiv CH_2=$CHCH_2Br$, in methanol, RT, 5 days; (ii) for **15c** and **16c**, 1 equiv $NaBF_4$, in acetone, RT, 48 h; for **15b** and **16b**, 1 equiv $NaBPh_4$, in acetone, RT, 48 h; (iii) 1/2 equiv $PdCl_2$, in dichloromethane, RT, 2 days.

Salts **15a** – **16c** were characterized using electrospray ionization mass spectrometry (ESI-MS), IR, ^{1}H and ^{13}C NMR spectroscopy. The positive ion ESI mass spectra of **15a**, **15c** and **15b** reveal a parent peak at *m/z* 123 corresponding to the expected cation, $[H_2C{=}CHCH_2{\lceil}N{=}C(H)N(CH_3)CH{=}C{\rceil}H]^+$. The ESI mass spectra of the bis-functionalized salts **16a**, **16b** and **16c** exhibit a parent peak at *m/z* 149 indicative of the cation, $[H_2C{=}CHCH_2{\lceil}N{=}C(H)N(CH_2CH{=}CH_2)CH{=}C{\rceil}H)]^+$. In negative ion mode, intense peaks at *m/z* 79/81, 87 and 319 demonstrating the presence of the bromide, tetrafluoroborate and tetraphenylborate anions are observed. In keeping with previous observations, aggregates composed of the anions and cations were also observed when the sample was diluted only moderately, but under high dilution essentially only the parent ions were observed with significant relative intensities. The IR spectra of **15b** – **16c** contain stretches between 3050 and 3100 cm^{-1} that correspond to =C─H vibrations, the C=C stretch is observed at c.a. 1645 cm^{-1}. The ^{1}H and ^{13}C NMR spectra of **15b** – **16c** are as expected, with little change in the spectra as the cation is varied. The proton at the 2-position in the imidazolium rings are observed in the range 8.20 – 9.20 ppm and the other ring protons between 7.36 – 7.85 ppm. Three protons on the allyl group are observed in the ranges 6.77 – 6.02, 5.37 – 5.85 and 4.75 – 5.25 ppm, as multiplet resonances, without any notable trend as the anion varies.

In dichloromethane, palladium(II) chloride reacts with two equivalents of **15a** or **16a** to form $[H_2C{=}CHCH_2{\lceil}N{=}C(H)N(CH_3)CH{=}C{\rceil}H]_2[PdCl_2Br_2]$ **17a** and $[H_2C{=}CHCH_2{\lceil}N{=}C(H)N(CH_2CH{=}CH_2)CH{=}C{\rceil}H)]_2[PdCl_2Br_2]$ **18a**, respectively, which are dark red solids at room temperature. The palladium complexes are air stable and decompose slowly in water and alcohols over prolonged periods. They are poorly soluble in chlorinated solvents such as chloroform and dichloromethane, but are soluble in coordinating solvents such as acetonitrile. Complex **7** has a melting point of 134 °C, however, complex **18a**, which has a higher molecular symmetry than **7,** melts at 58 °C and may therefore be classed as an IL based on the commonly accepted definition.[7] Such results infer that even the symmetry of the cation has an effect on the melting point of the salts; but it is not a decisive factor. It has been reported that the type of anion rather than the cation symmetry plays a substantial role in IL formation.[8]And in our case, the

flexibility of the side chain group on imidazolium ring also contributes to low melting point of the salt, which overtakes the symmetric influence.

The structures of **15b**, **16b** and **17a** have been established in the solid state using single crystal X-ray diffraction. Crystals suitable for X-ray diffraction studies were grown at room temperature from acetone-water solutions for **15b** and **16b** and from acetonitrile-diethyl ether for **17a**. Representations of the structures are shown in Figures 5.1, 5.2 and 5.3, respectively, and key bond distances and angles are provided in Table 5.1.

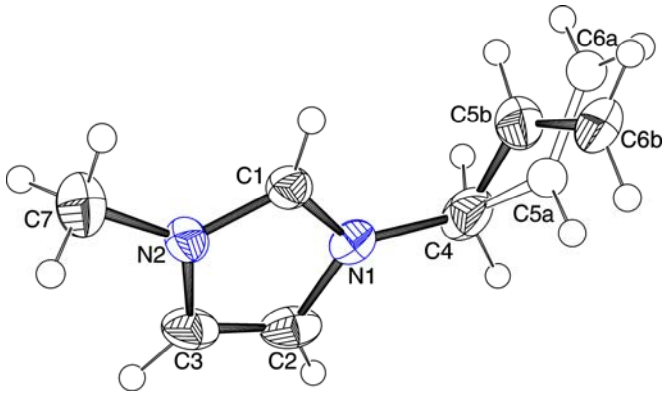

Figure 5.1 ORTEP-plot of 15b; ellipsoids are drawn at the 50 %-probability level.

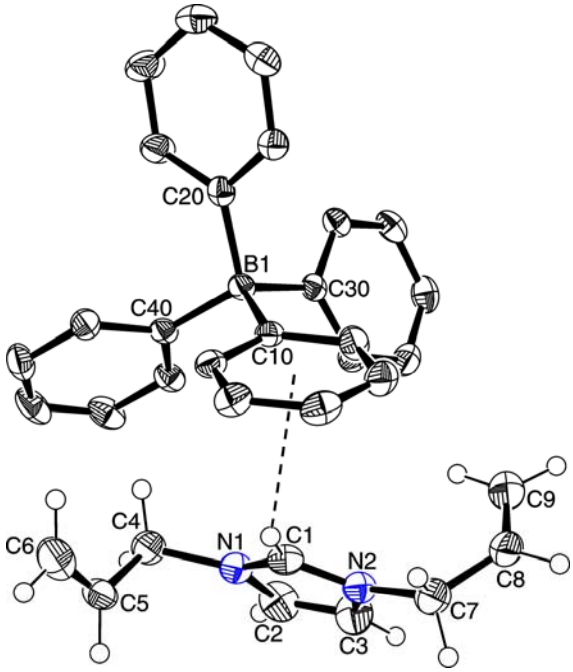

Figure 5.2 ORTEP-plot of 16b; ellipsoids are drawn at the 50 %-probability level.

There is some conformational disorder of the alkene moiety in structures of **15b** and **17a**, in that the alkene carbons are split over two positions, see experimental. Due to residual electron density close to Br1, which could no be refined satisfactorily, the quality of the structure of **17a** is poorer than the other structures.

Comparable structures of allylimidzolium cations are known and agree well with the parameters described herein.[9] In all structures, bond lengths and angles of the imidazolium ring are basically identical within experimental errors. The imidazolium ring is essentially planar and carbon atoms C4 and C7 deviate only very slightly from the plane. In **16b**, the two alkene moieties display almost identical bond distances, 1.301(2) and 1.303(2) Å, respectively. One alkene bond is basically parallel to the plane of the ring, whereas the other adopts a perpendicular orientation with respect to the imidazolium ring. In both **15b** and **16b** there is a weak C-H···π contact stemming from the acidic proton H1 to a phenyl ring on the $[BPh_4]^-$ anion [H1···C10–C15 centroid 3.019 and 2.722 Å, respectively]. Furthermore, in **15b** there is weak π-stacking between the imidazolium and a phenyl ring with the distance between the two ring centroids being 3.77 Å.

Table 5.1 Key bond lengths (Å) and angles (°) for 15b, 16b, 17a and 19.

	15b	**16b**	**17a**	**19**
C1-N1	1.323(3)	1.328(2)	1.30(2)	1.325(3)
C1-N2	1.320(3)	1.328(2)	1.35(2)	1.341(4)
C2-N1	1.378(3)	1.374(2)	1.40(2)	1.379(4)
C3-N2	1.372(3)	1.376(2)	1.39(2)	1.374(4)
C2-C3	1.337(3)	1.343(2)	1.37(2)	1.351(4)
N1-C4	1.478(3)	1.482(2)	1.48(2)	
N2-C7	1.466(3)	1.470(2)	1.46(2)	
C5-C6	disordered	1.301(2)	disordered	
C8-C9		1.303(2)		
Pd-N1				2.103(2)
Pd-Br1			2.401(2)	2.4389(3)
Pd-Cl1			2.350(3)	
N1-C1-N2		108.0(1)	109(1)	106.4(2)
C4-C5-C6	disordered	123.4(2)	disordered	
C7-C8-C9		128.0(2)		

In **17a** the palladium atom resides at a centre of inversion and has a square planar geometry with palladium-halide bond lengths and angles being as expected. The chloride is involved in extensive hydrogen-bonding to symmetry-related cations (5 contacts below 3 Å), whereas there is only one contact to the bromide.

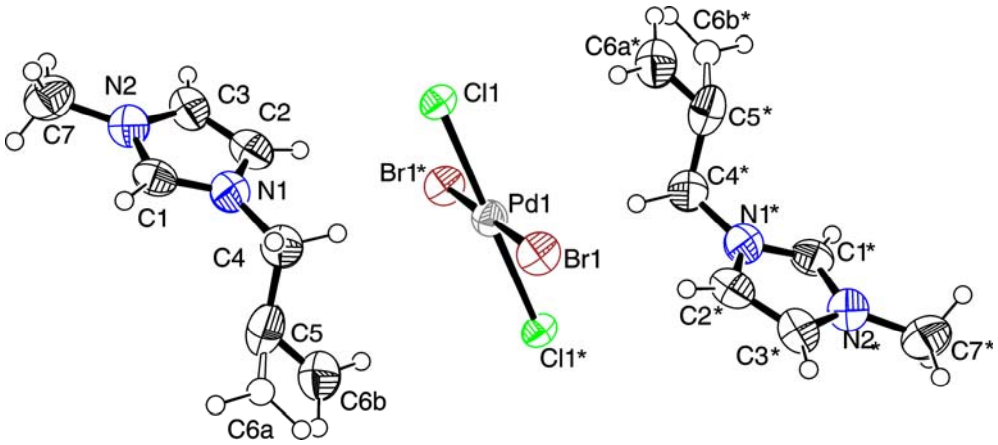

Figure 5.3 ORTEP-plot of 17a; ellipsoids are drawn at the 50 %-probability level. The starred atoms are obtained by the symmetry operation –x, –y, –z+2.

5.2.2 Reactivity of the allyl functionalised ILs

Attempts to polymerize the mono-F-ILs **15a**, **16a** and **17a** using a literature free radical initiator procedure[10] were unsuccessful. The reaction of **17a** with 2,2'-azobis(2-methylpropionitrile) (AIBN) as initiator in acetonitrile solution under reflux, led to the formation of **19**, in crystalline form, in 10 hours. Analysis of the crystals by single crystal X-ray diffraction identified the compound as *trans*-palladium(II)-bis-methylimidazole dibromide, see Figure 5.4. The palladium resides at a centre of symmetry and is almost perfectly square planar with N1-Pd1-Br1 angles being 89.92(7) and 90.08(7)°. The dihedral angle between the plane of the imidazole ring and the square plane around Pd is 131.9°. With the exception of the palladium-nitrogen distance, which is slightly longer due to higher electron density at the metal arising from the less electronegative bromine atoms [2.103(2) *vs* 2.011(4)] all other bonding parameters are identical within experimental errors. The structure of the chloride analogue has been published previously.[11]

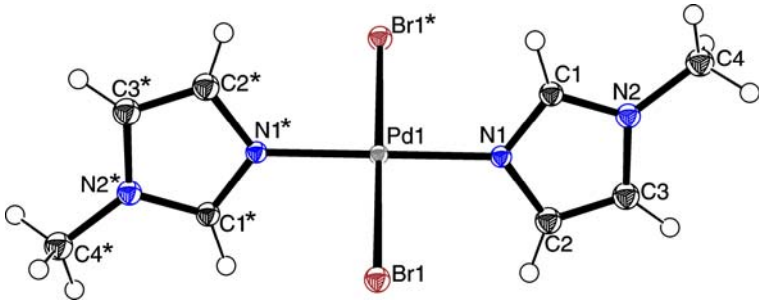

Figure 5.4 ORTEP-plot of 19; ellipsoids are drawn at the 50 %-probability level. The starred atoms are obtained by the symmetry operation –x, –y+1, –z+1

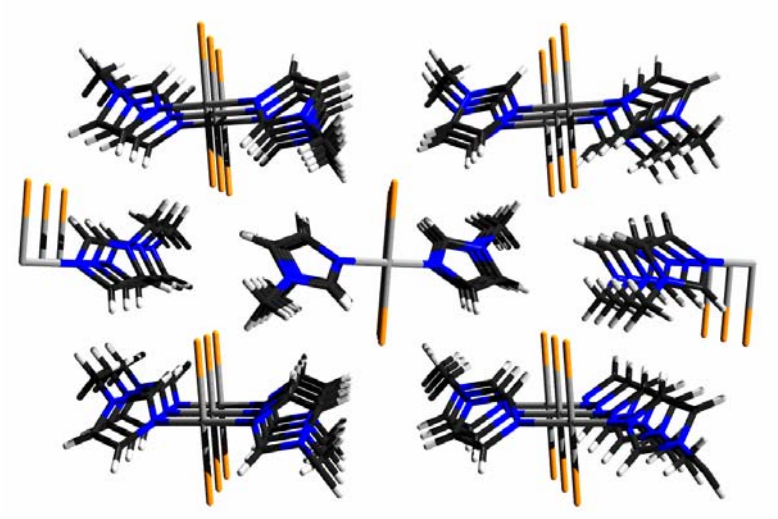

Figure 5.5 Crystal packing in 19

In the crystal, molecules of **19** form stacks in a parallel fashion with the distance between the molecules being 5.385 Å, see Figure 5.5.5. There are no inter- or intramolecular hydrogen bonds below 3 Å to the bromide ligands, thus, the molecules are held together by van-der-Waals forces and weak π-π stacking interactions.

Subsequent spectroscopic and analytical data of **19** was in agreement with the solid state structure. The ^{1}H NMR spectrum shows the protons on the imidazolium ring at 8.14, 7.20 and 7.16 ppm and the methyl group protons at 3.72 ppm. The formation of **19** presumably results from the formation of free radicals derived from AIBN which lead to the elimination of the allyl group from the imidazolium cation.

Addition reactions across the double bond in the allyl-F-ILs represent an important route to a wide a diverse range of new imidazolium salts, and hence ILs. To illustrate this utility, reaction of **15a** with benzene in the presence of triflic acid using literature method,[12] affords **20** (see Scheme 5.2). The ESI-MS spectra of **20** shows a parent peak at *m/z* 201 in positive ion mode corresponding to $[CH_3CH(C_6H_5)CH_2{}^{\lceil}N{=}C(H)N(CH_3)CH{=}C^{\rceil}H]$ and a peak at *m/z* 149 in negative ion mode which can be attributed to the $[CF_3SO_3]^-$ anion. The ^{1}H NMR spectrum of **20** exhibits a multiplet at 3.27 ppm corresponding to the $CH_2C\mathit{H}(Ph)CH_3$ proton and a doublet at 1.33 ppm [J_{HH} 7.0 Hz] corresponding to the methyl group protons. In addition, characteristic resonances for phenyl ring protons are observed between 7.21 and 7.34 ppm.

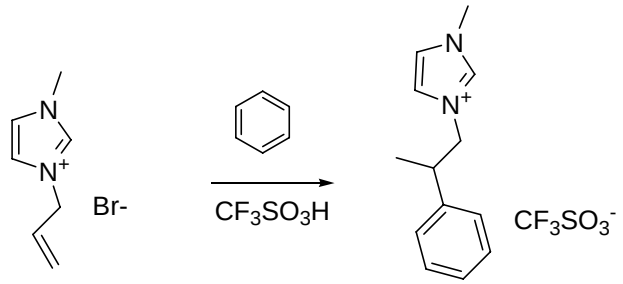

15a **20**

Scheme 5.2 Aryl addition of 15a catalyzed by the Brønsted super acid CF_3SO_3H to afford 20

In summary, we have synthesized a series of allyl F-ILs and demonstrated that they can be used as precursors to other new ILs via addition reactions across the unsaturated bond.

5. 3 Concluding remarks

Two imidazolium salts, 1-allyl-3-methylimidazolium bromide, **15a** and di-allylimidazolium bromide, **16a** were prepared from the direct reaction between allyl bromide and 1-methylimidazole or 1-allyimidazole. Exchange of the bromide anion in **15a** and **16a** with $[BPh_4]^-$ or $[BF_4]^-$ affords **15b**, **15c**, **16b**, and **16c**. Salts, **15a**, **16a**, **15c** and **16c** are liquids at room temperature. Reaction of $PdCl_2$ with salts **15a** and **16a** affords the palladium complexes **17a** and **18a**. Complex **18a** melts at 58 °C, and thus, may be classified as an IL. Attempts to polymerize **17a** resulted in the isolation of the palladium complex, **19**, rather than a polymer. In addition, further addition of **15a** was also undertaken affording **20**, another F-IL.

5. 4 Experimental

All chemicals were purchased from Acros and were used as received without further purification. Compound **1** and **2** were prepared according to literature method.[1] Reactions were performed under an inert atmosphere of dry nitrogen using standard Schlenk techniques in solvents dried using the appropriate reagents and distilled prior to use. IR spectra were recorded on a Perkin-Elmer FT-IR 2000 system. NMR spectra were measured on a Bruker DMX 400 MHz spectrometer, using $SiMe_4$ (^1H, ^{13}C) as external standards at 20 °C. Electrospray ionization mass spectra (ESI-MS) were recorded on a ThermoFinnigan LCQ™ Deca XP Plus quadrupole ion trap instrument on samples diluted in methanol or water. Samples were infused directly into the source at 5 μL min^{-1} using a syringe pump and the spray voltage was set at 5 kV and the capillary temperature at 50 °C.[13] Elemental analysis was carried out at the EPFL. Melting points of all the liquid compounds were measured using differential scanning calorimeter (DSC) performed with a SETARAM DSC 131 instrument by heating mode.

Synthesis of $[H_2C{=}CHCH_2{\ulcorner}N{=}C(H)N(CH_3)CH{=}C{\urcorner}H][BF_4]$ ***15c***

A) Metathesis method: A mixture of **15a** (6.09 g, 0.03 mol) and $NaBF_4$ (3.62 g, 0.033 mol) in acetone (80 ml) was stirred at room temperature for 48 h. The resulting solid was filtered and the solvent was removed under vacuum. The product was obtained as a pale yellow waxy solid. Yield: 5.86 g, 93%; Melting point: -81.1 °C; ESI-MS (H_2O, *m/z*): positive ion, 123 $[CH_2CH{=}CH_2im]^+$; negative ion, 87, $[BF_4]^-$; ^1H NMR (Aceton-d6): δ = 9.04 (s, 1H), 7.70 (s, 1H), 7.65 (s, 1H), 6.75 (m, 1H), 5.85 (s, 1H), 5.25 (m, 2H) 3.99 (s, 3H); ^{13}C NMR (Aceton-d6): δ = 136.2, 129.4, 124.3, 114.6, 114.42, 52.3, 35.7; IR (cm^{-1}): 3155 and 3117 ($\nu_{C\text{-}H}$ aromatic), 3088 ($\nu_{=C\text{-}H}$), 2978 ($\nu_{C\text{-}H}$ aliphatic), 1599 ($\nu_{C=C}$); Anal. Calcd. for $C_7H_{11}N_2BF_4$ (%): C 40.03, H 5.28, N 13.34; Found: C 40.02, H 5.25, N 13.26.

B) Halide-Free method: 1-Allylimidazole (5 ml) was added drop wise to a rapidly stirred suspension of trimethyloxonium tetrafluoroborate (1 mol equiv.) in hexane (20 ml) at -78°C over a period of 10 min. After the initial vigorous evolution of gas had ceased, the reaction mixture was allowed to warm to room temperature. The product was washed with diethyl ether (3 × 25 ml), then dried under vacuum to afford pale yellow liquid in quantitative yield. Melting point: -55.4°C. ESI-MS (H_2O, *m/z*): positive ion, 123 $[CH_2CH{=}CH_2im]^+$; negative ion, 87, $[BF_4]^-$; ^1H NMR (Aceton-d6): δ = 8.64 (s, 1H), 7.47 (s, 1H), 7.43 (s, 1H), 6.02 (m, 1H), 5.38 (s, 1H), 4.78 (m, 2H) 3.93 (s,

3H); ^{13}C NMR (Aceton-d6): δ = 136.1, 130.6, 124.0, 122.6, 121.1, 51.5, 35.7; IR (cm^{-1}): 3158 and 3120 (ν_{C-H} aromatic), 3089 ($\nu_{=C-H}$), 2977 (ν_{C-H} aliphatic), 1577 ($\nu_{C=C}$); Anal. Calcd for $C_7H_{11}N_2BF_4$ (%): C 40.03, H 5.28, N 13.34; Found: C 40.10, H 5.26, N 13.41.

Synthesis of $[H_2C{=}CHCH_2{\ulcorner}N{=}C(H)N(CH_3)CH{=}C{\urcorner}H][BPh_4]$ ***15b***

A mixture of **1** (6.09 g, 0.03 mol) and $NaBPh_4$ (11.29 g, 0.033 mol) in acetone (80 ml) was stirred at room temperature for 48 h. The resulting solid was filtered. Water (5 ml) was added to the filtrate and colorless crystals formed over a period of 3 days. The crystals were collected by filtration. Yield: 11.8 g, 89%; M. p.: 145.1 °C; ESI-MS (H_2O, *m/z*): positive ion, 123 $[CH_2CH{=}CH_2im]^+$; negative ion, 319, $[B(C_6H_5)_4]^-$; ^{1}H NMR (Aceton-d6): δ = 8.20 (s, 1H), 7.48 (s, 2H), 7.36 (t, 8H), 6.93 (t, 8H), 6.77 (t, 4H), 6.02 (m, 1H), 5.37 (m, 1H), 4.75 (m, 2H), 3.82 (s, 3H); ^{13}C NMR (Aceton-d6): δ = 164.8, 164.3, 163.8, 163.3, 136.4, 136.1, 131.0, 126.0, 125.2, 122.3, 121.4, 120.5, 51.4, 35.9; IR (cm^{-1}): 3137 (ν_{C-H} aromatic), 3082, 3053, 3033 ($\nu_{=C-H}$), 2999 and 2945 (ν_{C-H} aliphatic), 1599 ($\nu_{C=C}$); Anal. Calcd for $C_{31}H_{31}N_2B$ (%): C 84.16, H 7.06, N 6.33; Found: C 85.30 H 7.10, N 6.26.

Synthesis of $[H_2C{=}CHCH_2{\ulcorner}N{=}C(H)N(CH_2CH{=}CH_2)CH{=}C{\urcorner}H][BF_4]$ ***16c***

A mixture of **16a** (6.87 g, 0.03 mol) and $NaBF_4$ (3.62 g, 0.033 mol) in acetone (80 ml) was stirred at room temperature for 48 h. The resulting solid was filtered and the solvent was removed under vacuum. The product was obtained as a pale yellow waxy solid. Yield: 6.37 g, 90%; Melting point: -46.8 °C; ESI-MS (H_2O, *m/z*): positive ion, 149 $[DiCH_2CH{=}CH_2im]^+$; negative ion, 87, $[BF_4]^-$; ^{1}H NMR (Aceton-d6): δ = 9.18 (s, 1H). 7.71 (s, 2H), 6.18 (m, 2H), 5.41 (m, 4H), 5.01 (m, 4H); ^{13}C NMR (Aceton-d6): δ = 136.2, 129.5, 123.4, 121.8, 52.2; IR (cm^{-1}): 3145 (ν_{C-H} aromatic), 3077 ($\nu_{=C-H}$), 2941, 2852 (ν_{C-H} aliphatic), 1654 ($\nu_{C=C}$); Anal. Calcd for $C_9H_{13}N_2BF_4$ (%): C 45.80, H 5.55, N 11.87; Found: C 45.75, H 5.47, N 11.76.

Synthesis of [H_2C=$CHCH_2$⌜N=C(H)N(CH_2CH=CH_2)CH=C⌝H)][BPh_4] ***16b***

A mixture of **16a** (6.87 g, 0.03 mol) and $NaBPh_4$ (11.29 g, 0.033 mol) in acetone (80 ml) was stirred at room temperature for 48 h. The resulting solid was filtered off. Water (5 ml) was added to the filtrate and colorless crystals formed over a period of 3 days. The crystals were collected by filtration. Yield: 12.4 g, 88%; M. p.: 170.2 °C; ESI-MS (H_2O, *m/z*): positive ion, 149 [$DiCH_2CH$=CH_2im]$^+$; negative ion, 319, [$B(C_6H_5)_4$]$^-$; ^{1}H NMR (Aceton-D6): δ = 8.17 (s, 1H), 7.41 (s, 2H), 7.38 (t, 8H), 7.01 (t, 8H), 6.87 (t, 4H), 5.98 (m, 1H), 5.37 (m, 1H), 4.68 (m, 2H); ^{13}C NMR (Aceton-d6): δ = 164.9, 164.2, 163.6, 163.3, 136.3, 135.9, 131.0, 124.8, 123.2, 122.3, 120.4, 120.1, 51.4; IR (cm^{-1}): 3139 (ν_{C-H} aromatic), 3088, ($\nu_{=C-H}$), 2999 and 2945 (ν_{C-H} aliphatic), 1631 ($\nu_{C=C}$); Anal. Calcd for $C_{33}H_{33}N_2B$ (%): C 84.61, H 7.10, N 5.98; Found: C 84.64, H 7.10, N 5.86.

Synthesis of [H_2C=$CHCH_2$⌜N=C(H)N(CH_3)CH=C⌝H][$PdCl_2Br_2$] ***17a***

$PdCl_2$ (177 mg, 1.0 mmol) was added to a solution of **15a** (406 mg, 1.0 mmol) in dichloromethane (5.0 ml). The reaction mixture was stirred at room temperature for 2 days, during a dark-red suspension formed. The solid was collected by filtration followed by washing with dichloromethane (2 × 2.0 ml) and dried under vacuum. Yield: 553 mg, 95%; M. p.: 133.9 °C, (decomp.); ^{1}H NMR (DMSO-d6): δ = 9.16 (s, 1H), 7.65 (m, 2H), 5.91 (m, 1H), 5.19 (m, 1H), 4.77 (m, 2H), 3.78 (s, 3H); ^{13}C NMR (DMSO-d6): δ = 136.5, 132.1, 124.1, 121.7, 120.7, 51.4, 36.4 IR (cm^{-1}): 3138 (ν_{C-H} aromatic), 3091, 3071 ($\nu_{=C-H}$), 2973, (ν_{C-H} aliphatic), 1632 ($\nu_{C=C}$). Anal. Calcd for $C_{14}H_{22}Br_2Cl_2N_4Pd$ (%): C 28.82, H 3.80, N 9.60; Found: C 28.80, H 3.78, N 9.69.

Synthesis of [H_2C=$CHCH_2$⌜N=C(H)N(CH_2CH=CH_2)CH=C⌝H)]$_2$[$PdCl_2Br_2$] ***18a***

$PdCl_2$ (177 mg, 1.0 mmol) was added to a solution of **2** (458 mg, 1.0 mmol) in dichloromethane (5.0 ml). The reaction mixture was stirred at room temperature for 2 days, during which time a dark-red suspension formed. The solid was collected by filtration followed by washing with dichloromethane (2 × 2.0 ml) and dried under vacuum. Yield: 553 mg, 95%; M. p.: 58 °C; ^{1}H NMR (DMSO-d6): δ = 9.28 (s, 1H). 7.78 (s, 2H), 6.02 (m, 2H), 5.35 (m, 4H), 5.27 (m, 4H); ^{13}C NMR (DMSO-d6): δ = 136.7, 132.2, 123.5, 122.1, 51.4; IR (cm^{-1}): 3124 (ν_{C-H} aromatic), 3091 ($\nu_{=C-H}$), 2981, 2960 (ν_{C-H}

aliphatic), 1644 ($\nu_{C=C}$); Anal. Calcd for $C_{18}H_{26}Br_2Cl_2N_4Pd$ (%): C 34.02, H 4.12, N 8.81; Found: C 34.08, H 4.18, N 8.79.

Synthesis of H⌜C=CH(CH₃)N(H)C=N⌝Pd(Br)₂⌜N=C(H)N(CH₃)CH=C⌝H ***19***

2, 2'-Azobis(2-methylpropionitrile) (2 mg) was added to a solution of palladium complex **17a** (291.5 mg, 0.5 mmol) in acetonitrile (10 ml). The reaction mixture was heated at 80 °C for 10 h. The reaction mixture was then cooled to room temperature. Orange cubic crystals **9** formed over a period of 24 h were collected by filtration. Yield: 20 mg, 9%; M. p.: 248.9 °C, decompose; ^{1}H NMR (DMSO-d6): δ = 8.14 (s, 1H). 7.20 (s, 1H), 7.16 (s, 1H), 3.72 (s, 1H); ^{13}C NMR (DMSO-d6): δ = 137.7, 131.2, 124.2, 32.4; IR (cm^{-1}): 3138 (ν_{C-H} aromatic), 2951 (ν_{C-H} aliphatic); Anal. Calcd for $C_8H_{12}Br_2N_4Pd$ (%): C 22.32, H 2.81, N 13.01; Found: C 22.08, H 2.84, N 13.09.

Synthesis of [CH₃CH(C₆H₅)CH₂⌜N=C(H)N(CH₃)CH=C⌝H][CF₃SO₃] ***20***

Triflic acid (30 ml, excess) was added to a suspension of **15a** (2.03 g, 0.01 mol) in benzene (20 ml). The reaction mixture was refluxed for 6 h. After cooling down to 0°C and it was neutralized with NaOH aqueous solution (40%) (pH value approximately 7.1). The mixture is then extracted with CH_2Cl_2 (30 ml × 3) and the combined organic phase is washed with saturated aqueous ammonium chloride solution, dried with $MgSO_4$ and concentrated under vacuum to give a pale yellow liquid. Yield: 0.8 g, 22%; M. p.: -56°C, ESI-MS (CH_2Cl_2, *m/z*): positive ion, 201, $[CH_3CH(C_6H_5)CH_2mim]^+$; negative ion, 149, $[CF_3SO_3]^-$; ^{1}H NMR (Acetonitrile-d3): δ = 8.32 (s, 1H). 7.37 (s, 1H), 7.35 (s, 1H), 7.30 – 7.34 (m, 2H), 7.21 – 7.27 (m, 3H) 4.25 – 4.40 (m, 2H) , 3.76, (s, 3H), 3.27 (m, 1H), 1.32 (d, 3H); ^{19}F NMR (Acetonitrile-d3) δ = –79.7; ^{13}C NMR (Acetonitrile-d3): δ = 137.8, 124.8, 123.3, 123.1, 122.1, 119.4, 118.5, 51.5, 36.5, 31.8, 13.7; IR (cm^{-1}): 3151 (ν_{C-H} aromatic), 2969 (ν_{C-H} aliphatic); 1574, 1256, 1163, 1029. Anal. Calcd for $C_{14}H_{17}F_3N_2O_3S$ (%): C 47.99, H 4.89, N 7.99; Found: C 47.68, H 5.00, N 7.89.

X-ray data for ***15b****,* ***16b****,* ***17a*** *and* ***19***

Crystals of **15b** and **16b** suitable for X-ray diffraction studies were obtained at room temperature from in acetone/water (10:1) solution. Crystals of **17a** was obtained at room temperature from in

acetonitrile/diethyl ether (10:1) solution and crystal of **19** from dichloromethane solution. CrySingle crystals were mounted on a KUMA KM4/Sapphire CCD diffractometer. Data reduction was performed using CrysAlis RED.[14] Structure solution and refinement was performed using the SHELX97 software package,[15] graphical representations of the structures were made with ORTEP32.[16] Structures were solved by direct methods and successive interpretation of the difference Fourier maps, followed by full matrix least-squares refinement (against F^2). All non-hydrogen atoms were refined anisotropically. Hydrogen atoms were placed in their geometrically generated positions and refined using a riding model. An adsorption correction (DELABS) was applied for **17a** and **19**. In **15b**, carbon atoms C5 and C6 are split over two positions with an occupancy factor of 0.62. In **19**, carbon atom C6 is split over two positions (occupancy factor 0.67). Furthermore, there is considerable residual electron density close to Br1 which could not be refined.

Table 5.2 Crystallographic data and details of 15b, 16b, 17a, 19

	15b	**16b**	**17a**	**19**
Formula	$C_{31}H_{31}BN_2$	$C_{33}H_{33}BN_2$	$C_{14}H_{22}Br_2Cl_2N_4Pd$	$C_8H_{12}Br_2N_4Pd$
M	442.39	468.42	583.48	430.44
Crystal system	monoclinic	monoclinic	monoclinic	monoclinic
Space group	$P2_1/n$	$P2_1/n$	$P2_1/n$	$P2_1/c$
a/Å	9.6409(8)	10.8209(6)	8.870(2)	5.3852(5)
b/Å	17.647(2)	17.478(1)	12.110(4)	11.815(1)
c/Å	15.3633(8)	13.8763(9)	9.908(4)	9.7595(8)
α/°	90	90	90	90
β/°	104.137(7)	90.804(5)	101.98(3)	98.139(7)
γ/°	90	90	90	90
V/Å^3	2534.6(3)	2624.2(3)	1041.1(6)	614.73(9)
Z	4	4	2	2
Density [Mg/m^3]	1.159	1.186	1.861	2.325
T/K	140	140	140	140
Θ range/°	$3.07 \le \Theta \le 25.03$	$3.16 \le \Theta \le 25.03$	$3.27 \le \Theta \le 25.03$	$3.45 \le \Theta \le 25.03$
μ/mm^{-1}	0.067	0.068	4.989	7.983
Reflections measured	14982	15423	6349	3355
Unique reflections [$I>2\sigma$(	4250 (R_{int} = 0.0607)	4385 (R_{int} = 0.0374)	1844 (R_{int} = 0.0422)	1084 (R_{int} = 0.0272)
Final *R*1, *wR*2[$I>2\sigma(I)$]	0.0422, 0.0641	0.0362, 0.0775	0.0982, 0.2876	0.0215, 0.0529

5.5 References

[1] J. B. Jones, D. W. Hysert, *Can. J. Chem.* **1971**, *49*, 325.

[2] J. Wu, J. Zhang, H. Zhang, J. He, Q. Ren, M. Guo, *Biomacromolecules,* **2004,** *5*, 266.

[3] T. Mizumo, E. Marwanta, N. Matsumi, H. Ohno, *Chem. Lett.* **2004**, *33*, 1360.

[4] P. A. Z. Suarez, J. E. L. Dullius, S. Einloft, R. F. De Souza, J. Dupont, *Polyhedron* **1996**, *15*, 1217.

[5] P. J. Dyson, D. J. Ellis, G. Laurenczy, *Adv. Synth. Catal.* **2003**, *345*, 216.

[6] A. S. Larsen, J. D. Holbrey, F. S. Tham, C. A. Reed, *J. Am. Chem. Soc.* **2000**, *122*, 7264.

[7] P. Wasserscheid, T. Welton, ed. *Ionic Liquids in Synthesis* Wiley-VCH, Weinheim, Germany, **2002**. p1.

[8] J. Pernak, K. Sobaszkiewicz, J. Foksowicz-Flaczyk, *Chem. Eur. J.* **2004**, *10*, 3479.

[9] W. Chen, F. Liu, *J. Organomet. Chem.* **2003**, *673*, 5.

[10] (a) H. S. Bisht, A. K. Chatterjee, *J. Macromole. Sci., Polymer Rev.* **2001**, *C41,* 139; (b) C. J. Hawker, *Accoun. Chem. Res.* **1997**, *30*, 373.

[11] M. C. Navarrro-Ranninger, *Acta Cryst. C* **1983**, *C39*, 186.

[12] Y. Zhang, A: McElrea, G. V. Sanchez Jr, D. Do, A. Gomez, S. L. Aguirre, R. Rendy, D. A. Klumpp, *J. Org. Chem.,* **2003**, *68*, 5119.

[13] P. J. Dyson, J. S. McIndoe. *Inorg. Chim. Acta* **2003**, *354*, 68.

[14] Oxford Diffraction Ltd, 68 Milton Park, Abingdon, OX14 4 RX, UK, 2003.

[15] G. M. Sheldrick, *SHELX-97. Structure Solution and Refinement Package*. Universität Göttingen, 1997.

[16] L. J. Farrugia, *J. Appl. Crystallogr.* **1997**, *30*, 565.

6

“Dual-functionalized” ILs: Synthesis and Characterization of Imidazolium Salts with the Butylnitrile 3-trifluoroborate Anion

6.1 Introduction

It has been pointed out in chapter 1 that the fuctionalization of IL cations is the main methodoloy to obtain task-specific ILs. Although the synthesis of F-ILs via imidazolium cation modification is relatively straitforward, the main problem with such ILs is that their melting points and viscosities tend to be much higher, and some modified imidazolium salts are even solids at ambient temperature, when compared to closely related alkyl-substituted imidazloium salts.[1] Increased melting points and viscosity are not conducive to the application of ILs as solvents. In contrast, task-specific anion synthesis has not received much attention, however, IL functionalization through anion adaption represents a promising route to obtaine F-ILs with low melting points and viscosities.

The early examples of anion-F-ILs were prepared via anion exchange with readily available materials. For example, the aluminium chloride[2] and metal-carbonyl anions[3] were reported (Chart 6.1).

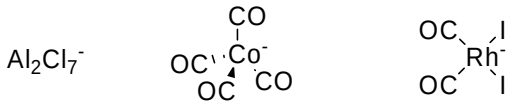

Chart 6.1 Aluminium chloride and metal carbonyl anion

Perfuluoroalkyltrifluoroborate anions that can lead to a series of ILs of low viscosity (Chart 6.2) have also been reported.[4]

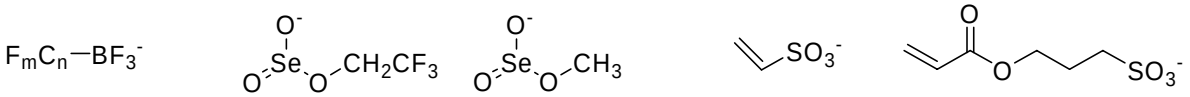

Chart 6.2 Perfluoroalkyltrifluoroboratea, selenite and vinyl functionalized anions

Selenite anions have also been prepared and used to form low-viscosity ILs that can be used as reaction media for oxidative carbonylation of aromatic amines (Chart 6.2).[5] An anion that has a polymerable vinyl group has also been prepared as a precursor for IL polymer synthesis (Chart 6.2).[6]

In chapters 2 and 4, we showed that after incoporating the nitrile functionality, the melting point and visocity of the resulting ILs increased. In this chapter, a series of "dual-functionalized" ILs, comprising imidazolium cations with various functionalities and the asymmetric nitrile

functionalized anion $[CH_3CH(BF_3)CH_2CN]^-$, aiming at reducing the melting point and visocity of FLs, will be described.

6.2 Results and discussion

6.2.1 Synthesis and characterization of inoic liquids with the nitrile functionalized anion $[CH_3CH(BF_3)CH_2CN]^-$

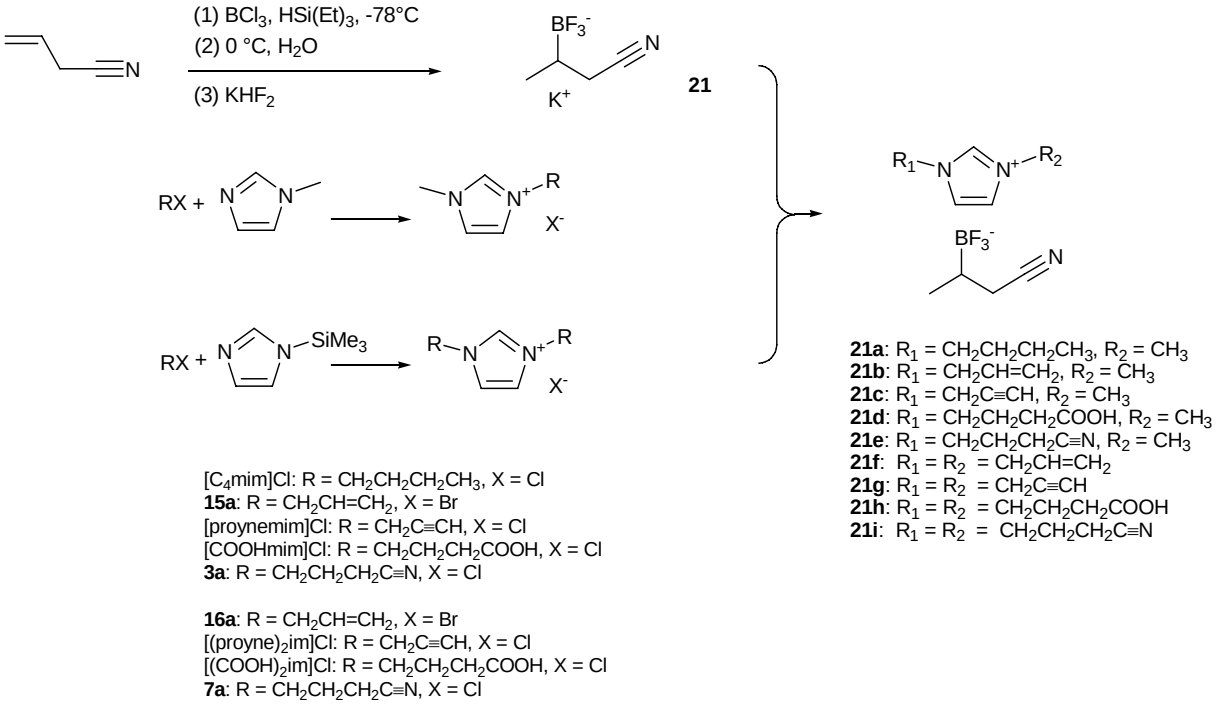

Scheme 6.5 Synthesis of ILs with the butyronitriletrifluoroborate anion

The synthetic strategy involves preparation of the functionalized anion as a simple potassium metal salt, followed by anion metathesis with various imidazolium halides (see Scheme 6.5), which represents the most widely used method to perpare ILs.[2] The first step of the anion synthesis involves hydroboration of allyl cyanide using boron trichloride and triethylsilane, followed by addition of water to afford **t**he boronic acid which was then stirred with KHF_2 in ether/H_2O at ambient temperature, in accord with a published protocol.[7,8] The product, $K[CH_3CH(BF_3)CH_2CN]$ **21**, was recrystallised from acteone-diethyl ether as white needles in 74% yield. The formation of **21** is somewhat unusual, since the related alkene $Cl(CH_2)_2CH=CH_2$ gave $K[BF_3(CH_2)_4CH_3]$ under the same conditions.[8] In the ^1H NMR spectrum of **21**, the CH group displays a broad multiple at 0.69 ppm; the CH_3 group enhibits a doublet at 0.97 ppm with a $^3J(HH)$ of 7.3 Hz; the CH_2 group shows two sets of doublets of doublets at 2.04 ppm and 2.47 ppm, the two H atoms are unidentical

as indicated by two different ^{3}J(HH) values of 4.3 Hz and 10.7Hz; the ^{2}J(HH) for the H-H coupling of CH_2 is -17.1Hz. Minor changes in the chemical shift are observed in different solvents. The signals in the ^{19}F and ^{11}B spectra are very broad even at low temperature in water or acetone. There are probably intense interactions between the F and H atoms within molecule or between molecule and solvent. However, the ^{1}J(BF) can be roughly resolved at 60 Hz, this value is in accordance with structurally similar compounds.[9] In order to acertain the molecular structure of **21**, attempts to crystals to grow crystals from different solvents were made, but the crystals were too small and no satisfactory results were obtained. Replacement of the potassium cation by the large organic cation bistriphenylphosphinoimine afforded crystals and the X-ray structure of the resulting salt confirmed the anion structure.

Table 6.1 Melting point, viscosity and solubility properties of dual-F-ILs.

Ionic liquids[a]	Melting Point (°C)	Viscosity (cp, 20°C)	Solubility in common solvents[b]					
			H_2O	Et_2O	EtOH	Acetone	Dichloromethane	Hexane
21a	-84.5	101.4	m	i	m	m	m	i
$[C_4mim][BF_4]$[21]	-81.0	115.2	m	i	m	m	m	i
21b	-89.2	25.8	m	i	m	m	pm	i
[CC=Cmim][BF_4] **15c**	-81.1	6110	m	i	m	m	pm	i
21c	-80.4	175.1	m	i	m	m	m	i
21d	-58.6	3047	m	i	m	m	i	i
$[C_3COOHmim][BF_4]$[12]	-58.0	4415	m	i	m	m	i	i
21e	-76.6	107.5	m	i	m	m	i	i
$[C_3CNmim][BF_4]$[13] **3c**	-71.9	230.0	m	i	m	m	i	i
$[DiCC{\equiv}Cmim][BF_4]$[20]	67.0	-	m	i	m	m	i	i
21f	-87.3	56.8	m	i	m	m	pm	i
21g	-55.1	1797	m	i	m	m	i	i
21h	38.0	-	m	i	m	m	i	i
21i	-69.8	402.4	m	i	m	m	i	i

[a]$[C_4mim][BF_4]$: 1-methyl-3-butylimidazolium tetrafluoroborate; [CC=Cmim][BF_4]: 1-methyl-3-allylimidazolium tetrafluoroborate; $[DiCC{\equiv}Cmim][BF_4]$: 1,3-di-akylimidazolium tetrafluoroborate; $[C_3COOHmim][BF_4]$: 1-methyl-3-proylcarboxylimidazolium tetrafluoroborate. [b]m for miscible, i for immiscible, p for partly miscible.

Commencing with 1-methyl-imidazole or 1-trimethylimidazole[10] a series of imidazolium halides were pepared using standard methods. Sunsequent metathesis of these imidazolium halides with **21** in acetone gave the DF-ILs **21a** – **21i** in high yield (typically 80 – 85%).

All the new salts were characterised by IR and NMR spectroscopy, electrospray ionisation mass spectrometry (ESI-MS) and elemental analysis. The IR spectra of the DF-ILs reveal that the

absorption between 2400 – 2880 cm^{-1} , indicative of the halide, has dissepeared, to be replaced by the characteristic absorption of the nitrile functionality on the anion (as well as the functional group attached to the cation). The C≡N vibration of the anion appear around 2236-2240 cm^{-1}. The ^{1}H and ^{13}C NMR spectra of the DF-ILs are not too dissimilar from their corresponding halide salts; the ^{19}F chemical shift of all the new DF-ILs differ also only very slightly, which are generally broad signals. The ESI mass spectra exhibit the parent peak for the cation (positive mode) and a strong molecular ion at *m/z* 136 in negative mode.

6.2.2 Physical properties

The melting point, viscosity and solubility data of the DF-ILs are compared with the analogous tetrafluoroborate salts in Table 1. Significantly, despite the presence of a functional group on the anion making it bulkier than BF_4^-, and also potentially taking part in intermolecular interactions, the DF-ILs exhibit lower viscosities and metling points. For example, the melting point of [CC=Cmim][$CH_3CH(BF_3)CH_2CN$] **21b** is only 8°C lower than that of [CC=Cmim][BF_4] but the viscosity is considerably reduced (25.8 versus 6110 cp). As far as we are aware, until now the IL with the lowest viscosity is 1-methyl-3-ethylimidazolium bis(trifluoromethane)sulfonimide which has a viscosity of 28 cp.[11] It is not unreasonable to attribute the reduced melting points and viscoities of these ILs onto the asymmetry of the anion, the related effect for asymmetric cations has been known for many years.[12] The BF_3 group may be coordinated to the imidazole ring, and the positive charge in the imidazole ring and the negative charge at the boron atom could be more delocalized, reducing the salt property of the whole molecule, and as a results, the viscosity decreased. Similar head-tail interactions have been observed in the solid state of nitrile-functionalized imidazolium salts where the N atom in the CN group interacts with the positive charged imidazole ring. The solubility of the DF-ILs in common organic solvents is similar to that of the analogous tetrafluoroborate salts as shown in the Table.

6.3 Concluding remarks

It has been shown that incorporating the $[CH_3CH(BF_3)CH_2CN]^-$ anion not only endows ILs with multiple functionality, but reduces the melting point and viscosity of the IL. The functionality on anion is not confined to the nitrile group, but other functioanal group can also be introduced using a similar strategy. Such combination of both functionalized the cations and anions will enrich the field of ILs by adding another dimension to IL design. The DF-ILs reported herein are composed of potential donor groups for transition metals, they dissolve a wide range of transition metal oxides and halide salts and may prove useful in many applications.

6.4 Experimental

The compounds $[C_4mim]Cl$[13], [proynemim]Cl[14], [COOHmim]Cl[15], **3a**[16], $[(proyne)_2im]Cl$[17], and $[(COOH)_2im]$[15] were prepared according to the literature methods or described in this thesis elsewhere. All chemicals are purchased from Acros® and were used as received without further purification. Synthesis was performed under an inert atmosphere of dry nitrogen using standard Schlenk techniques in solvents dried using the appropriate reagents and distilled prior to use. IR spectra were recorded on a Perkin-Elmer FT-IR 2000 system. NMR spectra were measured on a Bruker DMX 400, using $SiMe_4$ for ^1H, ^{13}C, $CFCl_3$ for ^{19}F and BF_3-Et_2O for ^{11}B as external standards at 20°C. Electrospray ionisation mass spectra (ESI-MS) were recorded on a ThermoFinnigan LCQ™ Deca XP Plus quadrupole ion trap instrument on sample diluted in methanol. Samples were infused directly into the source at 5 μL min-1 using a syringe pump and the spray voltage was set at 5 kV and the capillary temperature at 50°C. Elemental analysis was carried out at the Institute of Molecular and Biological Chemistry at the EPFL. Melting points of all the liquid compounds were measured using Differential scanning calorimetry performed with SETARAM DSC 131 instrument. Viscosities were measured with a Brookfield DV-II+ viscometer on 0.50 ml of sample. The temperature of the samples was maintained to 20 ± 1°C by means of an external temperature controller. The measurements were performed in duplicate.

*Synthesis of **21***

To a flask containing a mixture of allyl cyanide (5.37 g, 80 mmol) and $HSiEt_3$ (10.0 g, 85 mmol), a solution of BCl_3 (1.0 M in dichloromethane, 90 ml, 90 mmol) was added at –78°C under an inert atmosphere. The resulting solution was stirred at for 1 h and then allowed to warm to room temperature. The mixture was cooled to 0°C and water (100 ml) and diethyl ether (100 ml) were added slowly. The resulting suspension was stirred for 10 h and then extracted with ether (3 x 50 ml), dried over $MgSO_4$ overnight and filtered. After removal of solvent, a colorless liquid (8.02 g, 71 mmol) was obtained. This liquid was transferred to a PFA beaker and redissolved in diethylether following addition of KHF_2 (22.1 g, 284 mmol). The mixture was then stirred for 1 h and extracted with acetone (33 x 50 ml). The combined acetone extract were collected, the solvent removed under reduced pressure leaving a white solid. The solid was recrystallised from acetone-diethylether yielding colorless needles. Yield: 10.4 g, 74%; m.p.: 154°C; ESI-MS (H2O, m/z): positive ion, 39, $[K]^+$; negative ion, 136, $[CH_3(BF_3)CHCH_2CN]^-$; 1H NMR (d4-methanol): 2.36 (dd, ^1H, 2J(H, H) = 17.1 Hz, 3J(H, H) = 4.3 Hz), 1.93 (dd, 1H, 2J(H, H) = 17.1, 3J(H, H) = 10.7 Hz), 0.91 (d, 3H, 3J(H, H) = 7.3 Hz, 0.59 (m, 1H); ^{13}C NMR (d4-methanol): 121.8, 28.57, 20.24, 14.8; ^{19}F NMR (d4-methanol): -138.2 (m), -147.3 (m); ^{11}B NMR (d4-methanol): 7.20 (^1J(B, F) = 60 Hz. IR (cm-1):

2952, 2873, 2247; Anal. Calcd. for $C_4H_6NBF_3K$ (%): C 27.45, H 3.46, N 8.00; Found: C 28.11, H 3.51, N 7.96.

*Synthesis of **15a***

A mixture of 1-methylimidazole (8.21 g, 0.10 mol) and propenyl bromide (12.1 g, 0.10 mol) in methanol (50 ml) was stirred at room temperature for 5 days. The resulted pale yellow viscous liquid was washed with diethyl ether (3 x 100 ml) and then dried in vacuum. Yield: 18.67, 92%. ESI-MS (H_2O, *m/z*): positive ion, 123, $[CH_2CH{=}CH_2mim]^+$; negative ion, 80, $[Br]^-$; ^1H NMR (D_2O): δ 8.79 (s, 1H), 7.52 (s, 1H), 7.50 (s, 1H), 6.07 (m, 1H), 5.43 (m, H), 4.84 (m, 1H), 4.68 (s, 3H), 3.92 (s, 2H); ^{13}C NMR (D_2O): δ 137.01, 136.7, 124.07, 122.5, 120.6, 51.26, 35.93; IR (cm^{-1}): 3151, 3114, 2943, 2865, 1647; Anal. Calcd. for $C_7H_{11}N_2Br$ (%): C 41.40, H 5.46, N, 13.79; Found: C 40.41, H 5.41, N 13.27.

*Synthesis of **16a***

A mixture of 1-allylimidazole (10.8 g, 0.10 mmol) and propenyl bromide (12.1 g, 0.10 mol) in methanol (50 ml) was stirred at room temperature for 5 days followed by evaporation of solvent. The resulting pale yellow viscous liquid was washed with diethyl ether (3 x 30 mL). The product was dried in a vacuum for 24 h. Yield: 21.6 g, 95%; ESI-MS (H_2O, *m/z*): positive ion, 149 $[(allyl)_2im]^+$; negative ion, 80 $[Br]^-$; ^1H NMR (D_2O): δ 9.24 (s, 1H). 7.76 (s, 2H), 6.12 (m, 2H), 5.4 (m, 2H), 4.98 (m, 2H), 3.27 (s, 4H); ^{13}C NMR (D_2O): δ 136.05, 131.7, 122.07, 121.7, 120.8, 51.45; IR (cm^{-1}): 3143, 3087, 2943, 2866, 1646; Anal. Calcd. for $C_7H_{11}N_2Br$ (%): C 41.40, H 5.46, N, 13.79. Found: C 40.41, H 5.41, N 13.27.

*Synthesis of **7a***

A mixture of (trimethysily)imidazole (14.03 g, 0.10 mmol) and $Cl(CH_2)_3CN$ (24.86 g, 0.24 mol) was stirred at 80°C for 24 h. The resulting white solid was washed with diethyl ether (3 x 30 mL). The product was dried in a vacuum for 24 h. Yield: 22.4 g, 94%; m. p.: 100°C. ESI-MS (H_2O, *m/z*): positive ion, 203 $[(C_3CN)_2im]^+$; negative ion, 35, 37 $[Cl]^-$; ^1H NMR (D_2O): δ 8.56 (s, 1H), 7.52 (s, 2H), 4.48 (t, 4H, ^1J(H, H) = 7.15 Hz), 2.66 (m, 4H), 2.35 (t, 4H, ^1J(H, H) = 7.15 Hz); ^{13}C NMR (D_2O): 137.08, 123.44, 119.25, 48.37, 29.33, 25.17. IR (cm^{-1}): 3148, 3115, 2967, 2247, 1567; Anal. Calcd for $C_{11}H_{15}ClN_4$ (%): C 55.35, H 6.33, N 23.47. Found: C 54.98, H 6.08, N 23.55.

*Synthesis of **21a***

A mixture of **21** (1.0 g, 5.71 mmol) and $[C_4mim]Cl$ (0.997 g, 5.71 mmol) were stirred in acetone at room temperature for 24 h. The resulting suspension was filtered and the filtrate dried in vaccum. The resulted IL was purified by washing with diethyl ether following dryness of solvant. Yield: 1.32, 84%. Pale yellow liquid, m. p.: –84.5°C; ESI-MS (H_2O, *m/z*): positive ion, 139, $[C_4mim]^+$;

negative ion, 136, $[CH_3(BF_3)CHCH_2CN]^-$; ^{1}H NMR (d6-acetone): δ 8.28 (s, 1H). 7.16 (s, 1H), 7.11 (s, 1H), 4.45 (t, ^1J(H, H) = 7.15 Hz, 2H), 3.85 (s, 3H), 2.35 (dd, 1H, ^2J(H, H) = -17.1 Hz, ^3J(H, H) = 4.3 Hz), 1.94 (dd, 1H, ^2J(H, H) = -17.1, ^3J(H, H) = 10.7 Hz), 1.77 (m, 2H), 1.38 (m, 2H), 1.12 (t, 3H, J(H, H) = 6.98 Hz), 1.20 (m, 2H), 0.89 (d, 3H, ^3J(H, H) = 7.3 Hz), 0.56 (m, 1H); ^{13}C NMR (acetone): δ 142.16, 126.29, 124.45, 52.20, 38.79, 36.10, 34.22, 15.71; ^{19}F NMR (d6-acetone): -138.2 (m), -149.8 (m); ^{11}B NMR (d6-acetone): 7.25 (^1J(B, F) = 60 Hz); IR (cm^{-1}): 3154, 3117, 2962, 2872, 2239, 1574; Anal. Calcd. for $C_{12}H_{21}BF_3N_3$ (%): C 52.39, H 7.69, N, 15.27. Found: C 52.38, H 7.41, N 15.51.

*Synthesis of **21b***

The same method was used as synthesis of **21a** except **15a** (1.16 g, 5.71 mmol) was used instead of $[C_4mim]Cl$. Yield: 1.30g, 88%. Pale yellow liquid, m. p.: –89.2°C; ESI-MS (H_2O, *m/z*): positive ion, 123, $[CH_2CH{=}CH_2mim]^+$; negative ion, 136, $[CH_3(BF_3)CHCH_2CN]^-$; ^{1}H NMR (d6-acetone): δ 8.89 (s, 1H), 7.67 (s, 1H), 7.66 (s, 1H), 6.07 (m, 1H), 5.58 (m, H), 4.92 (m, 1H), 4.61 (s, 3H), 3.95 (s, 2H), 2.34 (dd, 1H, ^2J(H, H) = -17.1 Hz, ^3J(H, H) = 4.3 Hz), 1.96 (dd, 1H, ^2J(H, H) = -17.1, ^3J(H, H) = 10.7 Hz), 0.87 (d, 3H, ^3J(H, H) = 7.3 Hz, 0.54 (m, 1H); ^{13}C NMR (d6-acetone): 139.01, 136.7, 124.89, 122.7, 121.5, 121.7, 51.38, 35.99, 28.57, 20.24, 14.8; ^{19}F NMR (d6-acetone): -138.0 (m), -147.4 (m); ^{11}B NMR (d6-acetone): 7.20 (^1J(B, F) = 60 Hz). IR (cm^{-1}): 3151, 3114, 1647, 2943, 2865, 2238, 1647; Anal. Calcd. for $C_{11}H_{17}BF_3N_3$ (%): C 51.00, H 6.61, N, 16.22; Found: C 51.21, H 6.45, N 16.17.

*Synthesis of **21c***

The same method was used as synthesis of **21a** except [proynemim]Cl (0.89 g, 5.71 mmol) was used instead of $[C_4mim]Cl$. Yield: 1.20, 82%. Pale yellow liquid, mp –80.4°C; ESI-MS (H_2O, *m/z*): positive ion, 121, $[proynemim]^+$; negative ion, 136, $[CH_3(BF_3)CHCH_2CN]^-$; ^{1}H NMR (d6-acetone): δ 9.49 (s, 1H). 7.87 (s, 1H), 7.58 (s, 1H), 5.59 (d, 1H, ^1J(H, H) = 2.44 Hz), 4.37 (s, 3H), 3.21 (s, 2H); 2.36 (dd, 1H, ^2J(H, H) = -17.1 Hz, ^3J(H, H) = 4.3 Hz), 1.91 (dd, 1H, ^2J(H, H) = -17.1, ^3J(H, H) = 10.7 Hz), 0.89 (d, 3H, ^3J(H, H) = 7.3 Hz, 0.54 (m, 1H); ^{13}C NMR (acetone): δ 137.22, 124.28, 122.26, 121.25, 78.21, 75.29, 35.96, 29.30, 28.72, 20.53, 15.12; ^{19}F NMR (d6-acetone): -138.1 (m), -148.8 (m); ^{11}B NMR (d6-acetone): 7.15 (^1J(B, F) = 60 Hz). IR (cm^{-1}): 3251, 3158, 3116, 2960, 2867, 2238, 2131, 1697; Anal. Calcd. for $C_{11}H_{15}BF_3N_3$ (%): C 51.40, H 5.88, N, 16.35. Found: C 51.21, H 5.75, N 16.32.

*Synthesis of **21d***

The same method was used as synthesis of **21a** except [COOHmim]Cl (1.17 g, 5.71 mmol) was used instead of $[C_4mim]Cl$. Yield: 1.38, 88%. Pale yellow liquid, mp –58.6°C; ESI-MS (H_2O, *m/z*):

positive ion, 169, $[COOHmim]^+$; negative ion, 136, $[CH_3(BF_3)CHCH_2CN]^-$; ^{1}H NMR (d6-acetone): δ 10.33 (br, 1H), 9.01 (s, 1H), 7.75 (s, 1H), 7.72 (s, 1H), 4.35 (t, 2H, ^1J(H, H) = 7.05 Hz), 4.00 (s, 3H), 2.48 (p, 2H, ^1J(H,H) = 7.05), 2.39 (dd, 1H, ^2J(H, H) = -17.1 Hz, ^3J(H, H) = 4.3 Hz), 1.96 (dd, 1H, ^2J(H, H) = -17.1, ^3J(H, H) = 10.7 Hz), 1.20 (m, 2H), 0.89 (d, 3H, ^3J(H, H) = 7.3 Hz), 0.55 (m, 1H); ^{13}C NMR (d6-acetone): δ = 173.74, 136.01, 124.64, 121.17, 48.46, 35.19, 30.89, 28.99, 20.52, 15.16; ^{19}F NMR (d6-acetone): -138.1 (m), -148.8 (m); ^{11}B NMR (d6-acetone): 7.10 (^1J(B, F) = 60 Hz). IR (cm^{-1}): 3158, 3115, 2944, 2867, 2238, 1728; Anal. Calcd. for $C_{12}H_{19}BF_3N_3O_2$ (%): C 47.24, H 6.28, N, 13.77; Found: C 471.21, H 6.75, N 13.32.

*Synthesis of **21e***

The same method was used as synthesis of **21a** except **3a** (1.06 g, 5.71 mmol) was used instead of $[C_4mim]Cl$. Yield: 1.39, 85%. Pale yellow liquid, mp –76.6°C; ESI-MS (H_2O, *m/z*): positive ion, 150 $[CH_2CH_2CH_2CNmim]^+$; negative ion, 136, $[CH_3(BF_3)CHCH_2CN]^-$; ^{1}H NMR (d6-acetone): δ = 8.75 (s, 1H), 7.44 (s, 1H), 7.39 (s, 1H), 4.25 (t, 2H, ^1J(H, H) = 7.15 Hz), 3.82 (s, 3H), 2.50 (t, 2H, ^1J(H, H) = 7.15 Hz), 2.21 (t, 2H, ^1J(H, H) = 7.14 Hz), 2.30 (dd, 1H, ^2J(H, H) = -17.1 Hz, ^3J(H, H) = 4.3 Hz), 1.98 (dd, 1H, ^2J(H, H) = -17.1, ^3J(H, H) = 10.7 Hz), 1.20 (m, 2H), 0.87 (d, 3H, ^3J(H, H) = 7.3 Hz), 0.55 (m, 1H); ^{13}C NMR (d6-acetone): δ 134.11, 130.49, 120.01, 121.52, 116.19, 48.01, 30.87, 28.99, 25.96, 20.58, 13.63, 9.87; ^{19}F NMR (d6-acetone): -138.1 (m), -148.8 (m); ^{11}B NMR (d6-acetone): 7.40 (^1J(B, F) = 60.1 Hz). IR (cm^{-1}): 3375, 3241, 3065, 3029, 2974, 2949, 2927, 2239, 1692; Anal. Calcd. for $C_{12}H_{18}BF_3N_4$ (%): C 50.38, H 6.34, N, 19.58; Found: C 50.21, H 6.45, N 19.32.

*Synthesis of **21f***

The same method was used as synthesis of **21a** except **16a** (1.31 g, 5.71 mmol) was used instead of $[C_4mim]Cl$. Yield: 1.43, 88%. Pale yellow liquid, mp –87.3°C; ESI-MS (H_2O, *m/z*): positive ion, 149 $[DiCH_2CH{=}CH_2im]^+$; negative ion, 136, $[CH_3(BF_3)CHCH_2CN]^-$; ^{1}H NMR (d6-acetone): δ 9.25 (s, 2H). 7.86 (s, 4H), 6.12 (m, 2H), 5.40 (m, 2H), 4.99 (m, 2H), 3.25 (s, 4H) 2.31 (dd, 1H, ^2J(H, H) = -17.1 Hz, ^3J(H, H) = 4.3 Hz), 1.95 (dd, 1H, ^2J(H, H) = -17.1, ^3J(H, H) = 10.7 Hz), 1.20 (m, 2H), 0.88 (d, 3H, ^3J(H, H) = 7.3 Hz), 0.56 (m, 1H); ^{13}C NMR (d6-acetone): δ 136.05, 131.7, 122.07, 121.7, 120.8, 51.45, 29.46, 20.65, 15.32; ^{19}F NMR (d6-acetone): -138.2 (m), -149.8 (m); ^{11}B NMR (d6-acetone): 7.20 (^1J(B, F) = 60.5 Hz). IR (cm^{-1}): 3143, 3087, 2943, 2866, 2238, 1646; Anal. Calcd. for $C_{13}H_{19}BF_3N_3$(%): C 54.76, H 6.72, N, 14.74. Found: C 54.21, H 6.85, N 14.41.

*Synthesis of **21g***

The same method was used as synthesis of **21a** except $[(proyne)_2mim]Cl$ (1.03 g, 5.71 mmol) was used instead of $[C_4mim]Cl$. Yield: 1.38g, 86%. Pale yellow liquid, mp –55.1°C; ESI-MS (H_2O,

m/z): positive ion, 145 $[2alkyneim]^+$; negative ion, 136, $[CH_3(BF_3)CHCH_2CN]^-$; ^1H NMR (D_2O): δ = 9.02 (s, 1H), 7.55 (s, 2H), 4.91 (d, 4H, ^1J(H, H) = 2.44 Hz), 2.98 (t, 2H, ^1J(H, H) = 2.44 Hz) 2.35 (dd, 1H, ^2J(H, H) = -17.1 Hz, ^3J(H, H) = 4.3 Hz), 1.94 (dd, 1H, ^2J(H, H) = -17.1, ^3J(H, H) = 10.7 Hz), 1.20 (m, 2H), 0.89 (d, 3H, ^3J(H, H) = 7.3 Hz), 0.56 (m, 1H); ^{13}C NMR (D_2O): δ 138.91, 125.77, 121.71, 81.16, 74.82, 42.55, 29.29, 20.57, 15.42; ^{19}F NMR (d6-acetone): -138.2 (m), -149.8 (m); ^{11}B NMR (d6-acetone): 7.20 (^1J(B, F) = 59.9Hz); IR (cm^{-1}): 3394, 3208, 3086, 3010, 2239, 2125; Anal. Calcd. for $C_{13}H_{15}BF_3N_3$(%): C 55.55, H 5.38, N, 14.95; Found: C 55.21, H 5.45, N 14.69.

*Synthesis of **21h***

The same method was used as synthesis of **21a** except $[(COOH)_2im]Cl$ (1.58 g, 5.71 mmol) was used instead of $[C_4mim]Cl$. Yield: 1.83, 85%. Pale yellow liquid, mp –38°C; ESI-MS (H_2O, *m/z*): positive ion, 241, $[(COOH)_2im]^+$; negative ion, 136, $[CH_3(BF_3)CHCH_2CN]^-$; ^1H NMR (acetone): δ 8.76 (s, 1H), 7.44 (s, 2H), 4.18 (t, 4H, ^1J(H, H) = 7.05 Hz), 2.37 (dd, 1H, ^2J(H, H) = -17.1 Hz, ^3J(H, H) = 4.3 Hz), 2.37 (t, 4H, ^1J(H, H) = 7.05 Hz), 2.08 (m, 4H) 1.97 (dd, 1H, ^2J(H, H) = -17.1, ^3J(H, H) = 10.7 Hz), 1.21 (m, 2H), 0.89 (d, 3H, ^3J(H, H) = 7.3 Hz), 0.59 (m, 1H); ^{13}C NMR (d6-acetone): δ 179.73, 138.52, 125.51, 121.8, 51.60, 33.17, 28.44, 27.58, 20.30, 14.98; ^{19}F NMR (d6-acetone): -138.1 (m), -149.8 (m); ^{11}B NMR (d6-acetone): 7.20 (^1J(B, F) = 60.5 Hz); IR (cm^{-1}): 3422, 3104, 2921, 2582, 2512, 2246, 1710, 1558, 1461, 1433, 1406; Anal. Calcd. for $C_{13}H_{23}BF_3N_3O_4$(%): C 47.77, H 6.15, N, 11.14. Found: C 47.35, H 6.25, N 11.38.

*Synthesis of **21i***

The same method was used as synthesis of **21a** except **7a** (1.39 g, 5.71 mmol) was used instead of $[C_4mim]Cl$. Yield: 1.68, 87%. Pale yellow liquid, mp –69.8°C; ESI-MS (H_2O, *m/z*): positive ion, 203 $[Di(CH_2)_3C{\equiv}Nim]^+$; negative ion, 136, $[CH_3(BF_3)CHCH_2CN]^-$; ^1H NMR (acetone): δ 8.58 (s, 1H), 7.55 (s, 2H), 4.47 (t, 4H, ^1J(H, H) = 7.15 Hz), 2.66 (m, 4H), 2.37 (t, 4H, ^1J(H, H) = 7.15 Hz), 2.34 (dd, 1H, ^2J(H, H) = -17.1 Hz, ^3J(H, H) = 4.3 Hz), 1.99 (dd, 1H, ^2J(H, H) = -17.1, ^3J(H, H) = 10.7 Hz), 0.92 (d, 3H, ^3J(H, H) = 7.3 Hz, 0.58 (m, 1H); ^{13}C NMR (d6-acetone): 137.08, 123.44, 121.9, 119.25, 48.37, 29.33, 29.1, 25.17, 20.68, 13.68; ^{19}F NMR (d6-acetone): -138.1 (m), -148.8 (m); ^{11}B NMR (d6-acetone): 7.20 (^1J(B, F) = 60.1 Hz); IR (cm^{-1}): 3149, 3117, 2967, 2247, 1567; Anal. Calcd. for $C_{15}H_{21}BF_3N_5$(%): C 53.12, H 6.24, N, 20.65. Found: C 52.97, H 6.25, N 20.34.

6.5 References

[1] D. J. Brauer, K. Kottsieper, C. Liek, O. Stelzer, H. Waffenschmidt and P. Wasserscheid, *J. Organomet. Chem.*, **2001**, *630*, 177.

[2] J. S. Wilkes, J. A. Levisky, R. A. Wilson, C. L. Hussey, *Inorg. Chem.* **1982**, *21*, 1263.

[3] (a) R. J. C. Brown, P. J. Dyson, D. J. Ellis, T. Welton, *Chem. Commun*. **2001**, 1862; (b) P. J. Dyson, J. S. McIndoe, D. Zhao, *Chem. Commun*. **2003**, 508.

[4] (a) Z.-B. Zhou, H. Matsumoto, K. Tatsumi, *Chem. Eur. J.* **2004**, *10*, 6581; (b) Z.-B. Zhou, H. Matsumoto, K. Tatsumi, *Chem. Eur. J.* **2005**, *11*, 752.

[5] H. S. Kim, Y. J. Kim, H. Lee, K. Y. Park, C. Lee, C. S. Chin, *Angew. Chem. Int. Ed.* **2002**, *41*, 4300

[6] (a) M. Yoshizawa, W. Ogihara, H. Ohno, Polym. *Adv. Technol.* **2002**, *13*, 589; (b) H. Ohno, M. Yoshizawa, W. Ogihara, *Electrochim. Acta* **2004**, *50*, 752.

[7] D. Männig and H. Nöth, *Angew. Chem., Int. Ed.,* **1985**, *24*, 878.

[8] G. A. Molander, C-S. Yun, M. Ribagorda and B. Biolato, *J. Org. Chem.* **2003**, *68*, 5534.

[9] Z-B Zhou, M. Takeda and M. Ue, *J. Flourine. Chem.* **2004**, *125*, 471

[10] K. J. Harlow, A. F. Hill and T. Welton, *Synthesis* **1996**, *6*, 697.

[11] A. B. McEwen, H. L. Ngo, K. LeCompte, J. L. Goldman, *J. Electrochem. Soc.* **1999**, *146*, 1265

[12] Larsen, A. S.; Holbrey, J. D.; Tham, F. S.; Reed, C. A. *J. Am. Chem. Soc.* **2000**, *122*, 7264.

[13] P. J. Dyson, M. C. Grossel, N. Srinivasan, T. Vine, T. Welton, D. J. David Jr., A. J. P. White, T. Zigras, *J. Chem. Soc., Dalton Trans*. **1997**, 3465.

[14] H. Schottenberger, K. Wurst, U. E. I. Horvath, S. Cronje, J. Lukasser, J. Polin, J. M. McKenzie, H. G. Raubenheimer, *Dalton Trans.* **2003**, 4275.

[15] Z. Fei, D. Zhao, R. Scopelliti, T. J. Geldbach and P. J. Dyson, *Chem. Eur. J.* **2004**, *10*, 4886.

[16] D. Zhao, Z. Fei, R. Scopelliti and P. J. Dyson, *Inorg. Chem.* **2004**, *43*, 2197.

[17] Z. Fei, D. Zhao, R. Scopelliti and P. J. Dyson, *Organometallics* **2004**, *23*, 1622.

7

Development of an IL Polymer as Metal Nanoparticle Stabilizer

7.1 Introduction

Metal nanoparticles (NPs) continue to attract interest across diverse areas of science due to their unique physicochemical properties attributable to the quantum size effect and single electron transitions.[1] As a result of the kinetically unstable nature of NPs stabilizers are used to prevent aggregation. With different stabilizers, various techniques have been developed, allowing the synthesis of NPs with specific sizes and shapes.[2] Commonly used stabilizers include thiols, ammonium salts, polymers, etc.

NPs were first identified in ILs as species formed during Heck reactions using Pd(II) compounds as catalyst precursors.[8] Dupont *et al*. reported the deliberate preparation of transition metal NPs in ILs, without stabilizers, generated by reduction using molecular hydrogen, and demonstrated their application in hydrogenation and C-C coupling reactions.[9] It was suggested that both electrostatic and coordination effects of imidazolium cation contribute to NP stabilization by ILs.[10] However, aggregation of NPs in ILs still occurs if ILs are used without additional stabilizers. Thus PVP (poly(*N*-vinyl-2-pyrrolidone) has been used for NP synthesis in ILs,[11] in addition, thiol-functionalized ILs[12] and IL-like copolymers[13] have been developed to stabilize IL soluble NPs.

In this chapter, an alternative strategy for NP stabilization, using an IL monopolymer composed entirely of imidazolium units incorporating a hydrophobic benzyl group will be described. Several benefits may be envisioned with this design: first, a high molecular weight IL polymer should endow a steric stabilization effect in addition to an electrostatic effect;[14] second, cationic polymer units may interact with commonly used anionic metal precursors before reduction, hence a smaller particle size could be expected;[15] third, the amphiphilic nature of the polymer units should also help NP stabilization by micelle formation;[16] fourth, anion exchange or functionalization of the IL units could provide a pathway for NP surface modification.

7.2 Results and Discussion

Scheme 7.1 illustrates the synthesis of the IL polymer. Following the preparation of the IL halide precursor **22** via a standard method, polymerization is carried out in aqueous solution with the free radical initiator AIBN, thereafter acetone is added to precipitate the polymer, **2**, as a white amorphous solid. Polymer **23** is very hydroscopic, but slowly re-dissolves in water.

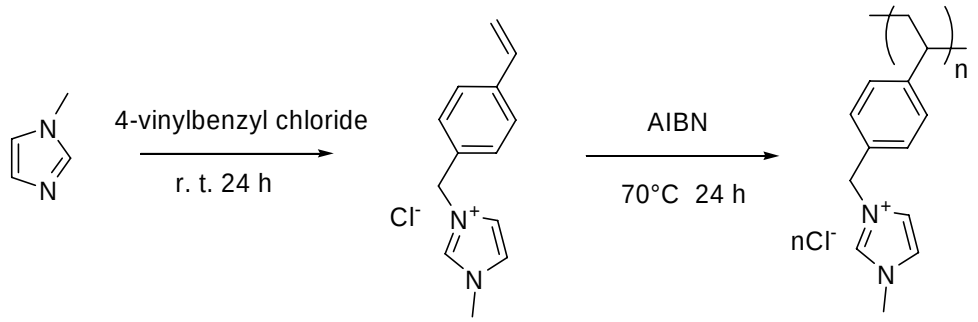

22 **23**

Scheme 7.1 Synthesis of ILPCl poly(1-methyl-3-vinylbenzyl-imidazolium chloride).

Since gold NPs have considerable potential in many applications, it was set out to investigate their stabilization by polymer **23**. $HAuCl_4$ was used as the precursor dissolved in water; to a solution of the metal precursor, a 2 ml aqueous solution of **23** (0.25 wt%) was added. Yellow precipitates were observed, indicative of a flocculation effect of **23** on the gold anion. The mixture was then vigorously agitated and an aqueous solution of $NaBH_4$ was added dropwise. The color of the solution rapidly changes from yellow to reddish-purple indicative of the formation of gold NPs. The UV-vis spectrum of the solution shows a peak at λ 518 nm, which originates from surface plasmon band of the gold NPs. TEM analysis indicates that the size range of the gold NPs is 8 ─ 12 nm (Figure 7.1). The NPs were precipitated by centrifugation at 6000 rmp. The IR spectrum of the separated NPs shows C-H absorptions between 3000 ─ 3350 cm^{-1} attributable to the imidazolium and benzyl moieties, as well as a peak at 1638 cm^{-1} for the C=C bond of the imidazolium ring, indicating that **23** binds to NPs. However, when re-dispersed in water, the color of the solution is blue and the UV-vis spectrum exhibits a red shift of λ to 528 nm, attribute to the aggregation of the NPs, which is induced by partial detachment of **23** from NPs during the centrifugation. With the aim of confirming the crystal phase and verifying the mean size of the gold NPs after centrifuge separation, X-ray diffraction (XRD) analysis was carried out. Figure 7.2 shows the nanoparticles featuring 2θ peaks at 38.2°, 44.5°, 64.6° and 77.6°, which correspond to the (111), (200), (220) and (311) planes of the standard face-centered cubic phase of

gold. The corresponding lattice constant is α = 4.077 nm that is within the error of the reported data (JCPDS File No. 7-0784; α = 0.4078 nm). The peak width of (111) Bragg reflection was chosen for nanoparticle mean size estimation by Debye-Scherrer formula[2e] which resulted in mean NP size of 31 ± 5 nm. The TEM image of the NPs post-centrifugation also confirms aggregation (about 30 nm, in accordance with XRD calculation result, see Figure 7.1)

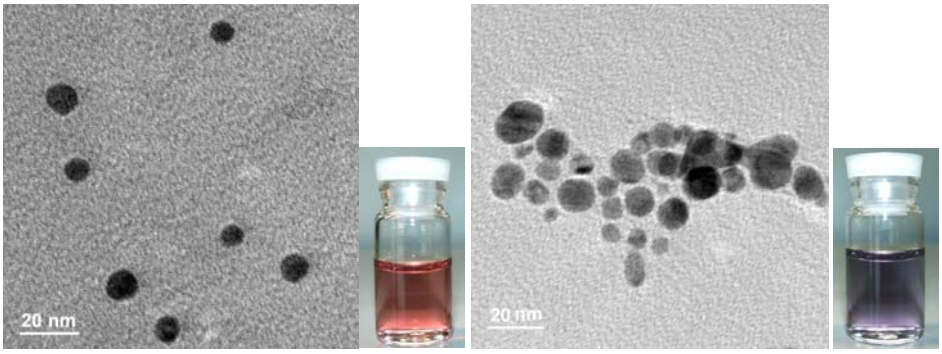

Figure 7.1 Color comparison and TEM images of ILPCl 23 stabilized gold NPs before (left, diluted 10 times) and after centrifugation (right, re-dispersed in water).

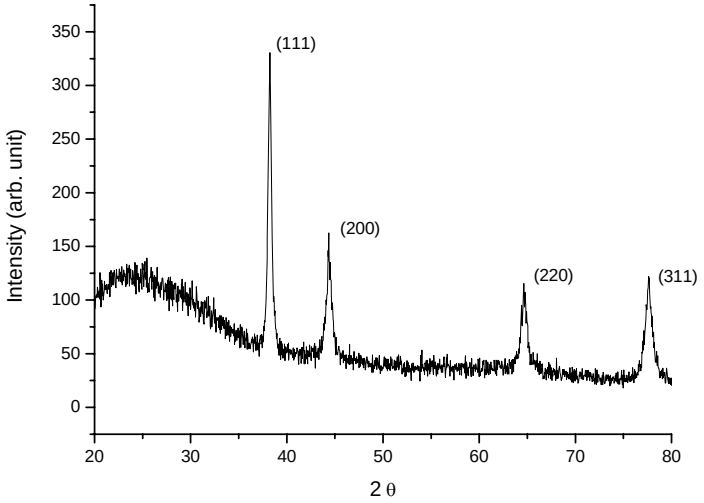

Figure 7.2 X-ray Diffraction patterns of gold NPs separated by centrifugation

Transferring nanoparticles from an aqueous phase to an organic phase is an important step in NP preparation, in general, requiring capping agents like thiols, amines or surfactants. In a recent report, it was shown that gold NPs can be transferred from aqueous solution to a hydrophobic IL [C_4mim][PF_6] (C_4mim = 1-butyl-3-methylimidazolium), although surfactant is required to prevent aggregation.[17]

In this study, a facile way to transfer the gold NPs to ILs without the need for surfactant was demonstrated. Mixing an aqueous solution of the gold NPs with [C_4mim][PF_6] followed by vigorous shaking results in the transfer of gold NPs from water to the IL. However, as described in the literature, NP precipitation due to aggregation is observed (Figure 7.3A),[17] which requires addition of a cationic surfactant to prevent NPs aggregation. Our new strategy is to modify the water miscibility of gold NPs by anion exchange of **23** from Cl^- to that of the IL, viz. PF_6^-. Following the same procedure, except using 0.1 ml HPF_6 (60 wt% aqueous solution), the gold NPs can be precipitated and on addition of [C_4mim][PF_6], they transfer completely into the IL (Figure 7.3B). The TEM analysis of the gold NPs in the IL confirms that the size of NPs is preserved after transfer into the IL (Figure 7.3, bottom left). In addition, the upper water phase was analyzed by UV-vis spectroscopy indicating that no gold NPs were present after transfer. [C_4mim][Tf_2N] (Tf_2N = bis(trifuoromethylsulfonyl)imide) is another important hydrophobic IL with relatively low viscosity.[18] When [C_4mim][Tf_2N] is mixed with an aqeous solution of the gold NPs, even after energetic shaking, the NPs cannot be completely transferred to the IL phase (Figure 7.3C). However, addition of Li[Tf_2N] into the gold NPs solution, followed by addition of [C_4mim][Tf_2N] with vigorous shaking, allows the efficient transfer of the gold NPs into [C_4mim][Tf_2N] (Figure 7.3D) also without aggregation.

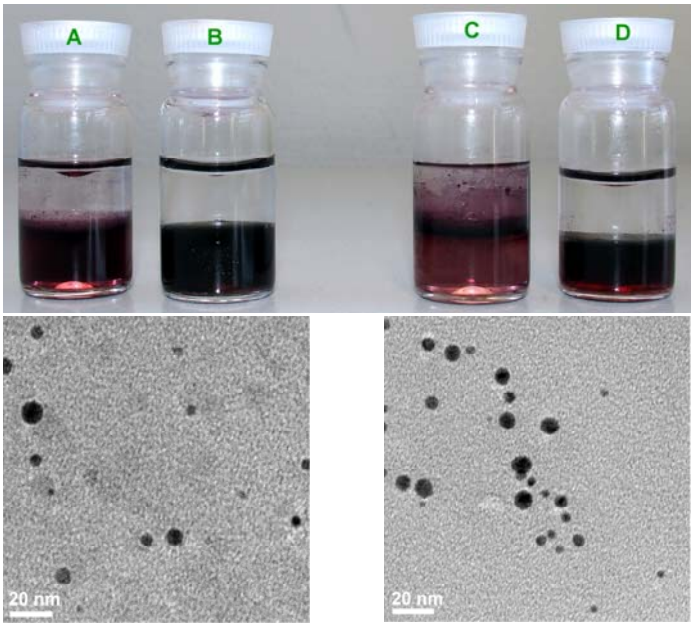

Figure 7.3 Gold NP transfer from water to ILs: *(A) water/[C_4mim][PF_6]; (B) water/[C_4mim][PF_6] with addition of HPF_6; (C) water/[C_4mim][Tf_2N]; (D) water/[C_4mim][Tf_2N] with addition of Li[Tf_2N]. TEM images: Gold NPs after transfer to [C_4mim][PF_6] following anion exchange with HPF_6 (left); Gold NPs after transfer to [C_4mim] [Tf_2N] following anion exchange with Li[Tf_2N] (right).*

A reference experiment has been carried out involving preparation of Au NPs without any stabilizer in order to rationalize the mechanism of the trasfer. Using the same procedure as described for ILP protected Au NPs, except without addition of the ILP, Au NPs can be obtained (Figure 7.4-1).

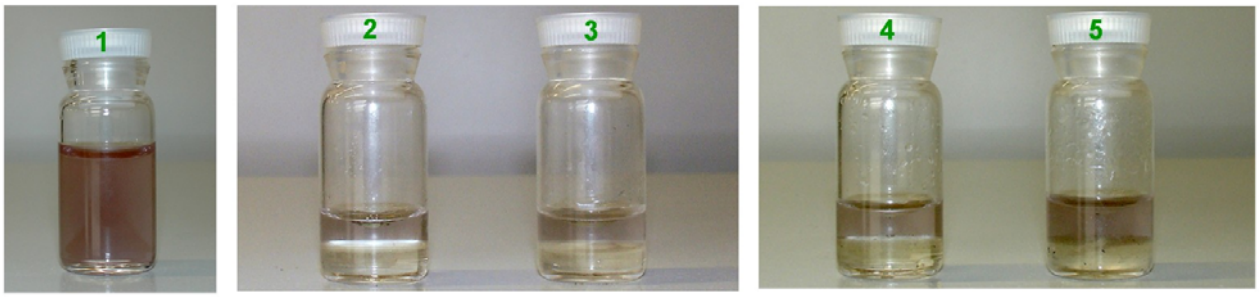

Figure 7.4 Photograph of 1: *Au NPs prepared by reducing $HAuCl_4$ using $NaBH_4$ without ILP* ***2. 2:*** *Attempt to transfer Au NPs into $[C_4mim][PF_6]$ directly.* ***3:*** *Attempt to transfer Au NPs into $[C_4mim][Tf_2N]$ directly.* ***4:*** *Attempt to transfer Au NPs into $[C_4mim][PF_6]$ with addition of $Na[PF_6]$.* ***5*** *Attempt to transfer Au NPs into $[C_4mim][Tf_2N]$ with addition of $Li[Tf_2N]$.*

However, the NP transfer from water to hydrophobic ILs proves impossible for the Au NPs without ILP as stabilizer (Figure 7.4-2,3), even with addition of $NaPF_6$ or $Li[Tf_2N]$ (Figure 7.4-4,5).

Another reference experiment was conducted by exchange the salts used to assist the NP transfer. KPF_6 was used for NP transfer to $[C_4mim][Tf_2N]$ while $Li[Tf_2N]$ used for transfer to $[C_4mim][PF_6]$ (see Figure 7.5). It can be seen that the transfer is not as efficient as using the counter anion salt containing the same anion as the IL.

Figure 7.5 Au NP transfer to hydrophobic ILs with addition of "false" counter anion salts (Left: $[C_4mim][PF_6]$; Right: $[C_4mim][Tf_2N]$)

The solubility of the polymer was also tested understand the NP transfer mechanism. The polymer **23** was dissolved in water and then an excess of HPF_6 or $Li[Tf_2N]$ was added; a white precipitate came out from the solution immediately (reaction shown in scheme 7.2). The precipitate was washed with water then centrifuged and dried in vacuum to give the polymers containing $[PF_6]^-$ (**24**) or $[Tf_2N]^-$ (**25**)in place of Cl^-. The solubility of these three polymers in ILs was tested.

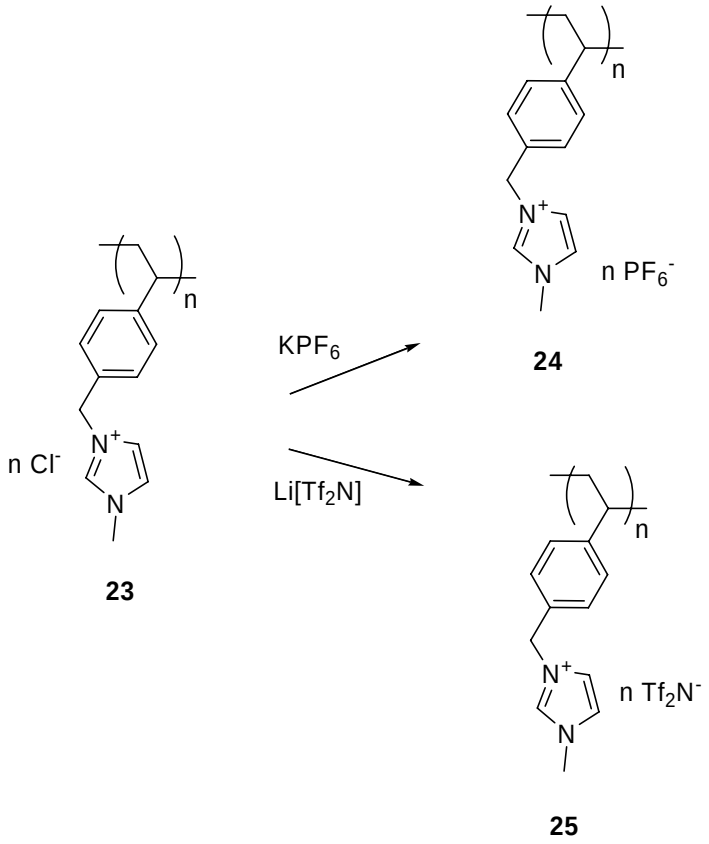

Scheme 7.2 Synthesis of ILPPF$_6$ 24 and ILPTf$_2$N 25

Polymer **23** only shows limited solubility in ILs, $[C_4mim][Tf_2N]$ and $[C_4mim][PF_6]$ ever after stirring at 80°C for 24 hours (Figure 7.6).

Figure 7.6 Polymer 23 solubility test (*Left: polymer powder; Middle: polymer in [C_4mim][PF_6] ; Right: polymer in [C_4mim][Tf_2N])*

On the contrary, polymer **24** and **25** are easily dissolved in ILs composed of the same anions using the same procedure described above (Figure 7.7).

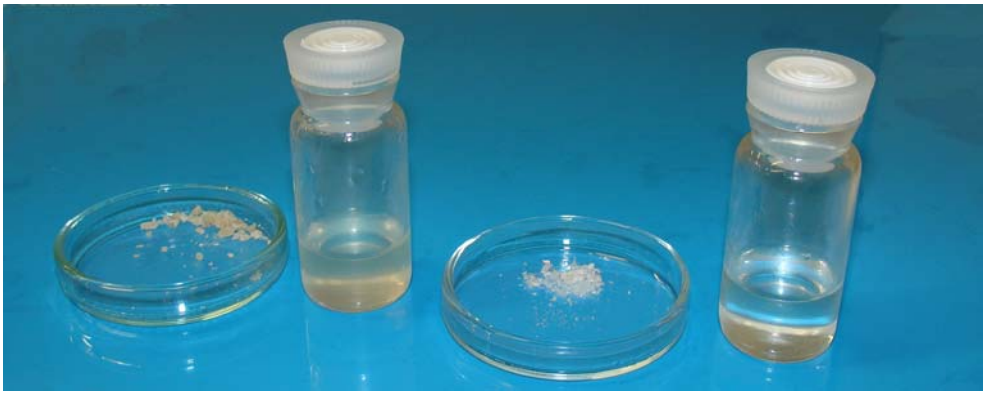

Figure 7.7 Polymer 24 and 25 solubility test (*Left: polymer powder 24 and in [C_4mim][PF_6] ; Right: Polymer powder 25 in [C_4mim][Tf_2N])*

From these experiments it is possible to conclude that, the NP transfer mechanism involves anion exchange of the polymer attached to NPs, which alters the NP affinity to hydrophobic ILs, the NP consequently can be transferred to the corresponding IL phase (Figure 7.8).

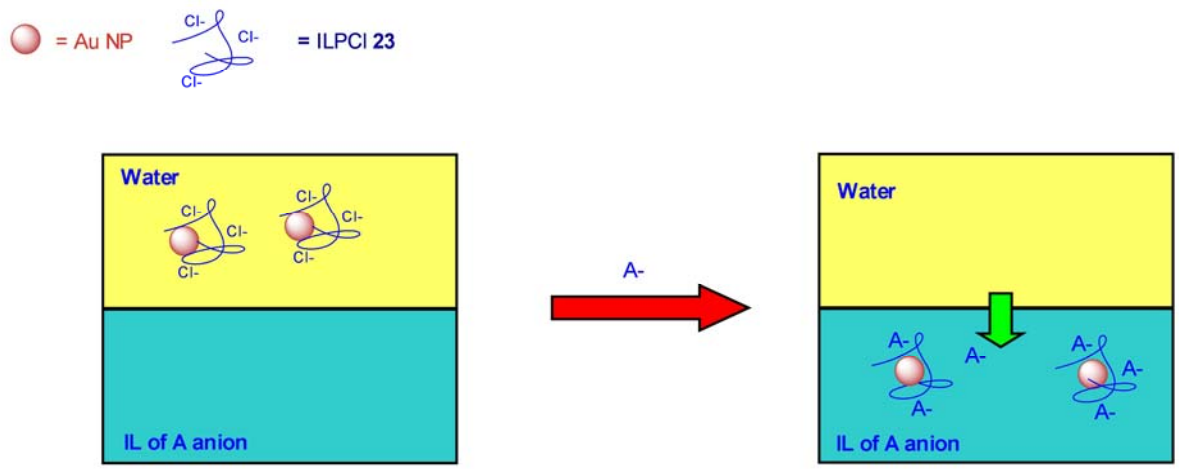

Figure 7.8 Proposed NP transfer mechanism

Platinum and palladium nanoparticles are finding increasing uses in catalysis because they have high catalytic activities and can be well dispersed in different media.[19] It was found that ILPCl **23** can also be used as a stabilizer for platinum and palladium NPs. Their preparation is essentially the same as that used for the gold NPs. Aqueous solution of K_2PtCl_6 or K_2PdCl_6 are mixed with **23** followed by addition of $NaBH_4$. The color of the solution changes immediately from yellow to dark brown, which indicates NP formation. TEM analysis of the Pt and Pd NPs indicates the size range of the Pt and Pd NPs is 1.5 ─ 4 nm for platinum and 1.5 ─ 3.5 nm for palladium (see Figure 7.9). The Pt and Pd NPs can be centrifuged and analyzed by XRD. The XRD patterns are identified as Pt(0) or Pd(0) crystalline of face-centered cubic lattice. (Figure 7.10; JCPDS File No. 88-2343 for Pt, No. 88-2335 for Pd). The sizes of the post-centrifuge NPs were calculated using Debye-Scherrer formula. The mean size of Pt NPs was found to be 10 ± 5 nm, and 18 ± 5 nm for the Pd NPs, indicating NP aggregation happens during the process of centrifugation.

The transfer of Pt or Pd NPs from water to hydrophobic ILs via prior anion exchange is as effective as that described for the gold NPs (Figure 7.11, for TEM images, see experimental section).

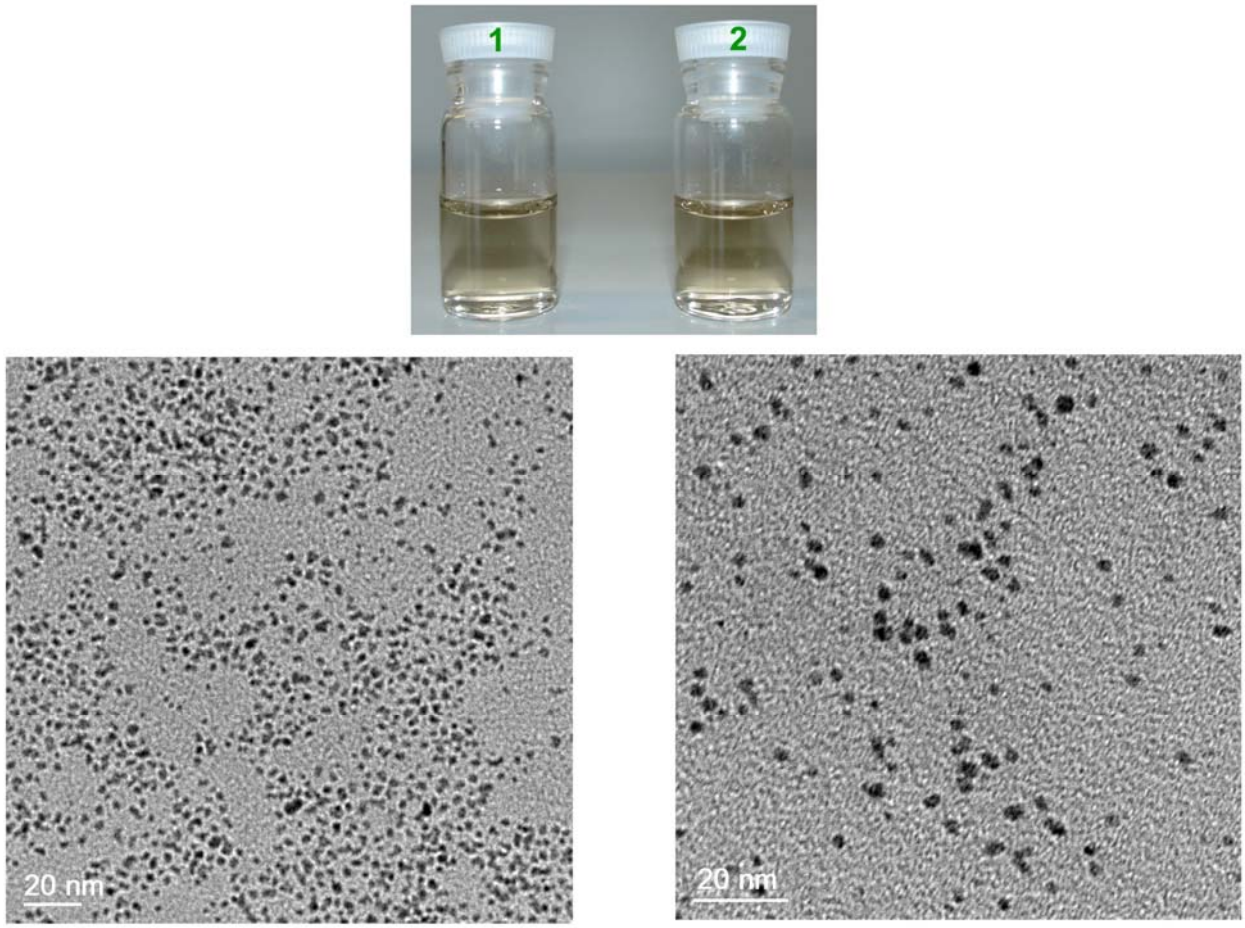

Figure 7.9 Pt and Pd nanoparticles stabilized by polymer 23 (1: Pt NPs; 2: Pd NPs)

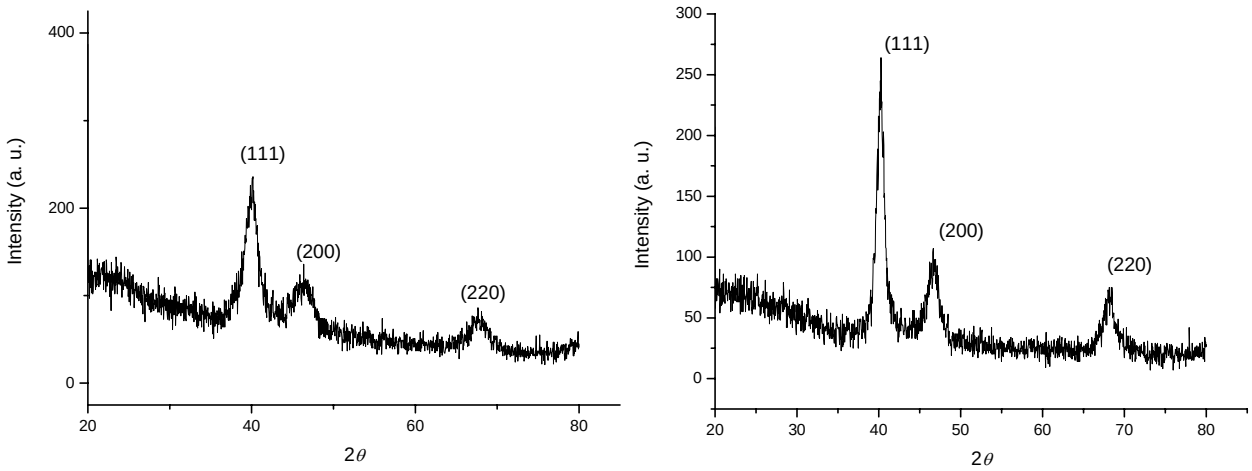

Figure 7.10 X-ray Diffraction patterns for (a) platinum NPs separated by centrifugation; (b) palladium NPs separated by centrifugation.

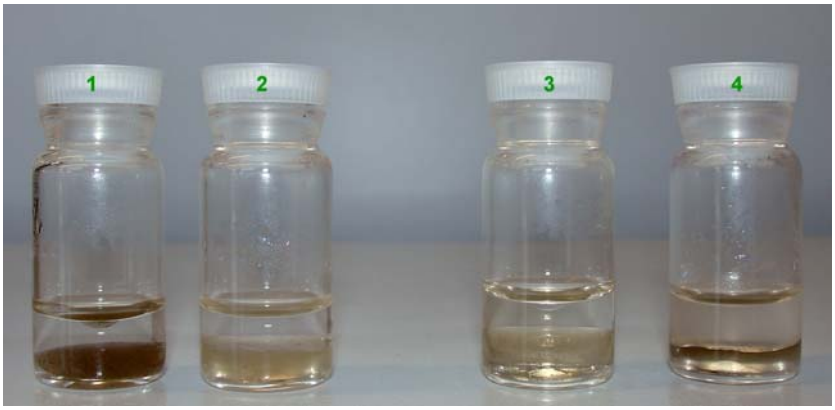

Figure 7.11 Photograph of Pt and Pd NP transfer to ILs (*1: Pt NPs transfer to C_4mim][PF_6]; 2: Pd NP transfer to [C_4mim][PF_6]; 3: Pt NP transfer to [C_4mim][Tf_2N]; 4: Pd NP transfer to [C_4mim][Tf_2N]**)*

7.3 Concluding Remarks

To conclude, it has been shown that the ILPCl **23** can be employed as an effective stabilizer for gold, platinum and palladium nanoparticles involving a simple preparation procedure. The synergism of steric, electrostatic and micelle effects of the ILPCl is believed to facilitate stabilization of the NPs. The NPs can be easily transferred to hydrophobic ILs without degradation or aggregation. Our approach opens up a novel methodology for the synthesis and stabilization of NPs, their facile transfer from water into ILs by anion exchange, and many potential applications can be envisaged.

7.4 Experimental

Fullerene, 4-vinylbenzyl chloride, 1-methylimidazole, 2,2'-azobisisobutyronitrile (AIBN) and 2,6-di-tert-butyl-4-methylphenol (DBMP) were purchased from Aldrich Chemical Co. 2,5-Dihydroxylbenzoic acid (DHB) was purchased from Fluka. Synthesis of imidazolium salts and the IL polymer was performed under an inert atmosphere of dry nitrogen using standard Schlenk techniques. Solvents were dried using the appropriate reagents and distilled prior to use. NMR spectra were obtained at 20°C with a Bruker DMX 400 instrument using $SiMe_4$ for ^1H, ^{13}C as external standards. IR spectra were recorded on a Perkin-Elmer FT-IR 2000 system. The UV-vis spectroscopic measurements were performed using a Cary 2200 spectrometer at temperature of 25°C±0.2°C. λmax was measured by taking the middle point of the peak. MALDI-MS spectra was recorded in reflectron mode (positive) on a Axima CFR Plus (Kratos/Shimadzu) MALDI-TOF instrument and calibrated using fullerene (C_{60}) at m/z 720.00. The X-ray diffraction samples were collected by accumulating centrifuged NPs and drying under vacuum. The

XRD measurements were carried out in the diffraction mode on a Siemens Kristalloflex 805 diffractometer operated at a voltage of 40 Kv and a current of 40 mA with Cu Kα radiation.

1-methyl-3-vinylbenzyl-imidazolium chloride ***22***

To a 250 ml flask 1-methylimidazole (8.2 g, 0.10 mol), 4-vinylbenzyl chloride (15.1 0.10 mol) and 2,6-di-tert-butyl-4-methylphenol (DBMP) (50 mg) was dissolved in methanol. The mixture was stirred at r.t. for 48 hours. The solvent was removed under vacuum. A waxy substance was obtained in a yield of 80%. ^{1}H NMR (D_2O, ppm): 8.22 (1H, s), 7.55 (1H, s), 7.53 (1H, s), 7.34 (2H, br), 7.02 (2H, m), 6.86 (1H, m), 5.90 (1H, d), 5.36 (1H, d), 5.23 (2H, s), 3.74 (3H, s); ^{13}C NMR (D_2O, ppm): 138.5, 135.9, 135.7, 128.9, 126.8, 121.8, 117.4, 114.9, 52.5, 35.9; FT-IR (cm^{-1}): $\upsilon_{C\text{-}H\ aromatic}$, 3023, $\upsilon_{C\text{-}H\ aromatic}$, 2851, $\upsilon_{C=C\ aromatic}$,1611.

Poly(1-methyl-3-vinylbenzyl-imidazolium chloride) (ILPCl) ***23***

Monomer **22** (3 g) and initiator AIBN (30 mg) was dissolved in water and the solution was heated at 70°C for 12 h. The polymer was precipitated by addition of methanol. The yield was 70%. H NMR (D_2O): 8.20 (1H, s), 7.55 (1H, br), 7.53 (1H, br), 7.34 (2H, br), 7.02 (2H, br), 6.86 (1H, m), 5.23 (3H, s), 3.43 (3H, br); FT-IR (cm^{-1}): $\upsilon_{C\text{-}H\ aromatic}$, 3023, $\upsilon_{C\text{-}H\ aromatic}$, 2851, $\upsilon_{C=C\ aromatic}$,1611.

Poly(1-methyl-3-vinylbenzyl-imidazolium hexafluorophosphate) (ILPPF6) ***24***

Polymer **23** (300 mg) was dissolved in 120 ml water and 5 g KPF_6. The polymer was precipitated was collected by centrifuge and then dried in vacuum. The yield was 82%. H NMR (Aceton-D6): 8.22 (1H, s), 7.41 (1H, br), 7.34 (1H, br), 7.28 (2H, br), 6.93 (2H, br), 6.48 (1H, m), 5.20 (3H, s), 3.41 (3H, br); FT-IR (cm^{-1}): $\upsilon_{C\text{-}H\ aromatic}$, 3033, $\upsilon_{C\text{-}H\ aromatic}$, 2848, $\upsilon_{C=C\ aromatic}$,1609.

Poly(1-methyl-3-vinylbenzyl-imidazolium bis(trifluoromethanesulfonyl)imide) (ILPTF2N) ***25***

The same procedure was used as Polymer **24** except 8 g Li[Tf_2N]. The yield was 85%. H NMR (Aceton-D6): 8.38 (1H, s), 7.54 (1H, br), 7.52 (1H, br), 7.18 (2H, br), 7.05 (2H, br), 6.88 (1H, m), 5.19 (3H, s), 3.40 (3H, br); FT-IR (cm^{-1}): $\upsilon_{C\text{-}H\ aromatic}$, 3024, $\upsilon_{C\text{-}H\ aromatic}$, 2847, $\upsilon_{C=C\ aromatic}$,1608.

MALDI-TOF Mass Spectrometry

The polymer **23** was predissolved in bidistilled water at 0.25% and 1.0% wt ratio while the matrices were prepared in 1:1 MeCN:H_2O. The analytes were prepared by the dried droplet method. The best result was obtained using 1.0% wt polymer and 10 mM DHB solution in 1:1 ratio, and the spectrum was recorded between m/z 100-400. No other significant peaks were observed.

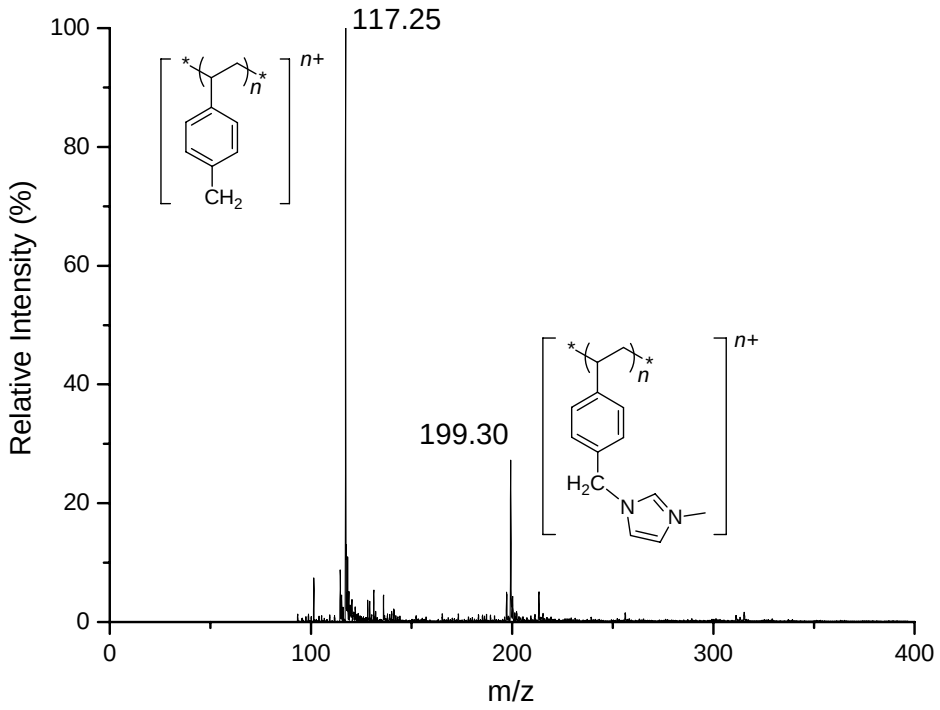

*Gold NPs stabilized by **23***

To a 2 ml solution of the $HAuCl_4$ (6×10^{-4} mol/L), a 2 ml aqueous solution of **23** (0.25 wt%) was added. The mixture is then vigorously agitated and 2 mg $NaBH_4$ dissolved in 1 ml water was added dropwise. The color of $HAuCl_4$ solution rapidly changes from yellow to redish-purple designating the formation of gold NPs.

UV-vis spectra of Au NPs before (1) and after (2) centrifugation

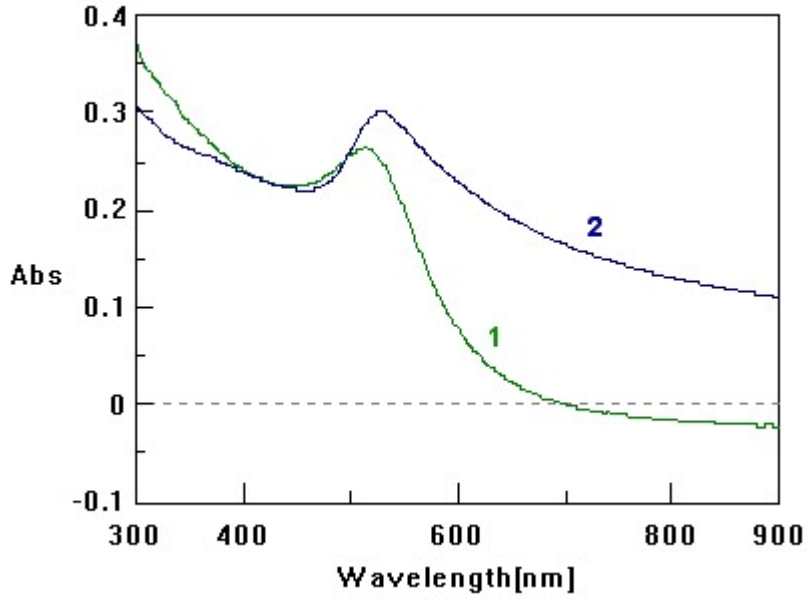

*Platinum NPs stabilized by **23***

To a 2 ml solution of $KPtCl_6$ (6×10^{-4} mol/L), a 2 ml aqueous solution of **23** (0.25 wt%) was added.. The mixture is then vigorously agitated and 2 mg $NaBH_4$ dissolved in 1 ml water was added dropwise. The color of $KPtCl_6$ solution rapidly changes from yellow to dark brown designating the formation of Pt NPs.

*Palladium NPs stabilized by **23***

To a 2 ml solution of $KPdCl_6$ (6×10^{-4} mol/L), a 2 ml aqueous solution of **23** (0.25 wt%) was added.. The mixture is then vigorously agitated and 2 mg $NaBH_4$ dissolved in 1 ml water was added dropwise. The color of $KPdCl_6$ solution rapidly changes from dark yellow to dark brown designating the formation of Pd NPs.

NPs transfer from aqueous solution to ILs

1) Transfer to [C_4mim][PF_6]

To 2 ml NPs aqueous solution, 0.1 ml HPF_6 (60 wt% aqueous solution) was added followed by addition of 2 ml [C_4mim][PF_6]. The mixture was shaked vigorously and then left to let the two phases separate.

2) Transfer to [C_4mim][Tf_2N]

To 2 ml NPs aqueous solution, 100 mg Li[Tf_2N] was added followed by addition of 2 ml [C_4mim][Tf_2N]. The mixture was shaked vigorously and then left to let the two phases separate.

TEM measurement

Specimens for TEM were prepared by depositing a drop of metal NPs aqueous solution on a carbon coated copper grid (400 mesh). The copper grid was then dried at ambient temperature. The TEM was carried out on PHILIPS CM 20 Transmission Electron Microscope. For the sample of NPs in [C_4mim][PF_6] and [C_4mim][Tf_2N], 0.5 ml of the IL containing NPs was diluted by 10 ml dichloromethane and then depositing a drop of such mixture onto copper grid. The EDX data were obtained by Thermo Noran installed with TEM. The nanosize distribution data was obtained by counting over 200 particles.

TEM image of gold NPs before centrifugation; EDX analysis of the gold NPs before centrifugation; Size distribution of the gold NPs before centrifugation

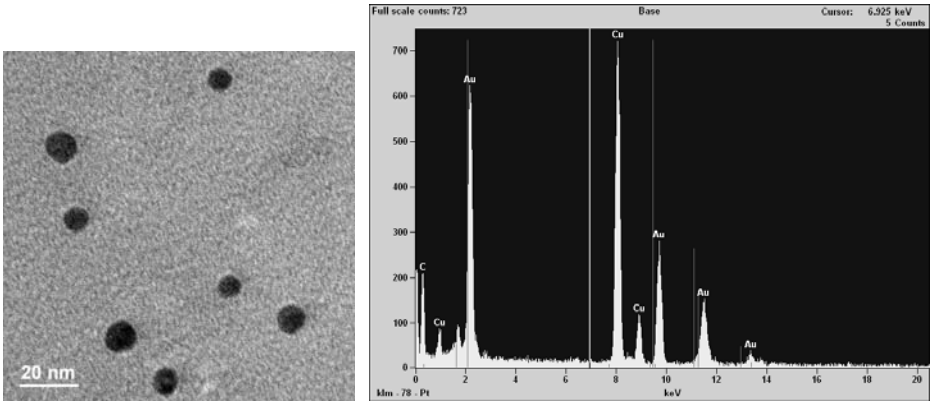

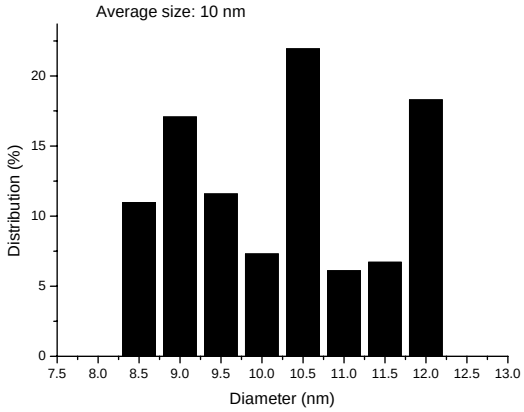

TEM image of gold NPs after centrifugation; EDX analysis of the gold NPs after centrifugation

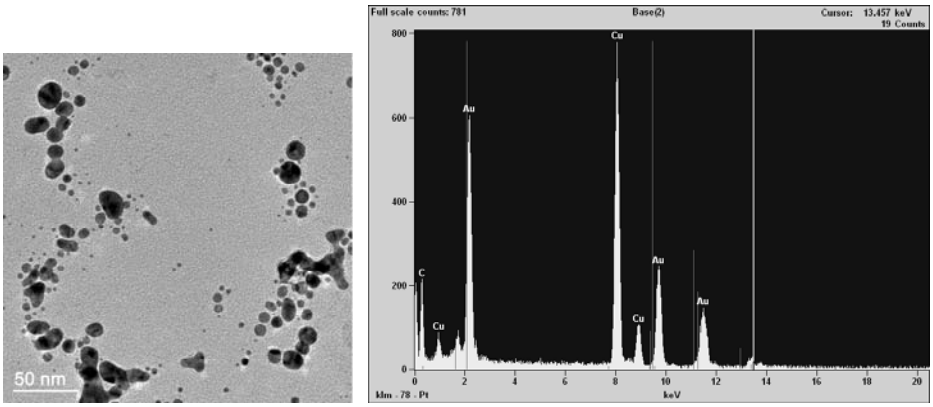

TEM image of platinum NPs; EDX analysis of the platinum NPs; Size distribution of the Pt NPs

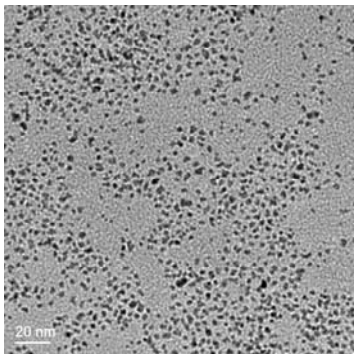

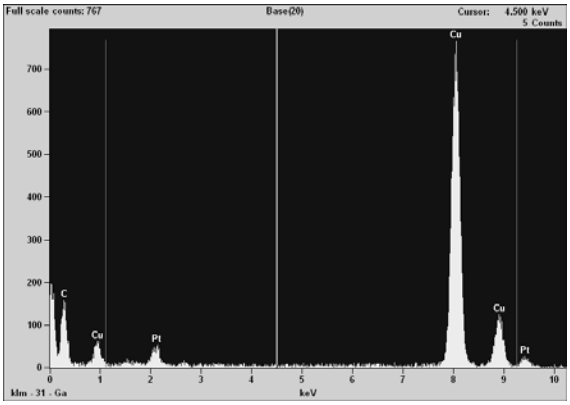

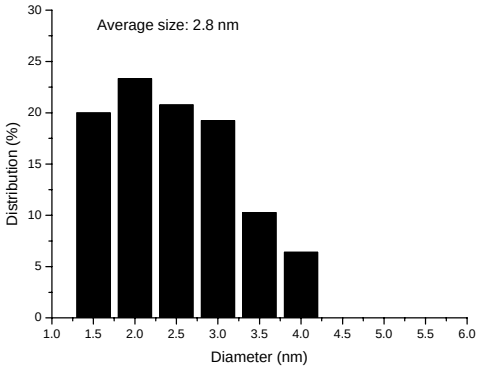

TEM image of palladium NPs; EDX analysis of the palladium NPs; Size distribution of the Pd NPs

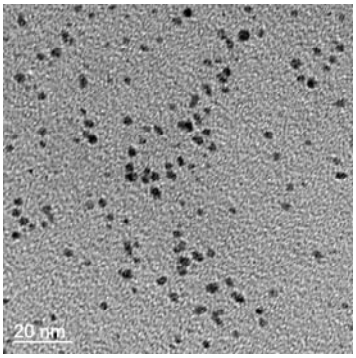

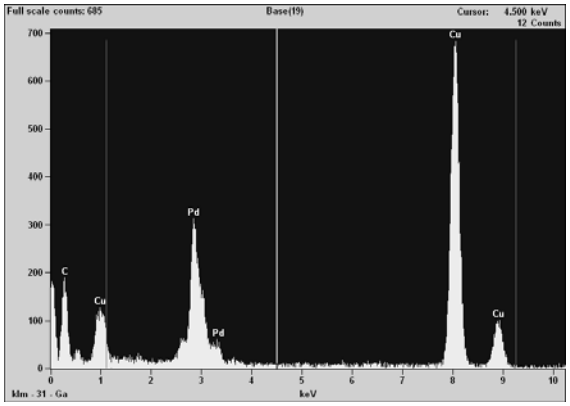

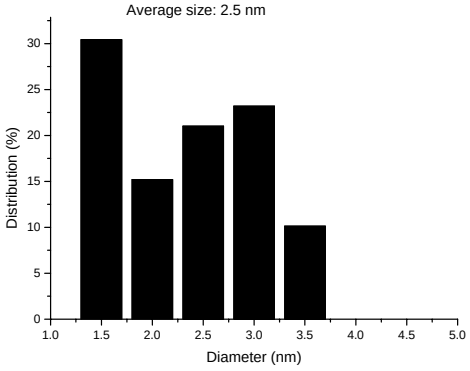

TEM image of gold NPs after transferred to [C_4mim][PF_6]; EDX analysis of the gold NPs after transferred to [C_4mim][PF_6]; Size distribution of the gold NPs after transferred to [C_4mim][PF_6]

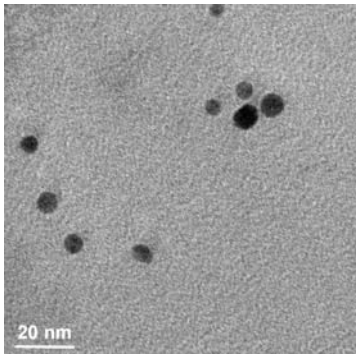

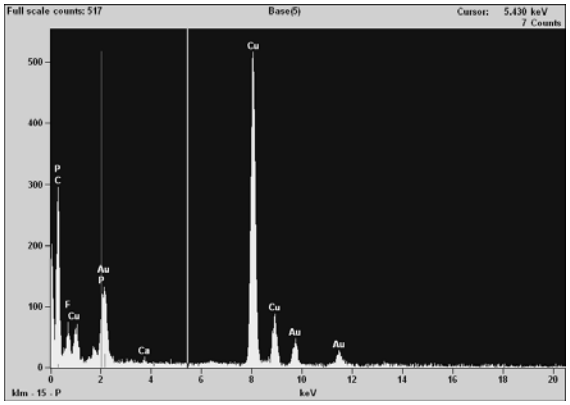

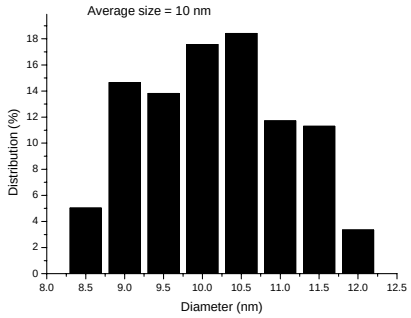

TEM image of gold NPs after transferred to [C_4mim][Tf_2N]; EDX analysis of the gold NPs after transferred to [C_4mim][Tf_2N]; Size distribution of the gold NPs after transferred to [C_4mim][Tf_2N]

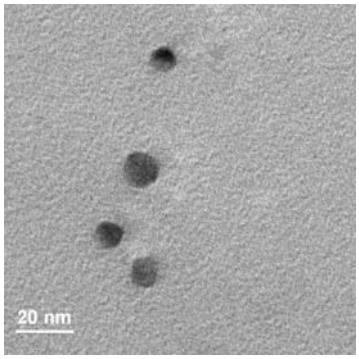

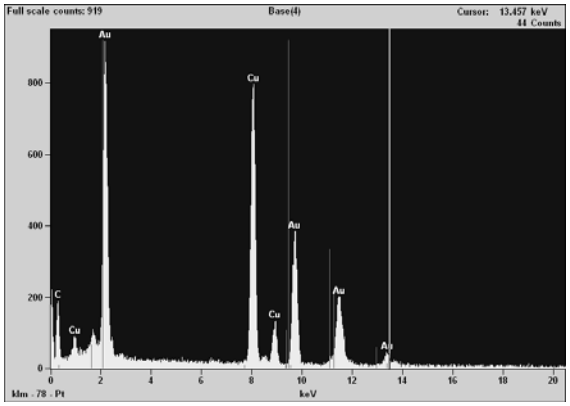

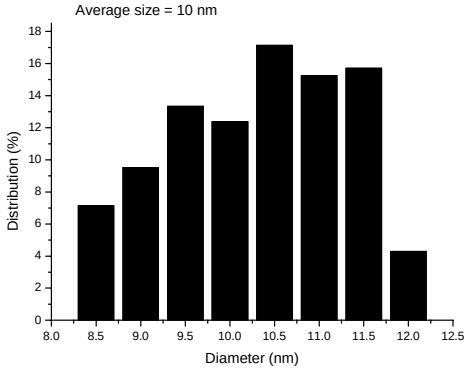

TEM image of platium NPs after transferred to [C_4mim][PF_6]; EDX analysis of the platinum NPs after transferred to [C_4mim][PF_6]; Size distribution of the Pt NPs after transferred to [C_4mim][PF_6]

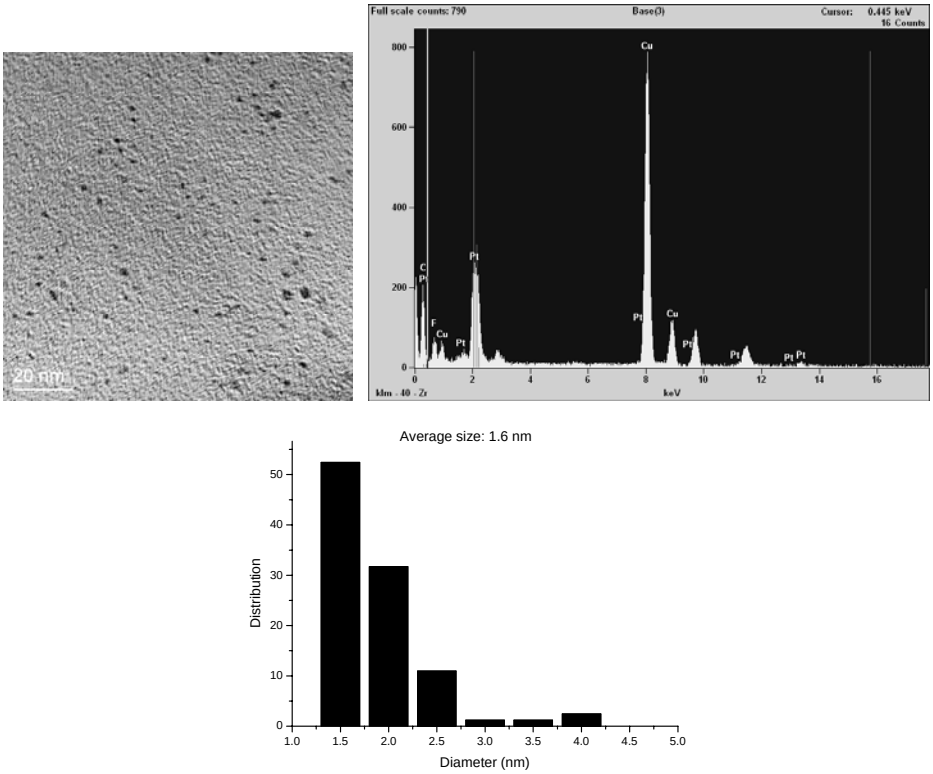

TEM image of palladium NPs after transferred to [C_4mim][PF_6]; EDX analysis of the palladium NPs after transferred to [C_4mim][PF_6]; Size distribution of the Pd NPs after transferred to [C_4mim][PF_6]

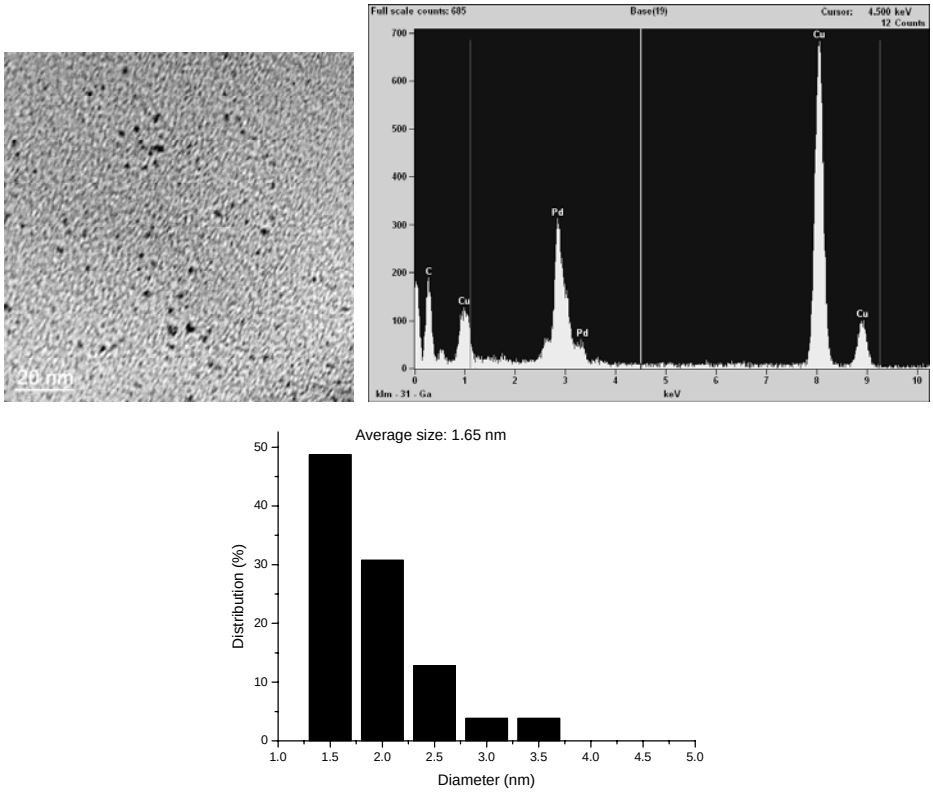

TEM image of platimun NPs after transferred to [C_4mim][Tf_2N]; EDX analysis of the platinum NPs after transferred to [C_4mim][Tf_2N]; Size distribution of the Pt NPs after transferred to [C_4mim][Tf_2N]

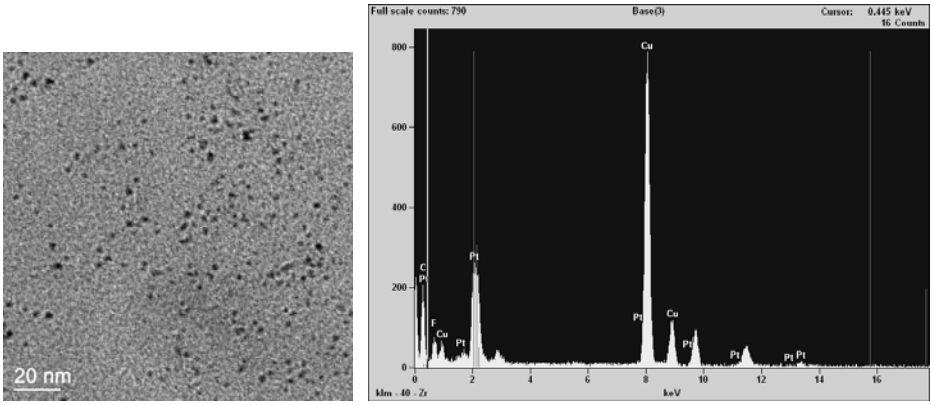

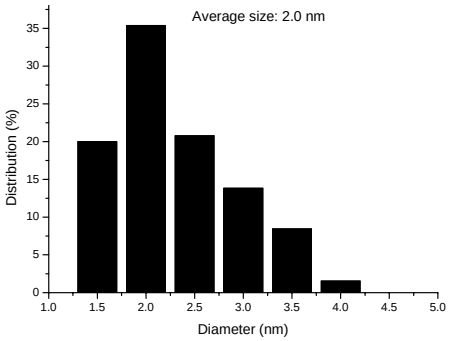

TEM image of palladium NPs after transferred to [C_4mim][Tf_2N]; EDX analysis of the palladium NPs after transferred to [C_4mim][Tf_2N]; Size distribution of the palladium NPs after transferred to [C_4mim][Tf_2N]

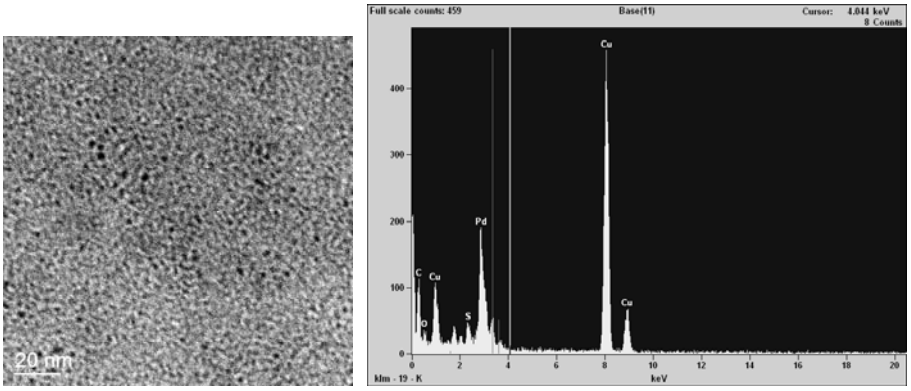

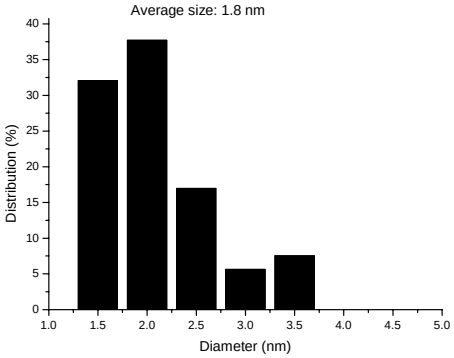

7.5 References

[1] For recent reviews, see: (a) A. Roucoux, J. Schulz, H. Patin, *Chem. Rev.* **2002**, *102*, 3757. (b) M. L. Brongersma, *Nature Mat.* **2003**, *2*, 296. (c) B. L. Cushing, V. L. Kolesnichenko, C. J. O'Connor, *Chem. Rev.* **2004**, *104*, 3893. (d) M. Daniel, D. Astruc, *Chem. Rev.* **2004**, *104*, 293. (e) M. Antonietti, D. Kuang, B. Smarsly, Y. Zhou, *Angew. Chem. Int. Ed.* **2004**, *43*, 4988.

[2] (a)J. Turkevitch, P. C. Stevenson, J. Hillier, *Discuss., Faraday Soc.* **1951**, *11*, 55. (b) M. Brust, J. Fink, D. Bethell, D. J. Schiffrin, C. Kiely, *J. Chem. Soc., Chem. Commun.* **1995**, 1655. (c) M. T. Reetz, W. Helbig, *J. Am. Chem. Soc.* **1994**, *116*, 7401. (d) D. V. Left, L. Brandt, J. R. Heth, *Langmuir,* **1996**, *12*, 4723. (e) Y. Yu, S. Chang, C. R. C. Wang, *J. Phys. Chem. B.* **1997**, *101*, 6661. (f) F. Kim, J. H. Song, P. Yang, *J. Am. Chem. Soc.* **2002**, *123*, 14316.

[3] For reviews, see: (a) C. M. Gordon, *App. Catal. A.* **2001**, *222*, 101. (b) H. Olivier-Bourbigou, L. Magna, *J. Mol. Catal. A*. **2002**, *182-183*, 419. (c) D. Zhao, M. Wu, Y. Kou, E. Min, *Catal. Today.* **2002**, *74*, 157. (d) J. Dupont, R. F. de Souza, P. A. Z. Suarez, *Chem. Rev*. **2002**, *102*, 3667. (e) C. E. Song *Chem. Commun.* **2004**, 1033; (f) P. J. Dyson, *Chimia,* **2005**, *59*, 66.

[4] (a) J.-C. Xiao, C. Ye, J. M. Shreeve, *Org. Lett*. **2005**, *7*, 1963. (b) D. Zhao, Z. Fei, T. J. Geldbach, R. Scopelliti, P. J. Dyson, *J. Am. Chem. Soc.*, **2004**, *126*, 15876. (c) T. J. Geldbach, P. J. Dyson, *J. Am. Chem. Soc.,* **2004**, *126*, 8114.

[5] (a) K. Jin, X. Huang, L. Pang, J. Li, A. Appel, S. Wherland, *Chem. Commun*. **2002**, 2872. (b) Z. Fei, T. J. Geldbach, D. Zhao, R. Scopelliti, P. J. Dyson, *Inorg. Chem.* **2005**, *44*, 5200. (c) J.-H. Liao, P.-C. Wu, Y.-H. Bai, *Inorg. Chem. Commun*. **2005**, *8*, 390. (b) Z. Fei, D. Zhao, T. J. Geldbach, R. Scopelliti, P. J. Dyson, S. Antonijevic G. Bodenhausen, *Angew. Chem. Int. Ed.*, **2005**, *44*, 5720.

[6] Z. Mu, W. Liu, S. Zhang, F. Zhou, *Chem. Lett*. **2004**, *33*, 524.

[7] B. S. Lee, Y. S. Chi, J. K. Lee, I. S. Choi, C. E. Song, S. K. Namgoong, S.-G. Lee, *J. Am. Chem. Soc.* **2004**, *126*, 480.

[8] R. R. Deshmukh, R. Rajagopal, K. V. Srinivasan, *Chem. Commun.* **2001**, 1544.

[9] (a) J. Dupont, G. S. Fonseca, A. P. Umpierre, P. F. P. Fichtner, S. R. Teixeira, *J. Am. Chem. Soc.* **2002**, *124*, 4228. (b) C. W. Scheeren, G. Machado, J. Dupont, P. F. P. Fichtner, S. R. Texeira, *Inorg. Chem.* **2003**, *42*, 4738. (c) G. S. Fonseca, A. P. Umpierre, P. F. P. Fichtner, S. R. Teixeira, J. Dupont, *Chem.-Eur. J.* **2003**, *9*, 3263. (d) L. M. Rossi, G. Machado, P. F. P. Fichtner, S. R. Teixeira, J. Dupont, *Catal. Lett.* **2004**, *92*, 149. (e) G. S. Fonseca, J. D. Scholten, J. Dupont, *Synlett.* **2004**, *9*, 1525. (f) E. T. Silveira, A. P. Umpierre, L. M. Rossi, G. Machado, J. Morais, G. V. Soares, I. J. R. Baumvol, S. R. Teixeira, P. F. P. Fichtner, J. Dupont, *Chem.- Eur. J.* **2004**, *10*, 3734. (g) C. C. Cassol, A. P. Umpierre,

G. Machado, S. I. Wolke, J. Dupont, *J. Am. Chem. Soc*. **2005**, *127*, 3298. (h) M. A. Gelesky, A. P. Umpierre, G. Machado, R. R. B. Correia, W. C. Magno, J. Morais, G. Ebeling, J. Dupont, *J. Am. Chem. Soc.* **2005**, *127*, 4588 (i) G. S. Fonseca, E. T. Silveira, M. A. Gelesky, J. Dupont, *Adv. Syn. & Catal.* **2005**, *347*, 847.

[10] (a) O. T. Starkey, M. L. Cline, M. Deetlefs, K. R. Seddon, R. G. Finke, *J. Am. Chem. Soc.* **2005**, *127*, 5758; (b) N. D. Clement, K. J. Cavell, C. Jones, C. J. Elsevier, *Angew. Chem., Int. Ed*. **2004**, *43*, 1277.

[11] X.-D. Mu, D. J. Evans, Y. Kou, *Catal. Lett.* **2004**, *97*, 151.

[12] (a) H. Itoh, K. Naka, Y. Chujo, *J. Am. Chem. Soc.* **2004**, *126*, 3026; (b) K.-S. Kim, D. Demberelnyamba, H. Lee, *Langmuir* **2004**, *20*, 556; (c) R. Tatumi, H. Fujihara, *Chem. Commun.* **2005**, 83.

[13] X.-D. Mu, J.-Q. Meng, Z.-C. Li, Y. Kou, *J. Am. Chem. Soc.* **2005**, *127*, 9694.

[14] D. H. Napper, *Polymeric Stabilization of Colloidal Dispersions*, **1983**, Academic Press, London.

[15] A. Warshawskz, D. A. Upson, *J. Polym. Sci., Part A: Polym. Chem.* **1989**, *27*, 2963.

[16] H. Hirai, N. Toshima, *Catalysis by Metal Complexes, Tailored Metal Catalysts,* ed. Y. Iwasawa. **1986**, Reidel, Dordrecht.

[17] G. Wei, Z. Yang, C.-Y. Lee, H.-Y. Yang, C. R. C. Wang, *J. Am. Chem. Soc.* **2004**, *126*, 5036.

[18] P. Bonhote, A.-P. Dias, N. Papageorgiou, K. Kalyanasundaram, M. Grätzel, *Inorg. Chem.,* **1996**, *35*, 1168.

[19] (a) G. A. Somorjai, *Appl. Surf. Sci*. **1997**, *121/122*, 1; (b) M. Moreno-Manas, R. Pleixats, *Acc. Chem. Res.* **2003**, *36*, 6

8

Conclusions

Ionic liquid functionalization enables us to obtain task-specific liquids that meet various application requirements. In this thesis, a series of functionalized ionic liquids illustrates this feature.

A series of imidazolium salts with the nitrile group attached to the alkyl side-chain, including both mono- and bis-substituted systems, have been prepared and characterized using spectroscopic methods. The majority of the nitrile-functionalized imidazolium salts can be classified as ILs since they melt below 100°C, and several are liquids well below room temperature. Key physical properties (density, viscosity and solubility in common solvents) of the low melting IL have been determined and are compared with those of the related 1-alkyl-3-methylimidazolium and 1-alkyl-2,3-dimethylimidazolium ILs. The results show that the incorporation of nitrile functionality affects the physical properties of the ILs, however, the ILs still retain low melting points, although viscosities increase slightly, but they can still be used as reaction media.

Palladium complexes of the nitrile functionalized imidazolium salts are among the first examples of transition metal complexes using the imidazolium cation as carrier for coordination center. The complexes are active catalyst precusors for Suzuki, Heck and Stille C-C coupling reaction as well as for hydrogenation. The most significant advantage of the Pd/CN-functionalised catalytic system, however, is the superior catalyst retetion and improved stability of the catalyst (evidenced by TEM due to the formation of nanoparticle catalyst resevoirs), by which a highly recyclable solvent/catalyst system results.

Pyridine, a cheaper ionic liquid precursor, was also functionalized with nitrile group and shows similar advanced ability to immobilized palladium catalyst for Suzuki and Stille reactions.

ILs with other functional groups were also prepared and characterised. In general, melting points and viscosities increase in these systems relative to non-functionalized analogues. However, during the course of the thesis work we discovered that by careful modification of the anion it was possible

to control the physical properties of the F-ILs. A K[$CH_3CH(BF_3)CH_2CN$] salt was prepared and was subsequently used to form various "dual functionalized ionic liquids" with various functionalized imidazolium cations. This anion not only endows ILs with multiple functionality, but reduces the melting point and viscosity of the ILs. The functionality on anion is not confined to the nitrile group, but other functional group can also be introduced using a similar strategy.

During the course of the thesis work nanoparticle catalyst resevoirs were found to be extremely well stabilized in F-ILS. Thus, other strategies were considered as methods to stabilize nanoparticles in ILs. Accordingly, an imidazolium salt functionalized by styrene group was polymerized to form a polyelectrolyte that can be employed as an effective stabilizer for gold, platinum and palladium nanoparticles involving a simple preparation procedure. The synergism of steric, electrostatic and micelle effects of the polymer is believed to facilitate stabilization of the NPs. The NPs can be easily transferred to hydrophobic ILs without degradation or aggregation. Our approach opens up a novel methodology for the synthesis and stabilization of NPs, their facile transfer from water into ILs by anion exchange, and many potential applications in catalysis and elsewhere can be envisaged.

Parts of the thesis have been published

Zhao, **Dongbin**; Fei, Zhaofu; Ang, Wee Han; Dyson, Paul J. **A Strategy for the Synthesis of Transition Metal Nanoparticles and Their Transfer Between Liquid Phases**, *Small, 2006, in press*

Zhao, Dongbin; Fei, Zhaofu; Geldbach, Tilmann J.; Scopelliti, Rosario; Dyson, Paul J. **Nitrile functionalised pyridinium ILs: synthesis, characterisation and application in Suzuki and Stille cross-coupling reactions.** *Journal of American Chemistry Society***, 2004,** *126*, 15876

Zhao, **Dongbin**; Fei, Zhaofu; Geldbach, Tilmann J.; Scopelliti, Rosario; Dyson, Paul J. **Allyl functionalised ILs: synthesis, characterisation and reactivity,** *Helvetica Chimica Acta,* **2005,** *88*, 665.

Zhao, Dongbin; Fei, Zhaofu; Ohlin, C. Andre; Laurenczy, Gabor; Dyson, Paul J. **Dual-functionalised ILs: synthesis and characterisation of imidazolium salts with a nitrile-functionalised anion.** *Chemical Communications,* **2004**, *21*, 2500.

Zhao, Dongbin. Analysis of Ionic Liquids and Dissolved Species by Electrospray Ionization MS. *Australian Journal of Chemistry,* **2004**, *57*, 509.

Zhao, Dongbin; Dyson, Paul J.; Laurenczy, Gabor; McIndoe, J. Scott. **On the catalytic activity of cluster anions in styrene hydrogenation: considerable enhancements in ILs compared to molecular solvents.** *Journal of Molecular Catalysis A: Chemical*, **2004,** *214*, 19.

Zhao, Dongbin; Fei, Zhaofu; Scopelliti, Rosario; Dyson, Paul J. **Synthesis and Characterization of Ionic Liquids Incorporating the Nitrile Functionality.** *Inorganic Chemistry* **2004**, *43*, 2197.

Fei Zhaofu, **Zhao Dongbin,** Geldbach Tilmann J., Scopelliti Rosario, Dyson Paul J., Antonijevic,Sasa Bodenhausen Geoffrey **A Synthetic Zwitterionic Water Channel: Characterization in the Solid State by X-ray Crystallography and NMR Spectroscopy**, *Angewandte Chemie International Edition*, **2005**, *44, 5720.*

Fei, Zhaofu; **Zhao Dongbin**; Geldbach Tilmann J. Scopelitti Rosario; Dyson Paul J. **Structure of nitrile functionalized alkyltrifluoroborate salts,** *European Journal of Inorganic Chemistry,* **2005**, 860.

Fei, Zhaofu; **Zhao, Dongbin**; Geldbach, Tilmann J.; Scopelliti, Rosario; Dyson, Paul J. **Bronsted acidic ILs and their zwitterions: Synthesis, characterization and pKa determination.** *Chemistry-A European Journal*, **2004**, *10*, 4886.

Fei, Zhaofu; **Zhao, Dongbin**; Scopelliti, Rosario; Dyson, Paul J. **Organometallic Complexes Derived from Alkyne-Functionalized Imidazolium Salts.** *Organometallics* **2004**, *23*, 1622.

Curriculum Vitae

Dongbin Zhao

Birthday: 14/11/1972

Nationality: P. R. China 

Education:

1990 - 1997: *Southwest Petroleum Institute, P. R. China,* **Master in Applied Chemistry.**

2002 - 2006: *EPFL, Lausanne, Switzerland,* **Ph. D in Inorganic Chemistry.**